AN EXPERIMENTAL INVESTIGATION ON DESIGN, CHARACTERIZATION AND ANALYSIS OF TWO NOVEL LEAD FREE SOLDER ALLOYS

A THESIS

Submitted by

JAYESH S

for the award of the degree

of

DOCTOR OF PHILOSOPHY

COCHIN UNIVERSITY OF
SCIENCE AND TECHNOLOGY

DIVISION OF MECHANICAL ENGINEERING
SCHOOL OF ENGINEERING
COCHIN UNIVERSITY OF SCIENCE AND TECHNOLOGY, KOCHI

MARCH 2020

DIVISION OF MECHANICAL ENGINEERING
SCHOOL OF ENGINEERING
COCHIN UNIVERSITY OF SCIENCE AND TECHNOLOGY

COCHIN UNIVERSITY OF
SCIENCE AND TECHNOLOGY

CERTIFICATE

This is to certify that the thesis entitled "**AN EXPERIMENTAL INVESTIGATION ON DESIGN, CHARACTERIZATION AND ANALYSIS OF TWO NOVEL LEAD FREE SOLDER ALLOYS"** submitted by Jayesh S to the Cochin University of Science and Technology, Kochi for the award of the degree of Doctor of Philosophy is a bonafide record of original research work carried out by him under my supervision and guidance at the Division of Mechanical Engineering, School of Engineering, Cochin University of Science and Technology. The contents of this thesis, in full or in parts, have not been submitted to any other University or Institute for the award of any degree or diploma. All the relevant corrections and modifications suggested by the audience during the pre-synopsis seminar and recommended by the Doctoral committee have been incorporated in this thesis.

Kochi-22

March 2020

Dr. Jacob Elias

(Supervising Guide)

DECLARATION

I hereby declare that the work presented in the thesis entitled "**AN EXPERIMENTAL INVESTIGATION ON DESIGN, CHARACTERIZATION AND ANALYSIS OF TWO NOVEL LEAD FREE SOLDER ALLOYS**" is based on the original research work carried out by me under the supervision and guidance of Dr. Jacob Elias for the award of degree of Doctor of Philosophy with Cochin University of Science and Technology. I further declare that the contents of this thesis, in full or in parts, have not been submitted to any other University or Institution for the award of any degree or diploma.

Kochi-22   **Jayesh S**
March 2020   Research Scholar

ACKNOWLEDGEMENTS

ABSTRACT

Soldering is a widely used metallurgical process to join two materials without actually melting it. The solder alloy forms a joint between the parent materials by wetting and joining. Sn-Pb alloy was used as solder material around the globe for many years. Sn-Pb has low melting point, good hardness and wetting properties and low cost which make it a famous solder material. Lead in the alloy is found to be toxic. Lead usage is discouraged to be used in solder alloy making because of its inherent toxicity. WEEE (Waste Electric and Electronic Equipment) and RoHS (Restriction on Hazardous Substances) norms also banned lead from alloy making. The toxic nature of the lead was not the only the reason to search for lead-free solder joints. According to the Moore's law, "the number of transistors in a dense integrated circuit doubles about every two years". As the transistor density increases the solder joint pattern also changes. The pitch of these solder arrangement will have adverse effect if Sn-Pb solder alloy is used in dense electronic packages. Behaviour of customer towards environmental friendly tag and economy is another reason. The 'environmental friendly' tag necessitated search for new alloys. Another reason is the need for high temperature solder alloys. With the ban of lead, researchers around the world were looking for new lead free solder alloys. Melting temperature, hardness, contact angle (wetting characteristics), shear strength and cost are some important properties that should be considered while developing new lead free solder alloys. Melting temperature, contact angle and cost should be minimal. Shear strength and hardness should be more. SAC305 (Sn-3Ag-0.5Cu) and SAC 405 (Sn-4Ag-0.5Cu) were emerged as the alternate solder joints in electronic industry. SAC 305 and SAC405 are having high cost due to patent coverage and silver content. None of them were

able to replace the Sn-Pb solder alloy in all respects.

In this investigation, two novel lead free solder joints were developed (Sn-0.5Cu-3Bi and Sn-1Cu-1Ni). The melting temperature was analysed using Thermo Gravimetric and Differential Thermal analysis (TG-DTA) set up. Hardness property was analysed using HMV-G micro Vickers hardness tester. Contact angle (wetting characteristics) measurement was done with the sessile drop method. Micro-force test system couple to software was used to measure shear strength of the alloys. The impact toughness property was analysed using Charpy test. The chemical composition of the alloys was tested using ICP-OES (Inductively coupled plasma - optical emission spectrometry) setup.

The effect of addition of Ag into the two alloys was experimentally investigated. With the addition of Ag, the properties were enhanced. Melting temperature and contact angle decreased, hardness, shear strength and impact toughness was increased. The corrosion tests were also carried out. It was found that the corrosion rate also decreased with the addition of Ag. The properties were compared with SAC305 and SAC405. From the comparison it was concluded that the novel alloys were having better properties than SAC305 and SAC405. The cost of the new alloys was found to be less than SAC305 and SAC405. The optimum amount of Ag that should be added was found to be 1% by wt. Therefore it can be concluded that Sn-0.5Cu-3Bi-1Ag and Sn-1Cu-1Ni-1Ag are two novel lead free solder alloys which can replace Sn-Pb alloy.

TABLE OF CONTENTS

CHAPTER 5: EFFECT OF ADDITION OF AG INTO Sn-0.5Cu-3Bi (SCB 305)

CHAPTER 6: EFFECT OF ADDITION OF AG INTO Sn-01Cu-1Ni (SCN 110)

CHAPTER 7: CORROSION PROPERTIES OF Sn-0.5Cu-3Bi-xAg

LIST OF TABLES

LIST OF FIGURES

LIST OF ABBREVIATIONS

Adj MS	Adjusted mean square
Adj SS	Adjusted sum of square
CI	Confidence interval
CR	Corrosion rate
DF	Degree of freedom
DoE	Design of Experiments
DTA	Differential Thermal Analysis
EDS	Energy Dispersive Spectroscopy
EHT	Electron High Tension
EMS	Electronics Manufacturing Services
FE SEM	Field Emission Scanning Electron Microscope
F-Value	Value in F-table
IMC	InterMetallic Compound
ICP-OES	Inductively Coupled Plasma Optical Emission Spectrometry
P-Value	Probability of significance
RoHS	Restriction on Hazardous Substances
R-sq	Pierson relation correlation coefficient
SAC	Alloy with Tin-Copper-Silver combination
SE Coef	Standard Error Coefficient
TGA	Thermo Gravimetric Analysis
VIF	Variance inflation factor
WD	Working Distance
WEEE	Waste Electric and Electronic Equipment

NOMENCLATURE

A	Area exposed
Ag	Silver
Au	Gold
Bi	Bismuth
Cu	Copper
F	Factors in DoE
gmd	$gm/m^2/day$
Hv	Hardness value
In	Indium
k	Levels in factorial regression
KX	1000 times
L	Number of levels
Ni	Nickel
Pb	Lead
Sb	Antimony
Sn	Tin
t	Time of exposure
w	weight loss
wt.	weight
Zn	Zinc
β	Coefficient in factorial regression
μm	micro meter

CHAPTER 1

INTRODUCTION

1.1.   SOLDERING PROCESS

Soldering is a metallurgical joining process happening without the melting of parent metals and occurs at a temperature less than 450°C. This joining process is very significant in the field of electronic package industries. Two solid metals (parent metals) or metal parts are joined using another material (solder alloy). The solder alloy is in a liquid state while this joining process is taking place (Schwartz, 2014). The solder alloy in the molten form during the joining process flows in the space in between the parent metals, wets the surface and after solidification joins them. Thus the principle behind the soldering operation is wetting and joining. The solder alloy will have low melting temperatures when compared to the parent metals. A bond is created between the parent metals after solidification (Handwerker, 2007).
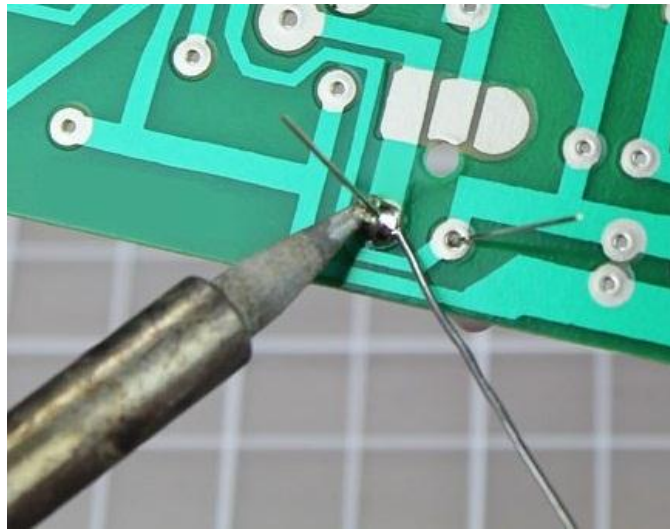
Fig. 1.1 Soldering process

The soldering process is very different from welding and brazing process. In welding process, the parent metals also melt to form the joint. While in brazing operation, parent metal substrates do not melt. The filler metal will have a higher melting temperature than the used solder alloy. Oxide layer should not be present on the External surface of the work piece or parent metal substrate. This is necessary to form a good solder joint. Soldering technology has a vital role in all the electronic devices and packages and also in the industries.
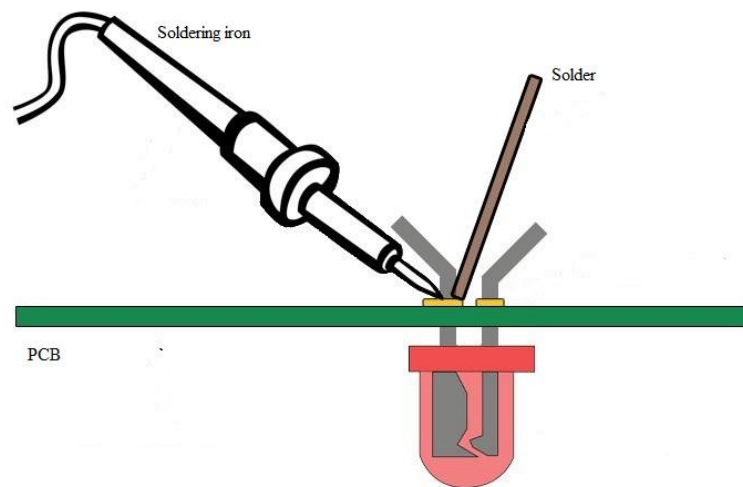
Fig. 1.2 Schematic diagram of soldering process

1.2. A SHORT HISTORY OF SOLDERING PROCESS

Soldering is a widely known joining process. Most of the people do not know the fact that soldering was in use for thousands of years already. The importance of joining for making tools and ornamental purposes, a primitive form of soldering was discovered.

Joining of metals for making tools and other materials were the necessities. From ancient times, ornaments had a vital role, people were often buried with their best jewellery. The burial sites were considered as sacred and therefore these sites were maintained and preserved well. Archeologists got immense information from these sites. Those pieces of information were helpful to identify the level of technical skills used by human beings in ancient times. The usage of fire in joining process was a revolution in the history of human beings. At very earlier stages after the usage of fire in joining process and metals, human beings uncovered the fact that metals can be easily melted using the wood fire. About 5500 years ago, the earliest data of hard solder were found in Sumeria and Egypt. In the figure 1.3 a painting of Egyptian goldsmith soldering with a blowing pipe on coal fire is shown (Demortier, 1989). This painting is from an Egyptian tomb, Thebe, 1475 BC. During this era, Ag-Cu, Au-Cu, and Pb-Cu alloys were used as solders. From the jewellery obtained from these places, the advancement in the skills was studied. The craftsmanship of the recovered jewellery items is so superior that it is very difficult to see that these are soldered joints.

Fig. 1.3 Painting of Egyptian goldsmith performing soldering with a blowing pipe on coal fire (Demortier, 1989)

Sn is used in the soldering operation to lower the melting point of the final alloy. It is known as soft solder. The exact period of starting the usage of Sn cannot be traced due to the fact that Sn will transform easily into Sn acids. Therefore several ancient artifacts using soft solder which were recovered is limited in number. Before 2000 BC, Sn was unknown to Egyptian society. 'Treasure of Priamos' gave light about the fact that the Greeks had mastered the jewelry soldering. These pieces of evidence were found during the excavations of Troje II during 2600 BC. The pieces of evidence after 1400 BC give strange observation that the soldering technique usage has a decreasing trend. During and after 350 BC, Greeks were able to come to their earlier level of soldering. The Greeks also used the soldering technique in machine building applications during these times. For machine making applications they generally used copper, lead and bronze.

Hippokrates, Theoprast, and Poseidonius of Apamea were famous Greek writers during 430 BC, 300 BC, and 139 BC respectively cited solder (Chrysokolla) in their works. Still, the exact composition of 'Chrysokolla' is a controversial topic (Hoover, 1950).

Tin-Lead (Sn-Pb) is introduced by the Romans. The famous example of this is the aqueducts. Aqueducts are mentioned in various works in ancient times like Pliny, Frontinus, and Vitruvius. These aqueducts are an example of the engineering construction and the architectural marvel. Lead pipes are used to carry water. These lead sheets are joined together by Sn-Pb solder. This fact described by Pliny in his work Historia Naturalis liber XXXIII (Vainco, 1993). Apart from Sn-Pb, Romans used 'Chrysokolla', Copper alloys and Gold alloys. As time passed, the price of Tin increased. Therefore they started using solder with only lead. Water vessels are made with lead and were used.

The soldering process also widely used in Europe. Irish ornaments (1500 BC), archeological findings in Central Europe (1200 BC) are the shreds of evidence for validating the point. Gauls and Celts worked with Tin alloys according to Caesar and Pliny. Holmiensis during 150 AD provided the first technical description about solder. Arabian, Persian and Syrian documentation in the course of the middle ages made the soldering practice highly efficient in the following couple of 100 years. The first legislation regarding the soldering process came around 1400 AD, regarding the solders using gold which is being diluted with noble metals in lesser quantities. In the same period, several documents appeared detailing the soldering. From the writings of

Leonardo Da Vinci (Codex Atlantico), it can be noted that the soldering was present and spread in Europe. Descartes, Paracelsus, and Galilei studied about the soldering operations and technique.

Newton was the first to add Bi into the Sn-Pb alloy which brings about the reduction of the melting point to less than 100°C (M.Kamal et al., 2011). Lowering the melting temperature of Sn-Pb alloy with Cd, Zn and Bi additions were common during the early 1900s. Thompson (1807) during the 19th century came up with the metallurgy of soldering and description of the process. He also explained the diffusion in liquids. There were some problems aroused with the discovery of Aluminium because no solder materials were able to wet Aluminium.

During the late 19th century the functions and uses of solder materials expanded. In addition to the metallurgical bond formed, solder finds applications in conductivity of electricity. Soldering and solder materials attained importance with the advances in electronics during the 20th century (Plumbridge, 1996).

1.3. SOLDERING METHODS AND CLASSIFICATIONS

Soldering is a metallurgical joining. Metal items are joined together by heating and then flowing a filler metal into the joint. Soldering is mainly done using the following methods:

1. Hand soldering
2. Wave soldering
3. Reflow soldering

1.3.1.   Hand soldering

The required amount of heat for the joint size should be selected from the heat source. Soldering iron of 25 Watts is inadequate for large electrical assemblies and a 100 Watt soldering iron is too much for printed circuit boards (PCB). The selection of heat is a very important step in hand soldering. Fine-pitch soldering is required in many cases. Therefore the hand soldering requires great skill. Too much heat can cause impairment to the sensitive components. But for BGA (Ball Grid Array) packages, hand soldering cannot be used. For hand soldering the alloy should be available in the form of wire. SAC(Sn-Ag-Cu) alloys and Sn-Cu alloys are available in the form of wires. SAC could be a superior choice citing its wetting characteristics. Figure 1.4 shows hand soldering

Fig. 1.4 Hand soldering

1.3.2.   Wave soldering

In wave soldering (figure 1.5) method, the PCB is passed above a pan of solder alloy in molten form. In this set up a pump produces an upsurge of solder which appears like a standing wave. The components get soldered to the board, as the circuit board creates direct contact with the wave. Important factors that should be considered while doing wave soldering are dissolution of copper, the temperature required, the formation of dross, wetting property and cosmetic effects. SAC305 (Sn-3Ag-0.5Cu) is a worthy candidate for this method as it is holding good properties.
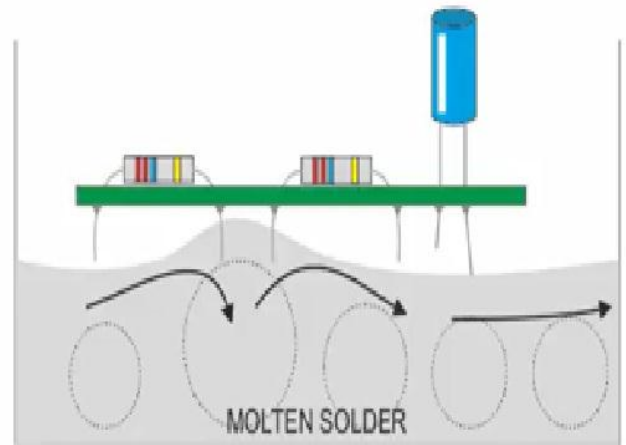
Fig. 1.5 Wave soldering process

1.3.3.   Reflow soldering

In this method, hundreds and thousands of small fine electronic components are temporarily attached to the contact pads using solder paste, followed by application of controlled heat. The source of heat is a reflow oven in the process. The solder paste will reflow in the molten state, producing permanent solder joints. In other processes, the solder alloys in the pure state are used for the soldering operation whereas solder paste is used in reflow soldering (Figure 1.6 and 1.7) process. By applying different fluxes

manufacturers can produce different solder paste for various purposes (Handwereker, 2007).
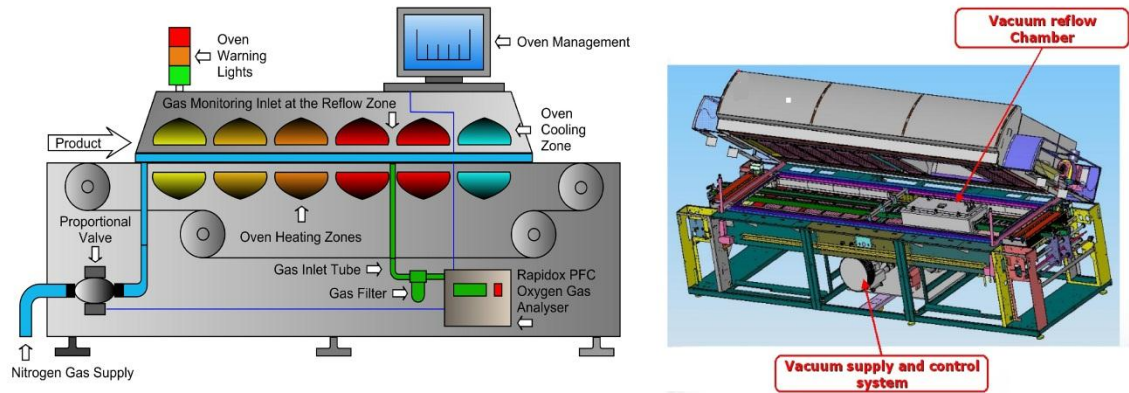
Fig. 1.6 Reflow soldering
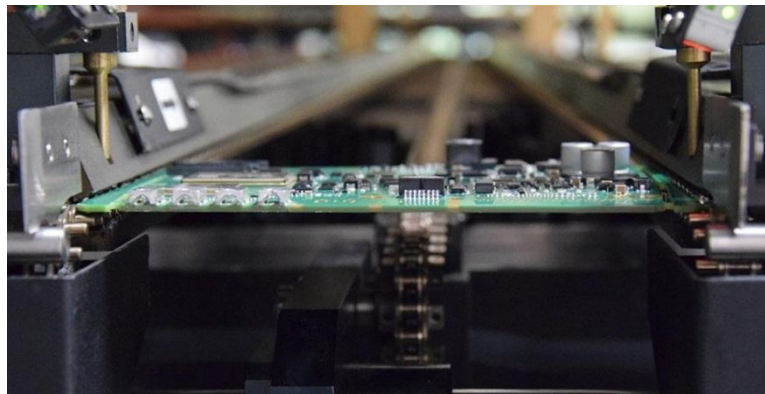
Fig. 1.7 Reflow soldering

1.4. Lead in solders

The soldering was in use for centuries, however the metallurgical study, descriptions and fundamental knowledge of the soldering came only in the 19th century. The lead-tin alloy which is widely used for soldering is having the composition of 63% tin and 37% lead by wt. Sn-Pb solder has been used in electronic package industries because of its virtuous

soldering properties, manufacturability, reliability and pricing. The melting temperature of Sn-Pb alloy is 183°C.

The reason to discuss the lead in the solder joints is environmental awareness. Sn-Pb alloy is the most commonly used soldering alloy. Lead toxicity among miners was first documented by Hippocrates (around 400 BC). The lead was extensively used by the Romans. They are also aware of the detrimental effects of the lead, as cited from the writings of Vitruvius in the books of architecture as follows:

'*Etiamque multo salubrior est ex tubulis aqua quam per fistulas, quod*

plumbum videtur esse ideo vitiosum quod ex eo cerussa nascitur, heac autem dicitur

esse nocens corporibus humanis. Itaque quod ex eo procreatur (si) id est vitiosum,

non est dubium quin ipsum quoque non sit salubre.'

Its translation is as follows:

'*Water conducted through earthen pipes is more wholesome than that through*

lead; indeed that conveyed in lead must be injurious, because from it white lead is

obtained and this is said to be injurious to the human system. Hence, if what is

generated from it is pernicious, there can be no doubt that itself cannot be a

wholesome body.'

There were claims from various historians that the decline of the Roman Empire was because of the usage of lead utensils mixed with the lead water pipes (Gilleo, 1994). Other examples can be taken from history. Sir John Franklin commanded a voyage to the Artic region with sufficient food supply for 3 years. His attempt failed following the death of the crew. This is not just because of the extreme weather, but also due to the lead poisoning of the food stored in the cans (Beattie, 2000).

With the rising consciousness regarding the environment, the inherent toxicity of the lead again came into light during the 1990s. The harmful effect of lead in the human body was also a concern. When lead enters inside the human body affects the nervous system, reproductive system, delay in neural and physical development, anemia, harmful effect on children's neurological development (Monsalve, 1984). The binding of lead to proteins is the major cause of these effects. The lead in the human body is detected by blood analysis. The limits for the amount of lead are determined by governments. For unpolluted human beings, the standard upper value is less than 130mg/L. For people who are working and exposed to lead during work, the upper limit is 300mg/L for women and 700 mg/L for men (German Biological Place of Work Tolerance values). The manufacturing environment causes less danger with lead. The great danger occur with breathing in, dried powder particles which occurs because of the violation of the safety measures. The disposal of electronics parts and electronic scrap pollutes the soil and the ground water.

Due to this inherent toxicity of lead, several suggestions were formed to ban, cut or tax the usage of lead in electronic package industries. Various legislation like RoHS (Restrictions of Hazardous Substances) and WEEE (Waste Electric and Electronic Equipment) and various environmental legislations, lead become a banned substance in the electronic package industry. China, Japan, South Korea, Turkey, and the United States also followed the ban of lead by making legislations (Cheng et al., 2017).

1.5.   LEAD-FREE SOLDER ALLOYS

The lead has been banned in solder alloy manufacturing due to its intrinsic toxicity nature. Therefore, a need for novel lead-free solder alloys aroused. Researchers around the world started looking for novel lead-free solder alloys for replacement of Sn-Pb alloy. The toxicity in lead was not only the reason for finding novel lead free solder alloys. The transistor density is increasing according to Moore's law. The pitch of the soldering also increases. The Sn-Pb alloy will not sufficient to accommodate the thick densities. These are the other two reasons for choosing lead-free solder alloys. Good hardness, low melting point, good wettability, availability of constituents, and price are some of the aspects that should be incorporated in the new lead-free solder alloys.

1.6   MOTIVATION

Lead is banned in solder making process due to its inherent toxicity which leads to the requirement of environment-friendly solder joint material to replace the Sn-Pb solder alloy. Many lead- free solder alloys were suggested, none of them were able to replace Sn-Pb in all aspects. SAC305 (96.5Sn-3Ag-0.5Cu) and SAC405 (95.5Sn-4Ag-0.5Cu) are two lead free solder alloys which are the prominent replacement. The two alloys are

protected by patent and contain silver (3 and 4 % by wt.) Thus the cost of silver and patent cost makes it an expensive alloy. There is a requirement of low cost lead free solder alloy. There is also a need for corrosion resistant solder alloy since there are equipments needed to implant in human body.

1.7   OBJECTIVES

Objectives of the work are:

➢   To synthesise novel lead free solder alloy with Sn, Cu, Bi, Ni.

➢   To experimentally analyze the effect of Ag addition into the solder alloy,

➢   To experimentally analyze the corrosion properties of the developed alloy

1.8   SCOPE

The scope of the present work is concentrated to:

- Development of new lead free solder alloys with Sn, Cu, Bi and Ni

- Alloys with low melting temperature, good hardness and good wetting properties.

- Experimentally investigate whether the addition of Ag in small quantities improves the desirable properties

- Experimentally investigate the impact toughness and shear strength of the the alloys

- Experimentally investigate the corrosion properties of the alloy

- Comparison of the properties with existing lead free alloys SAC305 and SAC405.

1.9 THESIS OUTLINE

Due to the ban on lead in alloy making, the need for new lead-free alloys became a necessity. Numerous researchers around the globe started developing novel lead-free solder alloys which can substitute the Sn-Pb alloy. In this work, two new lead free solder alloy compositions are developed. The effect of the addition of Ag into these two novel alloys is also examined. The mechanical properties, corrosion characteristics, cost analysis of these alloys are also conducted.

Chapter 1 – "Introduction" provides introduction to the work. Introduction to soldering, solder alloy. Various soldering processes and history of soldering is explained.

Chapter 2 – "literature survey" is the literature survey conducted for the work.

Chapter 3 – "Materials and methods" provides details of various experimental set up and materials used for the work.

Chapter 4 – "Development of two new novel lead free solder alloys"

illustrates the development of two new lead-free solder alloys. DoE is explained. Melting temperature, wetting characteristics, hardness, and microstructure of the alloys are discussed.

Chapter 5 – "Effect of addition of Ag into Sn-0.5Cu-3Bi (SCB 305)" investigates the effect of addition of Ag in to Sn-0.5Cu-3Bi. Melting temperature, wetting characteristics, hardness, shear strength, impact toughness and microstructure of the alloy is discussed.

Chapter 6 – "Effect of addition of Ag into Sn-1Cu-1Ni (SCN 110)" investigates the effect of addition of Ag in to Sn-1Cu-1Ni. Melting temperature, wetting characteristics, hardness, shear strength, impact toughness and microstructure of the alloy is discussed.

Chapter 7 – "Investigation on corrosion properties of Sn-0.5Cu-3Bi-xAg" is an experimental investigation for finding the corrosion properties of Sn-0.5Cu-3Bi in 3.5%by wt. NaCl.

Chapter 8 – "Investigations on the corrosion properties of Sn-1Cu-1Ni-xAg" is an experimental investigation for finding the corrosion properties of Sn-1Cu-1Ni in 3.5%by wt. NaCl.

Chapter 9 – "Conclusion" presents the overall conclusion of experimental works and also the scope for future work

Annexure I – provides the cost comparison of various lead free solder alloys.

CHAPTER 2

LITERATURE SURVEY

2.1   Sn-Pb SOLDER ALLOYS

Sn-Pb solder alloy has been used for more than 50 years in electronic package industries for joining electronic components. It has good soldering properties, low cost, reliability, and manufacturability.

2.2   WHY LEAD-FREE?

Lead is a very useful material having many useful properties and applications. But on the other hand, lead is a heavy metal and toxic. The inherent toxicity of lead is known for more than 2000 years. Many studies revealed the adverse effect of lead in the environment. Lead has no useful effect if contained in the human body. Lead is toxic in human beings. Regardless of the exposure to lead, it can cause serious health issues for human beings. Lead is considered as carcinogenic, can cause blood-related diseases, it can harm the reproductive organs. High quantity exposure to lead can cause death, malfunctioning of the brain and other physiological problems. Lead exposure in low quantity is enough to cause health imbalances in children. It will be present in the chemical, physical and biological environment once it is released into the atmosphere. Lead is toxic to plants, animals, and micro-organisms as well. Variety of electronic toys are present in the market. There are chances that these toys may come into contact with the child's mouth. This may result in the transfer of lead into the child's body.

Unless there is no sudden change in the adhesive joining technology, soldering will stand as an important technology. It is a very unlikely event to replace soldering with other technology. Tin will remain as the main component in the solder alloy. It is having a low melting temperature (232°C) and its usage is safe. Other additives has to be added into the Tin to make new lead free solder alloy. Not only melting temperature but also many other properties are there to consider like very good wetting characteristics, the strength of the joint, physical properties as that of Sn-Pb, non-toxic property, low cost, etc. Some elements form a low melting temperature phase with Pb. E.g., Ternary low melting point SnBiPb (96°C) is formed when the Sn-Bi eutectic reacts with Pb substrate. This is another reason for removing lead. This low melting temperature phase has an adverse effect on the reliability of the joint (Zoran, 1998).

2.3   SOLDER ADDITIVES

The following are the most common solder additives used: Copper, Bismuth, Nickel, Silver, Indium, Chromium, Silicon, Titanium, Platinum, Palladium, Cobalt, rare earth elements and nanoparticles. Cadmium and antimony are discarded due to toxicity concerns. Tin is the base metal in most solder alloys. The properties of these additives are listed in table 2.1. Inorder to reduce the growth of IMC, modify the microstructure and properties, the additives are added into the solder alloy. The addition of Ag (Kim et al., 2010, Laurila et al., 2009), Au (Laurila et al., 2010), Co (Anderson et al., 2004, Wang et al., 2009, Gao et al., 2006,), Cr (Kim et al., 2009), Cu (Wang et al., 2010), Fe (Ansderson et al., 2006), Mn (Anderson et al., 2006, Kim et al., 2009), Ni (Anderson et al., 2006, Wang et al., 2005, Yang et al., 2006, Liu et al., 2011), Pd (Ho et al., 2015, Ho

et al., 2012), Pt (Laurila et al., 2010), Si (Anderson et al., 2006) and Zn (Wang et al., 2006, Jee et al., 2007, Kim et al., 2010) have reduced the growth of Cu_3Sn.

The thermal aging performance of Sn-3.7Ag-0.6Cu-0.3Cr solder alloys were compared with Sn-3.7Ag-0.9Cu (Both for 100h and 1000h at 150°C). The shear ductility is found to be increasing with the addition of Cr along with extensive aging (Anderson et al., 2006). Laurila et al., 2010 studied the effect of adding Fe into the solder alloy. The reaction between Cu substrate and Sn base is studied. The CuSn IMC is slightly decreased but the ratio of the thickness (Cu_6Sn_5 to Cu_3Sn) remains the same. The addition of Mn has enhanced the shear ductility (Cheng et al., 2017). It also reduced the Cu_3Sn growth. There is a significant reduction in the $Cu_3Sn+Cu_6Sn_5$ combined intermetallic layer (Kim et al., 2009). The addition of Pd reduced the Cu_3Sn in the SAC solder joint. The mechanical reliability is found to be increased (Ho et al., 2012). The experimental observations obtained by the addition of Pt were not consistent (Laurila et al., 2010). The addition of Ni was also studied. The addition of Ni increases the fluidity. This will be helpful factor while performing wave soldering. With the addition of Ni, a complex compound $(CuNi)_6Sn_5$ is formed. In SAC alloys, the strength property is enhanced with the addition of Ni. The addition of Ni reduces the Cu_3Sn intermetallic growth (Henshall et al., 2009). Reaction between Sn-2.5Ag-0.8Cu and Cu alloys added with 0, 0.005, 0.01, 0.03, 0.06 and 0.1 % by wt. Ni with multiple reflow conditions was investigated. Thinner Cu_3Sn layer was formed with the addition of Ni (Wang and Kao, 2009).

Table 2.1 Solder additives and properties (Cheng et al., 2017)

Sl No	Element	Melting temperature (°C)	Properties
1	Tin (Sn)	232	Low melting point
			Base alloy metal
			Readily available
			Tin whiskers formed are not good
2	Copper (Cu)	1084	
			Inexpensive
			More difficult to remove the oxide layer
3	Bismuth (Bi)	271.5	It imparts good tensile strength
			Lowers the melting temperature
			Increases brittleness
			Becomes more brittle when contaminated with lead
4	Nickel (Ni)	1453	Copper dissolution is inhibited
5	Silver (Ag)	962	Expensive
			Absorbs copper
			Causes intermetallic growth with copper
6	Indium (In)	156.6	Very expensive
			Scarce
			Prone to corrosion
			extremely soft
			With high Indium content, mechanical strength reduces
			Fast formation of oxide during melting

			Corrodes fast
7	Zinc (Zn)	419.5	oxide formation
			Requires flux
8	Antimony (Sb)	630.5	Enhances mechanical properties
			Toxic (EACEM list "not to be used" substance)
9	Gold (Au)	1063	Increases melting temperature
			very expensive
			With increase in gold content, gold embrittlement issues exist
10	Cadmium(Cd)	321.1	Listed in RoHS
			Hazardous substance
11	Chromium(Cr)	1857	Improve the ductility of SAC solders
			Suppress void formation at Cu interface
12	Cobalt (Co)	1495	Hard, brittle material
			Ferromagnetic
13	Nano particle		Example- Silica, Titanium dioxide, Aluminum oxide, carbon nanotubes, etc.
			Wettability and melting temperature can be improved
			Problem in homogeneous distribution

2.4   PHASE DIAGRAMS

The phase diagrams of Sn-Pb (Fecht et al., 1989), Ag-Bi (Kattner and Boettinger, 2004 ,

Bi-Cu (Teppo et al., 1990), Bi-Sn (Lee and Shim, 1996), Cu-Sn (Shim and Lee, 1996),

Ag-Cu (Hayes et al., 1986), Ag-Sn (Oh et al., 1996) binary diagrams and Sn-Ag-Cu

ternary phase diagram is shown in the figures 2.1 to 2.9. The figure 2.9 is the plan (2D) of

the Sn-Ag-Cu ternary phase diagram. The hatched area in the figure indicates the near

eutectic region. The intermetallic compounds are formed with Sn, Cu, and Ag in SAC

alloys. The formation of these intermetallic compounds affects the properties of the alloy.

By analysing the binary phase diagrams, there are three vital possibilities for the

formation of intermetallic compounds. The reaction between Sn and Ag result in the

formation of Ag_3Sn. Cu and Sn reaction result in the formation of Cu_6Sn_5. Cu content

should be high enough for the formation of Cu_3Sn at the eutectic point at higher

temperatures. Ag and Cu will not form any intermetallic compounds. Only Ag rich α

phase and Cu rich β phase are formed due to the reaction between Ag and Cu (Hongtao

and Suhling, 2009).
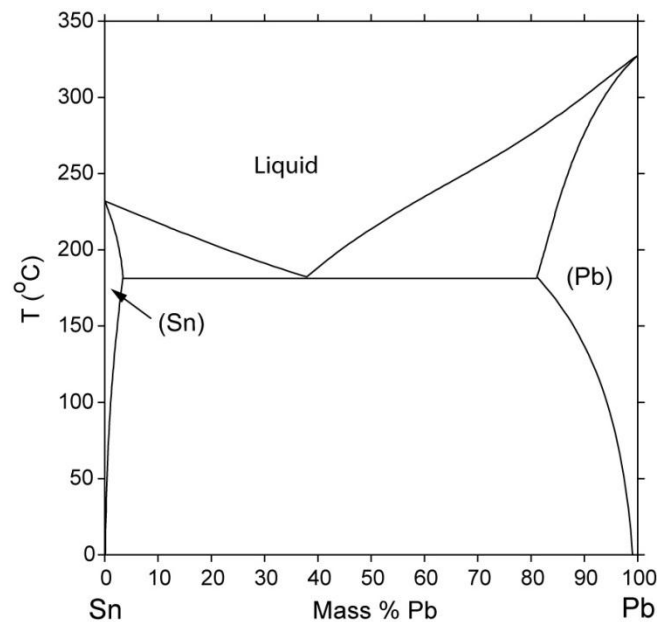
Fig. 2.1 Sn-Pb binary phase diagram
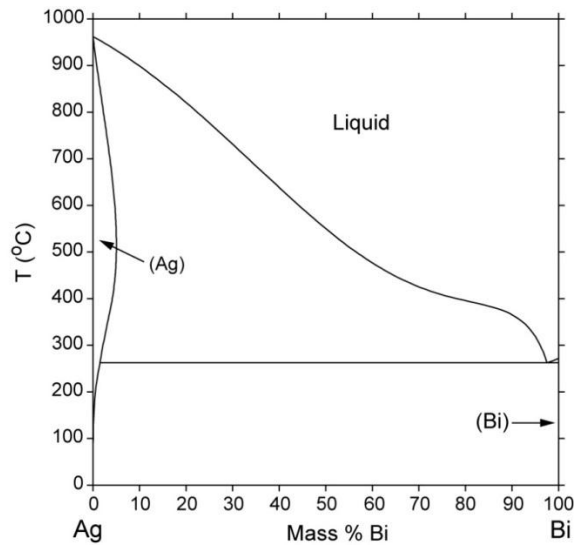
Fig.2.2 Ag-Bi phase diagram
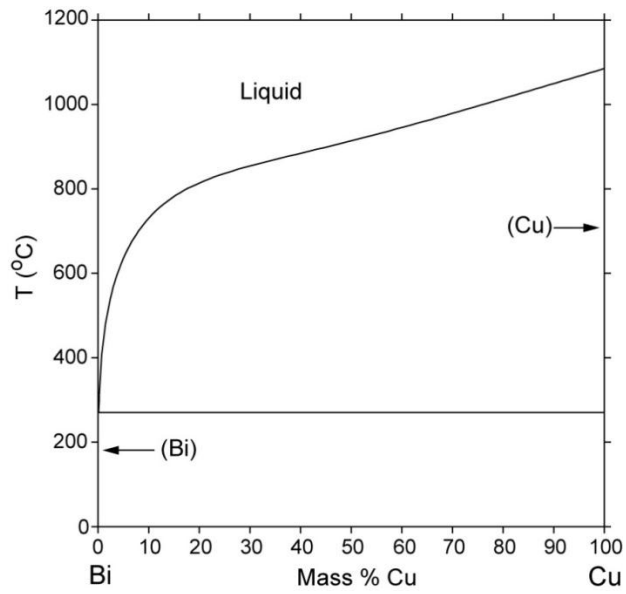
Fig.2.3 Bi-Cu Phase diagram
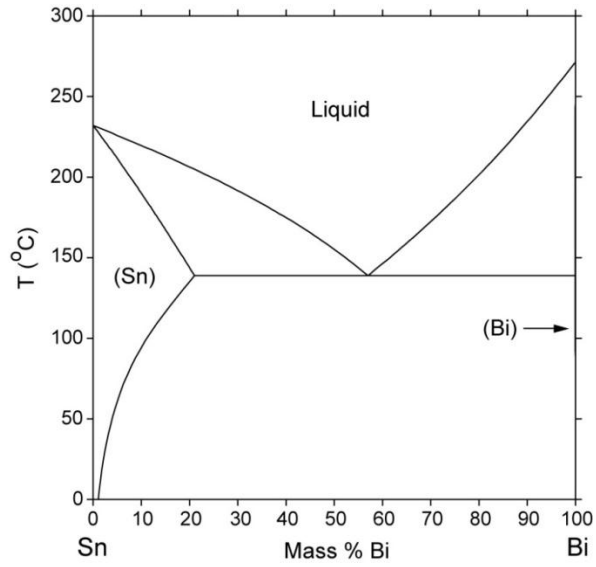
Fig.2.4 Bi-Sn Phase diagram
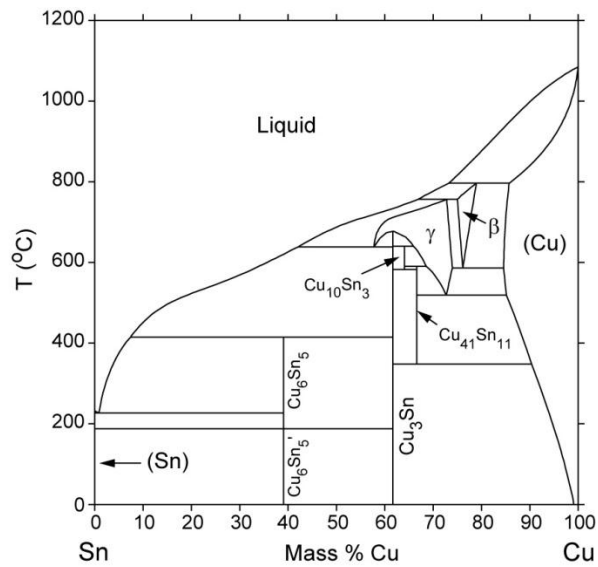
Fig.2.5 Cu-Sn binary phase diagram
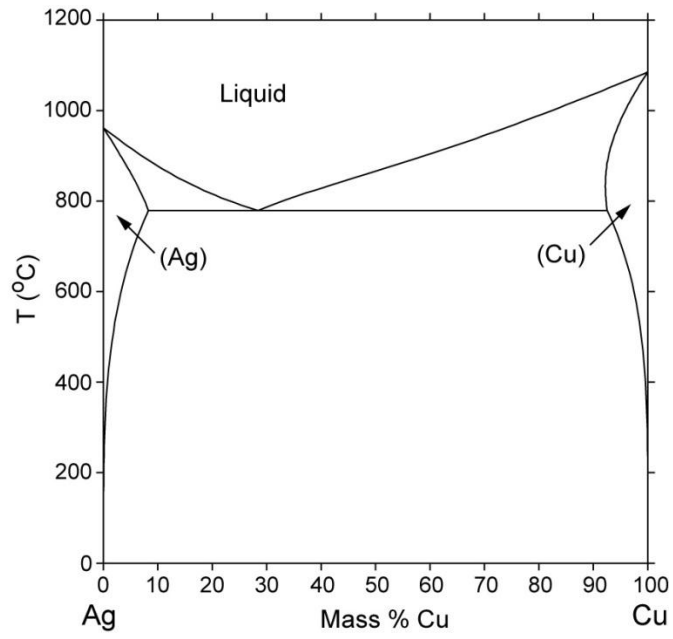
Fig.2.6 Cu-Ag binary phase diagram
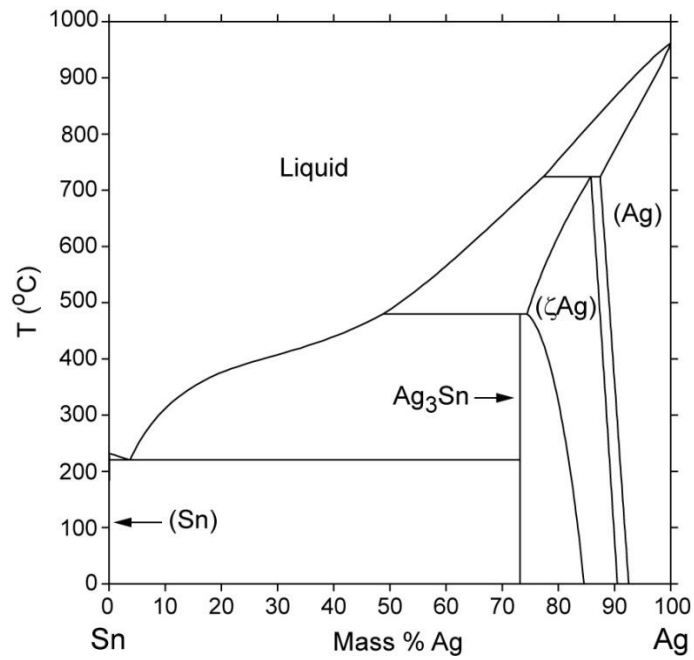
Fig.2.7 Ag-Sn binary phase diagram
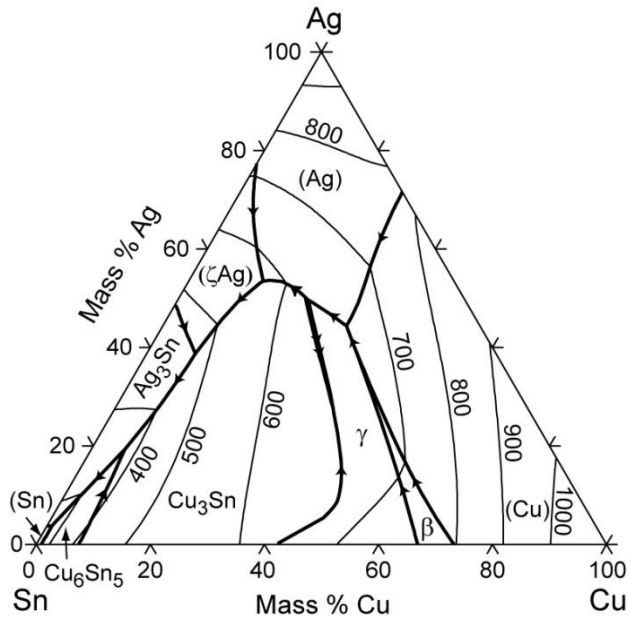
Fig.2.8 Liquidus projection of Sn-Ag-Cu ternary phase diagram
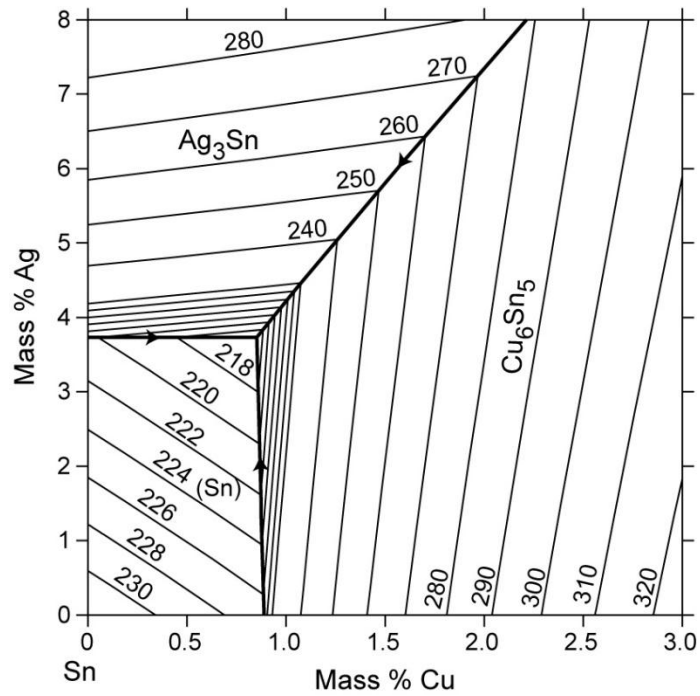
Fig 2.9 Sn-rich part of Sn-Ag-Cu ternary phase diagram

2.5   ALTERNATE SOLDER ALLOYS

Sn-Ag: 96.5Sn-3.5Ag.The melting temperature of this alloy is 221°C.   Wetting behaviour, as well as the strength of this alloy, is adequate to consider it as a solder alloy in the electronic packaging industry. When compared to Sn-Pb thermal fatigue of this alloy is also good. Damage due to thermal fatigue is found to be increased at elevated temperatures (Harad and Satoh, 1990). The solubility of Ag in the solder is limited in Sn-Ag system which results in better resistance to coarsening. Hence Sn-3.5 Ag has a uniformly distributed stable reliable microstructure. The diffusion of Cu in Sn will be more when this alloy is used to solder Cu base metals at higher temperature environments (Zhao et al., 2001).

Sn-Ag-Cu: This is a famous combination in solder alloys. Sn-4.0Ag-0.5Cu (Melting temperature 216-219°C) (Guo, 2001), Sn-3.8Ag-0.7Cu (Melting temperature 217-219°C) (Pang and Xiong, 2005), 95.0Sn-4.0Ag-1.0Cu (Melting temperature 216-219°C) (Zoran, 1998) and 93.6Sn-4.7Ag-1.7Cu;(Melting temperature 216-218°C) (Gayle et al., 2001) are widely accepted alloys. When exposed to elevated temperatures these alloys will withstand without melting whereas the Sn-Pb alloy (183°C) cannot be used (Kim et al., 2010). These alloys exhibit good wetting properties. The wetting property is increased when soldering is done in the Nitrogen atmosphere. The Cu dissolution rate of Sn-Ag-Cu is slower than Sn-Ag alloy. Corrosion damages were observed in the medical equipment assembled using this alloy.

Sn-Cu: Sn-0.7Cu has a melting temperature of 227°C. This alloy is a replacement in industries looking for silver-free and lead-free solder alloys. It is also suitable for automotive companies where temperature exposure is more. It also shows good resistance

to fatigue damage (Lee et al., 2002). Sn-Ag-Cu-Sb: Sn-2Ag-0.8Cu-0.5Sb has a melting temperature in the range of 217-220°C. This alloy is also known as Castin alloy. The properties of this alloy are almost similar to Sn-Ag-Cu alloy.

Sn-Ag-Bi: Sn-3.4Ag-4.8Bi (Melting temperature 200-216° C) is another lead-free solder alloy. Bismuth is added to the Sn-Ag alloy to reduce the melting temperature. The strength of the solder joint is also found to be improved with Bi addition. This alloy was developed by Sandia national labs. This alloy exhibits fatigue resistance. Sn-Bi: Sn-58bi is having a melting temperature of 138°C. The melting temperature is much lower. This alloy cannot be used in higher temperature exposed electronic packages. Little elasticity is another characteristic shown by this alloy.

Sn-Sb: Sn-5Sb solder alloy has a melting temperature of 232-240°C. Because of the high melting temperature, this alloy is suitable for high temperature applications. The strength and hardness of the alloy is enhanced due to the presence of Sb. Sb-Sn is an intermetallic compound formed that has a cubic structure. This IMC has high hardness. The wetting characteristics of this alloy are good when compared with Sn-Pb alloy. The tensile strength is reduced with the addition of more than 4% by wt. Sb.

Sn-Ag-Sb: Sn-25Ag-10Sb has a melting temperature of 230-235°C. This combination is also called as Motorola J alloy. This alloy exhibits better creep resistance. It was reported that this alloy is too strong that it may cause damage to the die. This is because of the presence of the large amount of Sb which leads to the formation of a large amount of intermetallic compound Sn-Sb. The greater strength of the alloy is due to the presence of Sb which makes the alloy stiff. The large amount of Sb results in very poor wetting. The amount of Ag (> 4% by wt.) is also a reason for poor wetting characteristics.

Sn-In: Sn-52In is another solder alloy with melting point 118°C. Because of the low melting temperature of the alloy, this is suitable only for low temperature applications. Good oxidation resistance is observed due to the presence of In. But in a humid environment, it is vulnerable to corrosion. Fatigue resistance at a higher temperature is very poor. This cannot be used everywhere because of the high cost and unavailability of Indium. Sn-In-Ag: Sn-20In-2.8Ag is another solder alloy with a melting temperature of 189°C. Binary low melting Sn-In phase (118°C) formed causes an adverse effect on the property of this alloy like poor thermal fatigue.

Sn-Zn: Sn-9Zn solder alloy has a melting temperature of 199°C. Corrosion and oxidation will be more due to the presence of Zn. This solder alloy reacts with alkalis and acids. Dross formation is more when wave soldering is done. Sn-Au: Sn-80Au is having a melting temperature of 280°C. Due to the limited availability of gold and the high cost, the usage is highly limited (Zoran, 1998).

Glazer (1994) reviewed the literature on the microstructure and mechanical properties of Sn-58Bi, Sn-52In, and Sn-3.5Ag alloys. Sn-Bi appears to have properties approaching those of eutectic Sn-Pb under most conditions, while eutectic Sn-In seems far inferior in most respects. Sharif and Chan (2004) in their work, investigation has been carried out to compare the dissolution kinetics of the Cu pad of the ball grid array (BGA) substrate into the molten conventional Sn–Pb solder and Sn–3.5Ag solder. Fundamental properties of lead-free solder alloys were discussed in detail by Handwerker et.al. (2007) in their book. WEEE directives (2000) laid down the rules which lead to the ban of lead in electronics package industries. Chang et.al. (2011) incorporated TiO_2 nanoparticles into Sn3.5Ag and Sn3.5Ag0.7Cu solder, to synthesize novel lead-free composite solders. Effects of the

TiO$_2$ nanoparticle addition on the microstructure, melting property, microhardness, and the interfacial reactions between Sn3.5AgXCu and Cu have been investigated. Hagler et.al. (2011) conducted studies on packaging technology for electronic applications in harsh high-temperature environments. Keller et al. (2011) investigated the mechanical stability of Pb-free SnAgCu solder connections in comparison to conventional eutectic SnPb. Salleh et.al. (2012) studied the mechanical properties of Sn–0.7Cu/Si$_3$N$_4$ lead-free composite solder in detail. Koo et al. (2014) made investigations on new Sn–0.7Cu-based solder alloys with minor alloying additions of Pd, Cr and Ca. Kotadia et al. (2014) published a detailed review on the development of low melting temperature Pb-free solders. Wang (2016) investigated the effect of Ag on the properties of solders and brazing filler metals. Gain and Zhang (2016) investigated the growth mechanism of the intermetallic compound and mechanical properties of nickel (Ni) nanoparticle doped low melting temperature tin–bismuth (Sn–Bi) solder. Cheng et al. (2017) discussed various elements of techniques in their detailed review of lead-free solder alloys in electronic applications.

Intermetallic Compounds: The long-term integrity of a solder joint very much counts on the intermetallic compounds that are formed during the soldering process. When soldered to copper or nickel, a formation of intermetallic compounds is necessary to achieve a good joint and their presence in the solder joint symbolize good wetting. However, if this layer becomes too thick the base metal or finish may be consumed by the solder and this leads to dewetting and poor joint reliability – more over some of the intermetallics are very brittle which decreases fatigue strength especially if this layer is thick. Intermetallic compounds continue to grow very slowly also at room temperature, but its also noted

29

that, under this condition they will not normally become thick enough to detrimentally influence the reliability of the joint. However, at elevated temperatures, when the time above the melting point during reflow is very long, the growth of an intermetallic layer will be very excessive and will very negatively influence the reliability of the solder joint. The melting points of intermetallic compounds (Cu_3Sn, Cu_6Sn_5, Ag_3Sn, Ni_3Sn_4, $AuSn$, $AuSn_2$, Ag_4Sn_4 etc.) gives an indication about the zone growth potential during room, or at working temperature . Rule of thumb: The lower the melting point, the larger the potential for growth The ductility and the firmness of the solder pad are negatively influenced by the excessive growth of intermetallic zones. The very low melting temperature of SnAu intermetallic compounds is consistent with fast gold dissolution into Sn containing alloys.

Based on the literature survey conducted, it can be concluded that the replacement of Sn-Pb alloy by a new one is not fully done in the industry. SAC305 and SAC405 are presently good, but limitations still exist. The high silver content adds the cost. Both the solder alloys are protected by high patent cost. The corrosion properties of these alloys are also not the best. Therefore there is still a room for a new lead free solder alloy alternative. In this project, lead free solder alloys with a combination of the following properties is aimed to synthesis. Low melting point, high hardness and strength, low contact angle, high corrosion resistance. This combination of properties are possible to synthesise using Sn, Cu, Bi, Ni and Ag.

CHAPTER 3

MATERIALS AND METHODS

3.1   MELTING TEMPERATURE ASSESSMENT

Melting temperature is an important characteristic property as far as lead-free solder joints are concerned. Preference will be more for a low melting temperature alloy. Melting temperature assessment of all samples in this work was conducted using TG-DTA. Thermo Gravimetric analysis (TGA) converts the weight gain or loss as a function of temperature; it can be dealing with the derivative of TGA concerning to time or temperature or time. Differential thermal analysis (DTA) is a method for noting down the temperature difference between a material and a reference material as a function of time or temperature. The two specimens are exposed to identical temperature regimes in an environment that is heated or cooled at a controlled rate. This analysis is performed at Sophisticated Test and Instrumentation Centre (STIC), CUSAT.
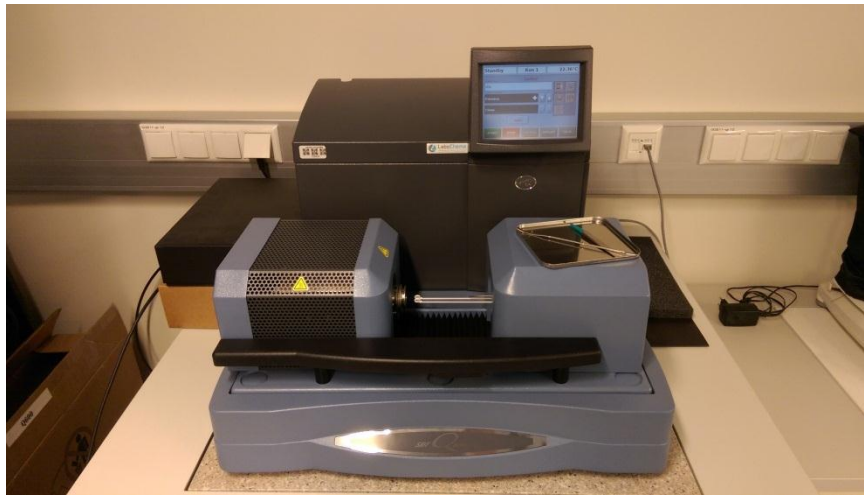
Fig. 3.1 Thermo Gravimetric and Differential Thermal analysis (TG-DTA) set up
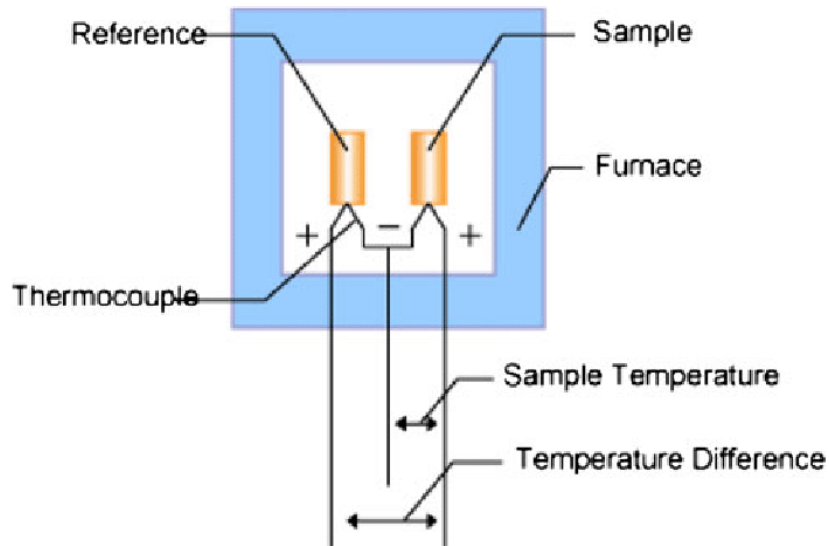
Fig. 3.2 Diagram of Thermo Gravimetric and Differential Thermal analysis (TG-DTA)

3.2   HARDNESS MEASUREMENT

Resistance to indentation of a material is known as the hardness of that material. It is a mechanical technique that involves the application of load (through indenter) onto the surface of the sample. Hardness tests were performed on the samples using HMV-G micro Vickers hardness tester. This measurement is done at Cochin Shipyard central laboratory, Kochi. Each Hv value of the sample is the average of ten different readings which were taken at random areas on the surface. For hardness tests to be performed on the sample, the surface should be smooth. Sample preparation was done using grinding by taking different grades of SiC papers. The samples were then polished on a polishing machine. The surfaces of the alloys were analysed in Axio vertical A1 metallurgical microscope before and after the microhardness test.

$$Hv = \frac{1.8544\,F}{d^2} \qquad\qquad (3.1)$$

Where F is the applied force and d is the diameter of the indentation.

Fig. 3.3 HMV-G micro Vickers hardness tester

3.3   CONTACT ANGLE MEASUREMENT

The capacity of molten solder to react with the bottom substrate is referred to as wetting. It forms a certain amount of intermetallic compound that acts as an adhesion layer to join the solder and the substrate (Ervina et al., 2010). The reaction between the solder and substrate is vital as it affects micro structure properties. It will also affect the mechanical strength of the solder joint. Sessile drop technique is used for the evaluation of the contact angle (wettability). There is a transparent silica work tube in this analysis set up. The tube is kept vertically inside a resistance furnace. this set up has a vacuum unit. There are two observation windows at the middle of the furnace. A crucible is required which is a ceramic tube with 1mm diameter drilled at one end. It is kept at the center-line of the silica tube. The alloy melted in the ceramic tube is permitted to fall on the substrate with the aid of gas pressure. A fast mode camera is placed in front of the observation window to capture the image of the droplet. Generally, if the wetting or contact angle lies

between 0° and 90° the system is said to be wet. If the wetting or contact angle is between 90° and 180° the system is considered to be non-wetting.

In more detail if $0° < \theta < 30°$it is considered as very good wetting,

if $30° < \theta < 40°$ it is considered as good wetting,

if $40° < \theta < 55°$ it is considered as acceptable wetting,

if $55° < \theta < 70°$ it is considered as poor wetting and

$\theta > 70°$ is considered as very poor wetting,

Where θ is the contact angle.
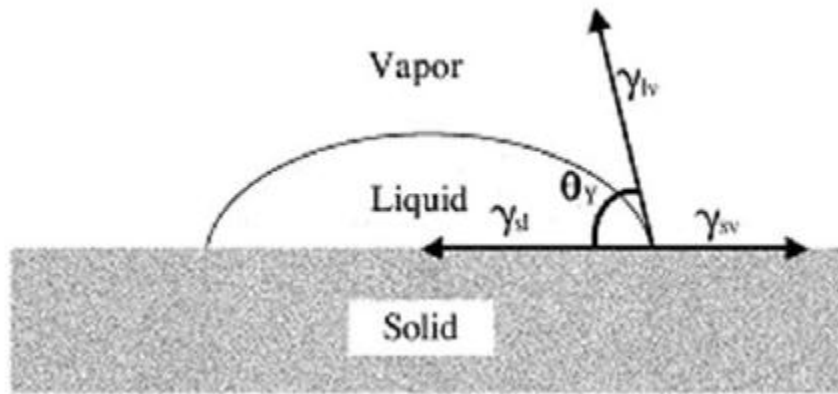
Fig. 3.4 Contact angle measurement with the sessile drop method.

The various forces occurred are linked together according to Young's equation:

$$\gamma_{sy} = \gamma_{sl} + \gamma_{lv}cos\theta \hspace{5cm} (3.2)$$

Where, γ_{sy}, γ_{sl} and γ_{lv} represent the "surface tensions" of the interface solid/gas, solid/liquid and liquid/gas, respectively, and θ represents the contact angle.

3.4 CHEMICAL COMPOSITION ASSESSMENT

Chemical compositions of the alloys were analyzed using ICP-OES (Inductively coupled plasma - optical emission spectrometry) (Krachler et al., 2016). This is one method of optical emission spectrometry. ICP- OES (Figure 3.5 and 3.6) is evaluated as a multipurpose analysis method. The elements (atoms) in the components are excited using plasma energy which is given to the specimens from outside. After excitation, excited atoms come back to the low energy position. Spectrum rays are released in the course of time. The emission rays equivalent to the photon wavelength is recorded. The element type is determined from the position of photon rays. The content of each element is confirmed using the rays' intensity obtained. The next step is the production of plasma. Torch coil is provided with argon gas and the work coil is supplied with high frequency electric current (tip of the torch tube). An electromagnetic field is created in the torch tube due to the high-frequency current applied. Plasma is generated which is followed by the ionization of gas. The generated plasma has high electron density as well as high temperature (10000 K). Using this energy, excitation energy of the specimen is done. The specimens are introduced into the plasma in an atomized state through the narrow tube in the center of the torch tube. This analysis is performed at Sophisticated Test and Instrumentation Centre (STIC), CUSAT.
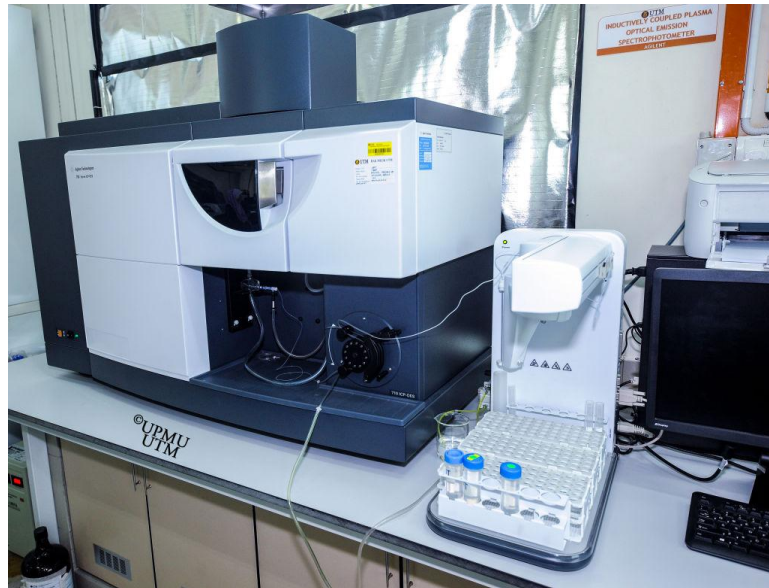
Fig. 3.5 ICP-OES apparatus
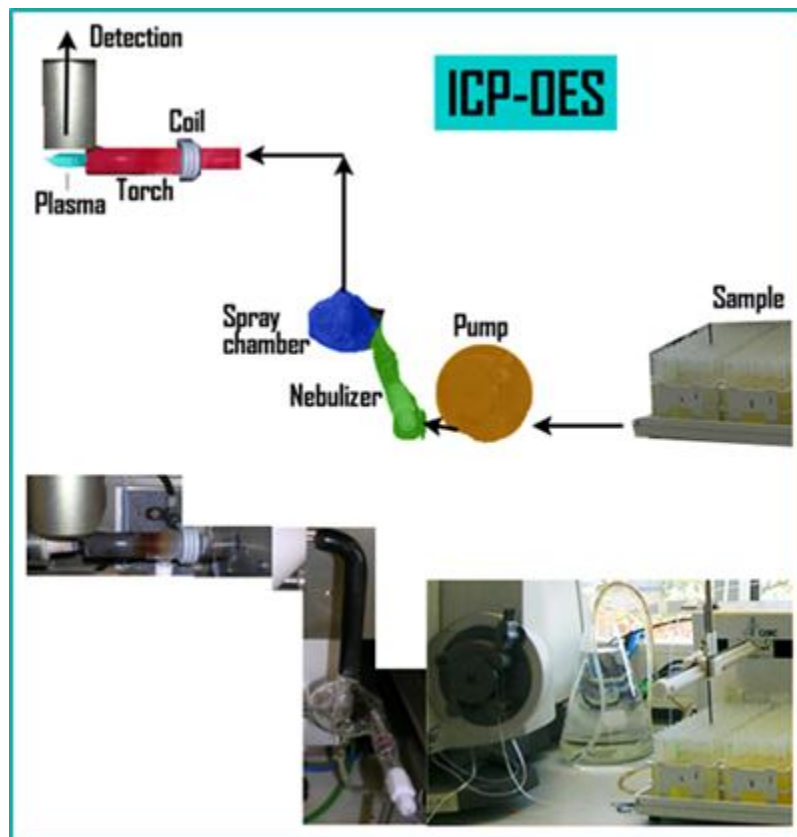
Fig. 3.6 Principle of ICP-OES apparatus

3.5   MICROSTRUCTURE ANALYSIS

The surface details of the samples were examined by field-emission scanning electron microscopy (FE-SEM, Carl Zeiss Sigma). FESEM can be considered as a microscope working with electrons (negative charge particles) instead of light. A field emission source is used to liberate these electrons. The sample is scanned in a zig-zag pattern by electrons. The topographic details of the entire samples' surface can be obtained for visualization. Observations as small as 1nm (1 billionth of mm) is obtained using FE SEM. The electrons proceed from a field emission source which is accelerated in a high electric field gradient. The primary electrons inside the high vacuum column are focused and the electrons are deflected using electronic lenses. As a result, a narrow scan beam is generated which will bombard on to the object. The bombardment causes the emission of secondary electrons from each spot of the object. The angle and velocity of these secondary electrons is equivalent to the surface structure of the object. The detector absorbs the secondary electrons and electronic signals are produced and generated electronic signals are amplified and a scanned image is created. These images are analyzed in the monitor and can be saved for future analysis. All the images were taken at a magnification of $5.00 - 100KX$, scale = $1\mu m$, Electron High Tension (EHT) = 5.00 KV, Working Distance (WD) = 3.2 mm. This analysis is performed on FE-SEM set up (Figure 3.7) available at physics department, CUSAT.

Fig. 3.7 FE SEM analysis set up

3.6 SHEAR STRENGTH ANALYSIS

A shear load is a force that tends to produce a sliding failure on a material along a plane which is parallel to the direction of the force. The solder alloys should be strong in shear strength. Samples were made ready for the shear strength analysis following the sample specimen-making procedure. Five samples of each alloy were tested in a similar condition. For the shear test to be conducted, micro lap shear solder joint samples were made. The same is shown schematically in the figure 3.8. The amount of shear on the specimen is measured and the specimen is loaded in the apparatus between the grips. Force is applied at a controlled rate to the specimen until it breaks. The maximum force is

noted down. All the five sample set were ground using SiC paper, followed by polishing to remove any excess solder at the edges. Micro-force test system was used to conduct the shear strength test, the system is controlled by software and test data are collected. The shear strength tests were conducted on the five samples at room temperature. 5×10^{-4}/s is the strain rate used. The results were averaged among the five data.
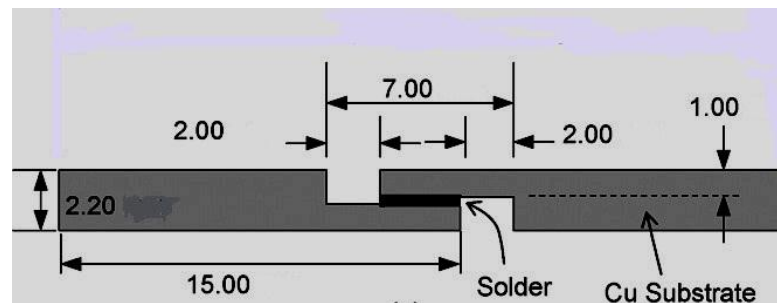
Fig. 3.8 Shear strength test specimen

3.7 IMPACT TOUGHNESS TEST

The ability of a material to absorb the impact energy and plastically deform without failure is known as impact toughness. To conduct the impact test, Charpy impact tests with pendulum-type impact tester were used. The pendulum effective weight was 21 Kg. Five specimens of each alloy are prepared with dimensions 70mm long x 5mm wide x 5mm thick. The schematic diagram provided in the figure 3.9 shows the analysis set up (Charpy impact test). The pendulum is lifted to a height H. This is considered as the initial position. E1 is the initial potential energy. Then the pendulum is allowed to swing and hit the specimen. After hitting the specimen it rises to a height of h. E2 is the energy at this stage and it is considered as the final energy. During hitting the specimen, some amount of energy E is absorbed by the specimen. The impact absorbed energy was obtained. The same procedure is repeated for all the five samples. The test data obtained

is then averaged. The data regarding the absorbed energy obtained during the test helps in analyzing the impact toughness of the alloys.
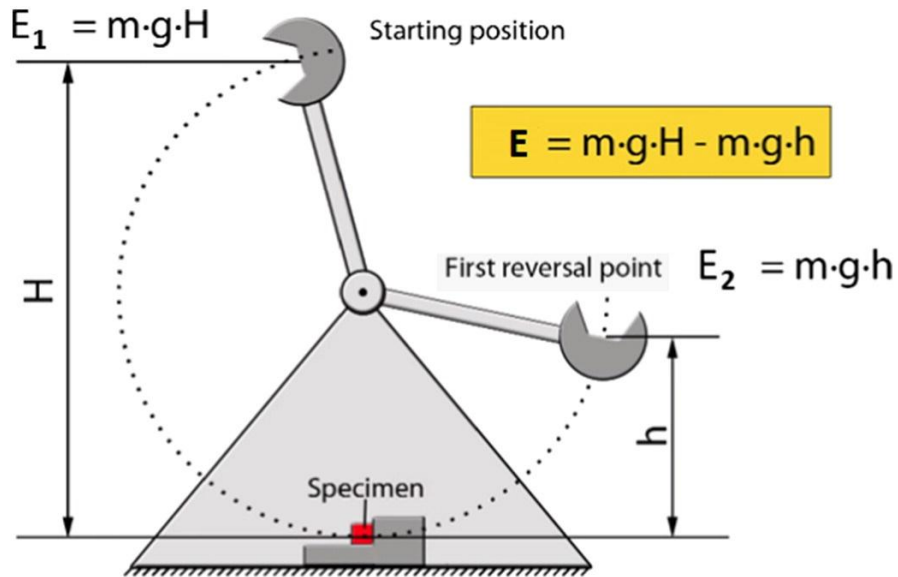
Fig. 3.9 Impact test principle

3.8   MATERIALS AND SUPPLIER

The materials required for this work are Sn, Cu, Bi, Ni and Ag. These materials and the supplier are shown in the table 3.1.

Table 3.1 Materials and supplier

Sl No.	Material	Supplier
1	Tin (Sn)	Merck
2	Copper (Cu)	Loba chemie
3	Bismuth (Bi)	Loba chemie
4	Nickel (Ni)	Rankem
5	Silver (Ag)	Rankem, RFCL Limited

3.9 SAMPLE PREPARATION

Samples are prepared from the pure metals which were in powder form. Composition of the alloys required taken in adequate quantities.. Sn, Cu and Bi in the powder form were weighed in the required weight proportions using sensitive weighing machine. Five specimens are made using induction furnace with Argon gas (inert gas to avoid unwanted oxidations). The samples were melted in induction furnace at more than 1000°C for 45 minutes and the poured to cylindrical moulds of diameter 5 cm. Quenching process in done for all these alloys by making use of the annealing furnace. The solder alloys were melted and maintained 100 ° C above their melting point for 20 minutes in Argon atmosphere. Then the specimen was quenched in water which was at 24 ° C. This is done to maintain good mechanical properties. This is the quenching cycle implemented for this experiment. The samples were kept in the room temperature for two days to completely relieve the stresses. Argon gas is used in the process as the inert gas which will avoid the unwanted oxide formations. All the five alloys were undergone visual inspection of the surface and accepted.

3.10 DESIGN OF EXPERIMENTS

Design of experiments is a methodology proposed by Robert Fischer in 1935. This methodology is used to design any job that plans to explain the variations under conditions. There are hypothesis to reflect such variations (Fischer, 1949). The change in one or more independent variables is generally hypothesized to result in a change in one or more dependent variables. The method also identifies control variables that must be kept constant, to avoid the external factors to affect the results. The main concerns in the

DoE are the reliability, replicability and validity (Hicks and Charles, 1964). In this work, with the aid of design of experiments, the optimum composition of new lead free solder alloy is predicted. This new composition contains Sn, Cu, Bi and Ni.

3.10.1 Full factorial Design

Full factorial and fractional factorial designs at 2 and 3 levels are the most commonly used experiments designs in the manufacturing industry field. Factorial designs help the researcher to analyse the joint effect of the design or process parameters on an output or response. A factorial design can be full factorial or fractional factorial. This chapter discusses the full factorial design at level 2. When the number of process parameters is less than or equal to 4, full factorial design is a good choice. This is done at early stage of experiment work. For studying k factors at 2 levels, number of experiments required is 2^k. The response is almost linear over the range of the factor settings selected. It is one of the assumptions in this analysis. In factorial regression, there are more possible combinations of distinct levels for the continuous predictor variables than there are cases in the data set. To simplify matters, full-factorial regression designs are defined as designs in which all possible products of the continuous predictor variables are represented in the design.

Regression models points out the relationship between a set of predictor variables (x's) and one or more responses (y's). Most often, the model or the equation is of the linear form.

$$E(y) = \beta_0 + \beta_1 x_1 + \beta_2 x_2 + \dots \dots \dots \dots \dots \dots \dots + \beta_p x_p \qquad (4.1)$$

Where, β is the coefficient to be estimated from the data.

If X is the (n x p) matrix of predictor variables related with n observations, then regression model can be written as:

$$E(Y) = X\beta \tag{4.2}$$

Where Y is the (n x 1) vector of responses and β is the (p x 1) vector of regression coefficients. Equation (4.1) is a model linear in the parameters (Ronald, 1977).

The aim of this section is to find a new lead free solder alloy with Tin (Sn), Copper (Cu) and Bismuth (Bi). The Sn is considered to be the base metal. Small amount of Cu and Bi is added to make the required alloy. With the addition of Cu and Bi, the melting temperature and contact angle is expected to be decreased. The hardness of the alloy is expected to be increased. This analysis has to be done prior to our experiments. An optimum composition of Cu and Bi is studied and tried to predict so that the melting point and contact angle is lower. This alloy should exhibit good hardness properties.

CHAPTER 4

DEVELOPMENT OF TWO NEW NOVEL LEAD FREE

SOLDER ALLOYS

Two novel lead free alloys with new composition are developed, i.e. Sn-0.5Cu-3Bi (SCB 305) and Sn-1Cu-1Ni (SCN110). The composition of SCB305 is 0.5 % Cu, 3% Bi and rest Sn (by wt.) The composition of SCN110 is 1% Cu, 1%Ni and rest Sn (by wt.).Design of experiments is conducted at the initial stage in the alloy development, from which the percentage by weight of Cu, Bi and Ni are confirmed.

4.1   DEVELOPMENT OF Sn-Cu-Bi SOLDER ALLOY

4.1.1   Results of DOE

The experiment was run with two factors (F), which is Cu & Bi composition and two levels (L), which is 0.5 and 1 for Cu, 3 and 4 for Bi. The composition is expressed in % by wt. 8 runs were conducted with 2 replications, as per the formula: (L^F), $(2^2) = 4 \times 2$ replications $= 8$. Three responses were recorded as output out of each run, Melting temperature, Contact Angle & Hardness. It is shown in the table 4.1.

Table 4.1 Output from the eight runs conducted

Experiment Runs	Factors		Response		
	Cu %	Bi %	Melting Temp(°C)	Contact angle (°)	Hardness (Hv)
1	0.5	4	245.35	33.25	14.5
2	0.5	3	231.15	28.74	19.8

3	0.5	3	231.25	28.82	19.7
4	1	3	243.12	42.22	12.3
5	1	4	238.12	43.12	11.7
6	1	3	243.41	42.3	12.8
7	1	4	238.68	43.5	11.3
8	0.5	4	246.1	32.91	14.65

Eight runs were conducted with Cu varying from 0.5 and 1% by wt. Bi varying from 3 % and 4% by wt. With Cu 0.5% by wt. and Bi 1% by wt., the melting point, contact angle and hardness can be seen as the optimum value. The aim which is specified is to minimize melting temperature and contact angle and increasing the hardness value.

4.1.2 Factorial Regression: Melting Temperature versus Cu, Bi

Factorial regression of melting temperature versus Cu and Bi were conducted. The analysis of variance is shown in the table 4.2. The model summary is tabulated in the table 4.3. The coded coefficients details are shown in the table 4.4

Table 4.2 Analysis of variance for Melting Temperature versus Cu, Bi

Source	DF	Adj SS	Adj MS	F-Value	P-Value
Model	3	245.878	81.959	675.81	0
Linear	2	57.892	28.946	238.68	0
Cu	1	11.234	11.234	92.63	0.001
Bi	1	46.658	46.658	384.73	0
2-Way Interactions	1	187.986	187.986	1550.08	0
Cu*Bi	1	187.986	187.986	1550.08	0
Error	4	0.485	0.121		
Total	7	246.363			

Table 4.3 Model summary for Melting Temperature versus Cu, Bi

S	R-sq.	R-sq. (adj)	R-sq. (pred)
0.348246	99.80%	99.66%	99.21%

Table 4.4 Coded coefficients for Melting Temperature versus Cu, Bi

Term	Effect	Coef.	SE Coef.	T-Value	p-Value	VIF
Constant		239.648	0.123	1946.4	0	
Cu	2.37	1.185	0.123	9.62	0.001	1
Bi	4.83	2.415	0.123	19.61	0	1
Cu*Bi	-9.695	-4.847	0.123	-39.37	0	1

Regression Equation in Uncoded Units for the range of Cu (0.5 and 1%) and Bi(3 and 4% by wt.) is given by:

$$Melting\ temperature = 117.39 + 140.47Cu + 33.915\ Bi - 38.78\ Cu * Bi \quad (4.4)$$

The p value from table 4.4 signals about the significance of the variables. The R-sq (pred) is found to be 99.21%

4.1.3 Factorial Regression: Contact angle versus Cu, Bi

Factorial regression of contact angle versus Cu and Bi were conducted. The analysis of variance is shown in the table 4.5. The model summary is tabulated in the table 4.6. The coded coefficients details are shown in the table 4.7.

Table 4.5 Analysis of variance for Contact angle versus Cu, Bi

Source	DF	Adj SS	Adj MS	F-Value	P-Value
Model	3	300.675	100.225	2939.15	0
Linear	2	295.393	147.697	4331.28	0
Cu	1	281.082	281.082	8242.88	0

Bi	1	14.311	14.311	419.68	0
2-Way Interactions	1	5.281	5.281	154.88	0
Cu*Bi	1	5.281	5.281	154.88	0
Error	4	0.136	0.034		
Total	7	300.811			

Table 4.6 Model summary for Contact angle versus Cu, Bi

S	R-sq.	R-sq. (adj)	R-sq. (pred)
0.184662	99.95%	99.92%	99.82%

Table 4.7 Coded coefficients for Contact angle versus Cu, Bi

Term	Effect	Coef	SE Coef	T-Value	p-Value	VIF
Constant		36.8575	0.0653	564.54	0	
Cu	11.855	5.9275	0.0653	90.79	0	1
Bi	2.675	1.3375	0.0653	20.49	0	1
Cu*Bi	-1.625	-0.8125	0.0653	-12.44	0	1

Regression Equation is represented by:

$$Contact\ Angle = -7.35 + 46.46\ Cu + 7.55\ Bi - 6.5 Cu * Bi \qquad (4.5)$$

4.1.4   Factorial Regression: Hardness versus Cu, Bi

Factorial regression of hardness versus Cu and Bi were conducted. The analysis of variance is shown in the table 4.8. The model summary is tabulated in the table 4.9. The coded coefficients details are shown in the table 4.10.

Table 4.8 Analysis of variance for Hardness versus Cu, Bi

Source	DF	Adj SS	Adj MS	F-Value	P-Value
Model	3	80.6709	26.8903	486.15	0
Linear	2	72.1631	36.0816	652.32	0

47

Cu	1	52.7878	52.7878	954.36	0
Bi	1	19.3753	19.3753	350.29	0
2-Way Interactions	1	8.5078	8.5078	153.81	0
Cu*Bi	1	8.5078	8.5078	153.81	0
Error	4	0.2212	0.0553		
Total	7	80.8922			

Table 4.9 Model summary for Hardness versus Cu, Bi

S	R-sq.	R-sq. (adj)	R-sq. (pred)
0.234186	99.73%	99.52%	98.91%

Table 4.10 Coded coefficients for Hardness (Hv) versus Cu, Bi

Term	Effect	Coef	SE Coef	T-Value	p-Value	VIF
Constant		14.5937	0.0832	175.51	0	
Cu	-5.1375	-2.5688	0.0832	-30.89	0	1
Bi	-2.1125	-1.5562	0.0832	-18.72	0	1
Cu*Bi	2.0625	1.0312	0.0832	12.4	0	1

Regression Equation is given by

$$Hardness = 54.85 - 39.15Cu - 9.3Bi + 8.25\ Cu * Bi \tag{4.6}$$

4.1.5   Response Optimization: Hardness, Contact angle, Melting Temperature

The optimized response from the analysis is shown in the table 11 and table 12. The prediction of the optimized composition is shown in the table 13. It can be found that the composition of Cu is 0.5% and of Bi is 3% by wt.

Table 4.11 Parameters: Hardness, Contact angle, Melting Temp(C)

Response	Goal	Lower	Target	Upper	Weight	Importance
Hardness	Maximum	11.3	19.8		1	1
Contact Angle	Minimum		28.74	43.5	1	1
Melting temperature	Minimum		231.15	246.1	1	1

Table 4.12 Solution

Solution	Cu	Bi	Hardness fit	Contact Angle fit	Melting Temperature fit	Composite Desirability
1	0.5	3	19.75	28.78	231.2	0.99602

Table 4.13 Multiple response prediction

Variable	Setting
Cu	0.5
Bi	3

Table 4.14 Best fit model

Response	Fit	SE Fit	95%CI	95% PI
Hardness	19.75	0.166	(19.288, 20.212)	(18.950, 20.550)
Contact Angle	28.78	0.131	(28.417, 29.143)	(28.152, 29.408)
Melting temperature	231.2	0.246	(230.516, 231.884)	(230.016, 232.384)

4.1.6 Main effects plots

The mean response of the level factors can be represented in the main effect plots. This is done by connections made by the lines. It can be interpreted that there is no main effect if horizontal line is present in the diagram. Little deflection from the horizontal direction means that it will significantly affect the response. Lines with higher slope give the information that the magnitude of the main effect is higher. The effect can be defined as the variations in melting temperature, hardness and the contact angle when the factor changes from one level to another level. Calculations are done at minimum and maximum values of each factor (Bharath, 2019). The information about the direction of the effect (i.e. Increase or decrease in the average response value) is obtained from the sign of the main effect plot. The strength of the effect is obtained from the magnitude (Jiju, 2014). The main effect diagrams give vital information about the information about the factor influence in the properties such as melting temperature, hardness and the contact angle of SCB305. The main effect plots for melting temperature, hardness and contact angle is given in the figure 4.1, figure 4.2 and figure 4.3.
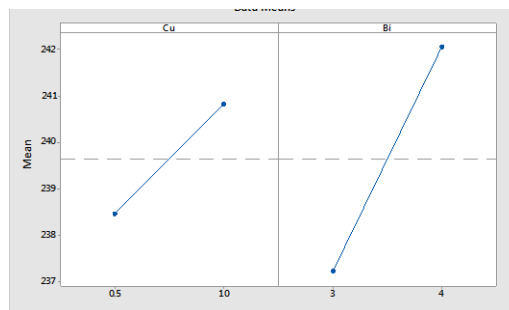
Figure 4.1 Main effects plot for melting temperature
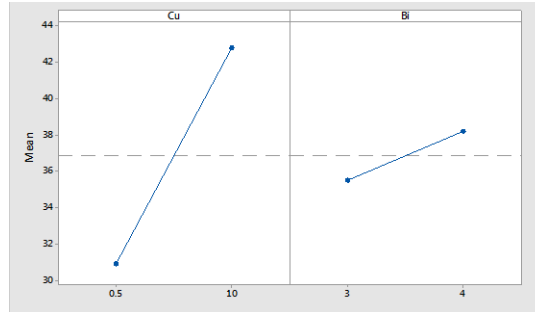
Figure 4.2 Main effect plot for contact angle
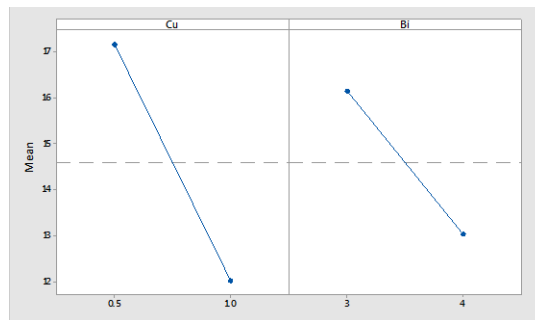
Figure 4.3 Main effect diagram for hardness

4.1.7   Interaction plots

The behaviour of one variable which is depending on the value of another variable is better understood by interaction plots. An interaction plot displays the levels of one variable on the X axis and has a separate line for the means of each level of the other variable. The Y axis is the dependent variable. The interaction effects are analyzed in the regression analysis, ANOVA and DOE. The influence of one factor and a continuous response with the value of the second factor can be identified from the interaction plots (Geshev, 2018). The lines in the diagram can be used to interpret how the relation between the factor and the response are affected. If there are parallel lines, it means that there is no interaction. Non-parallel lines in the diagram interprets that there is interaction

occurring. The strength of the interaction is proportional to number of non-parallel lines. Interaction plot for hardness, contact angle and melting temperature is shown in the figure 4.4, figure 4.5 and figure 4.6. It can be interpreted that the influence of these factors are present.
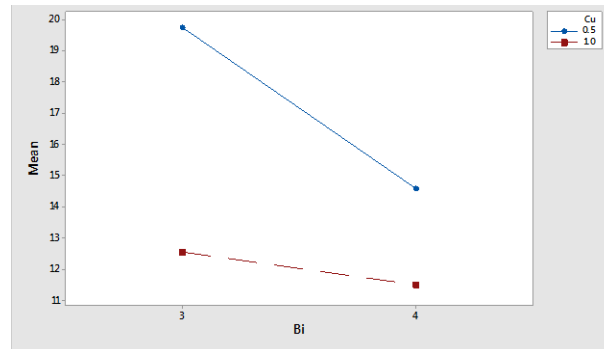
Figure 4.4 Interaction plot for hardness
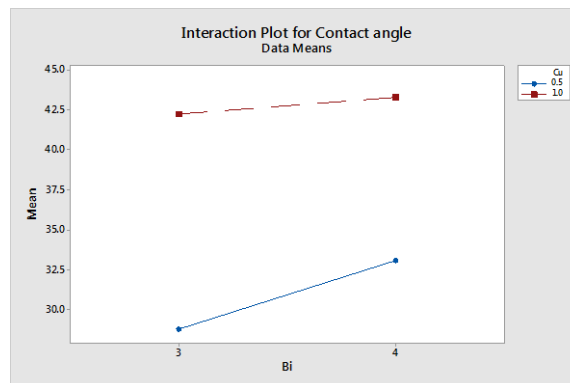
Figure 4.5 Interaction plot for contact angle
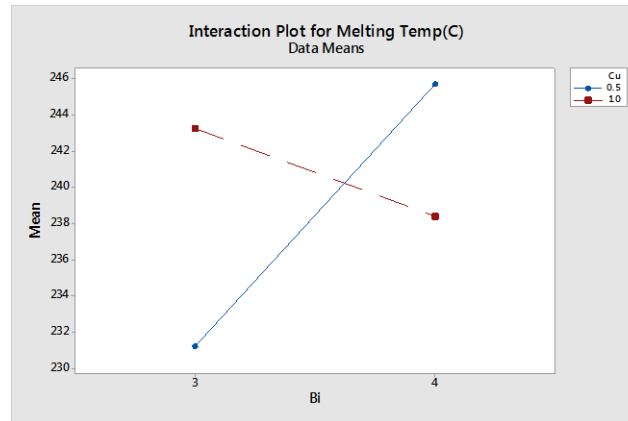
Figure 4.6 Interaction plot for melting temperature

This part of the work, using design of experiments (DoE) checks the use of Sn, Cu and Bi to make a new lead free solder alloy. By design experiments it has been found that, the selected parameters are the most impacting factors for response. The ANOVA evidently shows with its P- values having less than 0.05 that Cu and Bi composition in the alloy is having significant impact in the melting temperature, contact angle and hardness. The R square values of the regression equation is calculated to be more than 95% which denotes that model is best and convey us that there are no other factors impacting the factors. The same can be seen graphically in the Mean effects plot. The Interaction plot shows the interaction between the Cu & Bi with the factors. From the results of Design of Experiments we can infer that Cu-0.5% and Bi-3% (by wt.) is the best optimized composition for the new solder alloy. Therefore Sn-0.5Cu-3Bi will be an optimum composition of the new lead free solder alloy.

4.2   DEVELOPMENT OF SCB 305

After Design of Experiments, Sn-0.5Cu-3Bi (0.5% Cu, 3 % Bi by wt. and remaining Sn) is developed as a new lead free solder alloy.

Table 4.15 The chemical composition required for SCB305

Solder alloy	Sn (%)	Cu (%)	Bi (%)	Ni (%)
SCB305	96.5	0.5	3	0

4.2.1 Properties of SCB305 alloy

4.2.1.1 Chemical Composition results

The required composition of the alloy is shown in table 4.15. Chemical compositions of the alloys were analysed using ICP-OES. The results of the analysis are shown in the table 4.16. Composition results of all the five alloy samples are listed. From this list of alloys, one alloy is selected for further investigations.

Table 4.16 Chemical Composition results

Solder alloy	Sn (%)	Cu (%)	Bi (%)
SCB305 Sample 1	96.3967	0.4865	3.1098
SCB305 Sample 2	96.5101	0.4976	2.9834
SCB305 Sample 3	96.5155	0.5011	2.9783
SCB305 Sample 4	96.3843	0.5122	3.0945
SCB305 Sample 5	96.3406	0.4876	3.1701

4.2.1.2 Melting temperature

Melting temperature is one of the main characteristic properties as far as a solder alloy is concerned. A solder alloy with good properties but of higher melting temperature is not

accepted, because the high temperature may damage the electronic package. A low melting alloy with narrow pasty solder range can be considered as desired property for a good solder alloy. Analysis for SCB305 was conducted using Thermo Gravimetric and Differential Thermal analysis (TG-DTA). Thermo Gravimetric analysis (TGA) measured the weight loss or gain as a function of temperature ,the TGA trace appear as steps, it can be deal with the derivative of TGA with respect to time or temperature. Differential thermal analysis (DTA) is a technique for recording the difference in temperature between a substance and a reference material as a function of time or temperature as the two specimens are subjected to identical temperature regimes in an environment heated or cooled at a controlled rate. Melting temperature of the new alloy SCB305 (231.15±0.07) is shown in the table 4.17.

Table 4.17 Melting temperature results of SCB305

Solder alloy	Melting temperature (° C)
SCB305 Sample 1	231.15
SCB305 Sample 2	231.25
SCB305 Sample 3	231.1
SCB305 Sample 4	231.24
SCB305 Sample 5	231.05
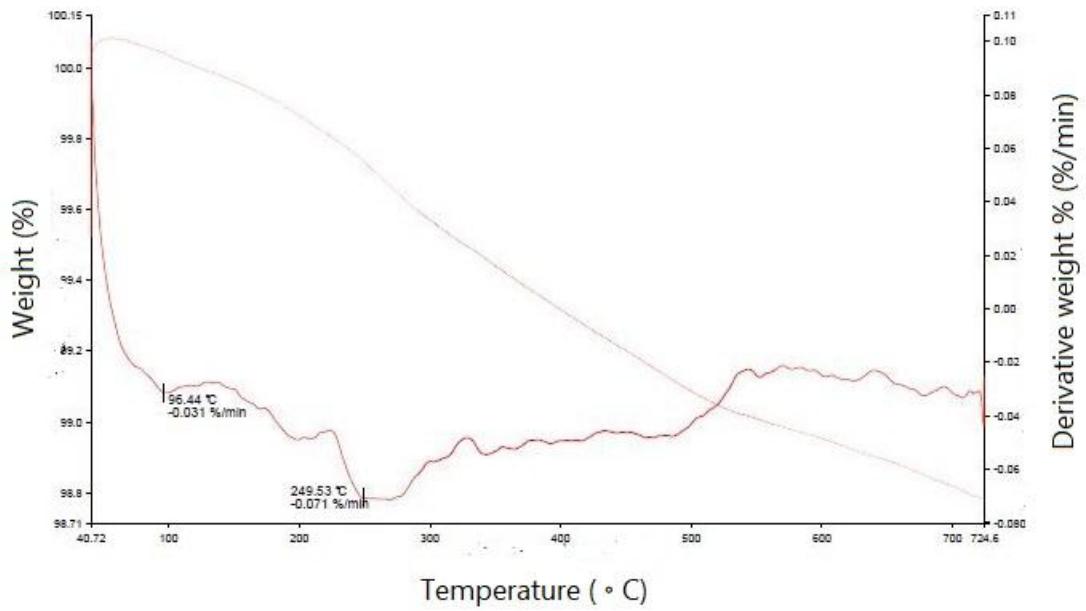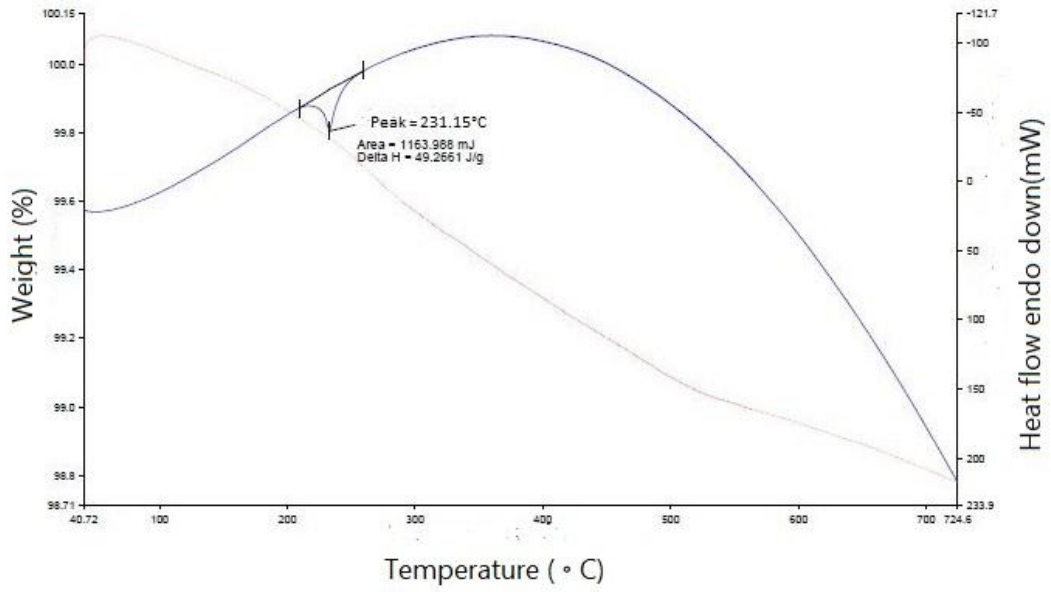
Figure 4.7 DTA and TGA results of SCB305

4.2.1.3 Contact angle and hardness

Contact angle measured for SCB305 are shown in the table 4.18. The presence of Bi has enhanced the wetting property of Sn-Cu. Solder wettability is found to be enhanced with the presence of Bi in SCB305. The presence Bi in the alloy strengthens the solder alloy. Contact angle of SCB305 is less than 30°. Therefore it is exhibiting very good wetting property(28.74 ±0.08)

Table 4.18 Contact angle measurement results

Solder alloy	Contact angle (°)
SCB305 Sample 1	28.76
SCB305 Sample 2	28.84
SCB305 Sample 3	28.85
SCB305 Sample 4	28.7
SCB305 Sample 5	28.82
SCB305 Sample 6	28.65
SCB305 Sample 7	28.76
SCB305 Sample 8	28.55
SCB305 Sample 9	28.73
SCB305 Sample 10	28.76
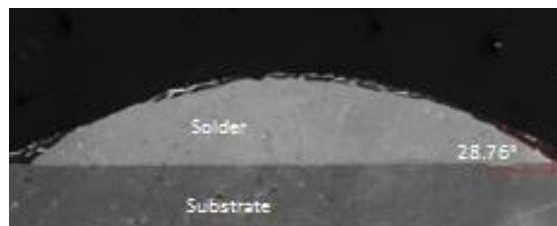
Figure 4.8 Contact angle measurement of SCB305 sample

Hardness values measured for SCB305 are shown in the table 4.19. Good hardness values (19.81 ± 0.13) are obtained for SCB305 solder alloys.

Table 4.19 Hardness measurement results

Solder alloy	Hardness (Hv)
SCB305 Sample 1	19.8
SCB305 Sample 2	19.9
SCB305 Sample 3	19.7
SCB305 Sample 4	19.5
SCB305 Sample 5	19.8
SCB305 Sample 6	19.9
SCB305 Sample 7	19.8
SCB305 Sample 8	20
SCB305 Sample 9	19.9
SCB305 Sample 10	19.9

4.3 DEVELOPMENT OF Sn-Cu-Ni ALLOY

Sn-1Cu-1Ni (1% Cu, 1% Ni by wt. and rest Sn) is developed as a new lead free solder alloy. This new solder alloy will be termed as SCN110 hereafter. The aim of this section is to find a new lead free solder alloy with Sn, Cu and Ni. The Sn is considered to be the base metal. Small amount of Cu and Ni is added to make the required alloy. With the addition of Cu and Ni, the melting temperature and contact angle is expected to be decreased. The hardness of the alloy is expected to be increased beacuase of the addition of Ni . This analysis has to be done prior to our experiments. An optimum composition of Cu and Ni is studied and tried to predict so that the melting point and contact angle is lower.

4.3.1 Design of Experiments

The experiment was run with two factors (F), which is Cu & Ni composition and two levels (L), which is 0.5 and 1 for Cu, 0.5 and 1 for Ni. The composition is expressed in % by wt. 8 runs were conducted with 2 replications, as per the formula :$(L)^F$, $(2)^2 = 4 \times 2$ replications = 8. Three responses were recorded as output out of each run, Melting temperature, Contact Angle & Hardness. It is shown in the table 4.20.

Table 4.20 Output from the eight runs conducted

Experiment Runs	Cu (% by wt.)	Ni (% by wt.)	Melting Temp(°C)	Contact Angle(°)	Hardness (Hv)
1	1	0.5	239.12	38.66	8.1
2	1	0.5	238.76	39.1	8.22
3	1	1	232.2	36.75	16.1
4	0.5	1	240.12	38.12	10.2
5	0.5	0.5	238.12	43.22	7.9
6	0.5	0.5	238.34	43.58	7.6
7	0.5	1	240.34	38.48	10.39
8	1	1	232.45	36.82	16.2

4.3.2 Factorial Regression: Melting Temperature versus Cu, Ni

Factorial regression of melting temperature versus Cu and Ni were conducted. The analysis of variance is shown in the table 4.21. The model summary is in the table 4.22. The coded coefficients details are in the table 4.23

Table 4.21 Analysis of variance for Melting Temperature versus Cu, Ni

Source	DF	Adj SS	Adj MS	F-Value	P-Value
Model	3	73.6422	24.5474	679.75	0
Linear	2	22.5906	11.2953	312.78	0
Cu	1	17.3911	17.3911	481.58	0
Ni	1	22.536	22.536	624.04	0
2-Way Interactions	1	37.1091	37.1091	1027.6	0
Cu*Ni	1	37.1091	37.1091	1027.6	0
Error	4	0.1445			
Total	7	73.7867			

Table 4.22 Model summary for Melting Temperature versus Cu, Ni

S	R-sq.	R-sq. (adj)	R-sq. (pred)
0.190022	99.80%	99.66%	99.22%

Table 4.23 Coded coefficients for Melting Temperature versus Cu, Ni

Term	Effect	Coef	SE Coef	T-Value	p-Value	VIF
Constant		226.905	0.672	337.72	0	
Cu	37.3	18.65	0.85	21.94	0	10
Ni	42.46	21.23	0.85	24.98	0	10
Cu*Ni	-68.92	-34.46	1.07	-32.06	0	19

Regression Equation in Uncoded Units is given by

$$Melting\ Temperature = 226.905 + 18.65\ Cu + 21.23\ Ni - 34.46\ Cu * Ni \quad (4.7)$$

4.3.3 Factorial Regression: Contact Angle versus Cu, Ni

Factorial regression of contact angle versus Cu and Ni were conducted and the analysis of variance is shown in the table 4.24. The model summary is tabulated in the table 4.25. The coded coefficients details are shown in the table 4.26.

Table 4.24 Analysis of variance for Contact Angle versus Cu, Ni

Source	DF	Adj SS	Adj MS	F-Value	P-Value
Model	3	48.6096	16.2032	283.21	0
Linear	2	13.1941	6.5971	115.31	0
Cu	1	11.3251	11.3251	197.95	0
Ni	1	13.1382	13.1382	229.64	0
2-Way Interactions	1	4.515	4.515	78.92	0.001
Cu*Ni	1	4.515	4.515	78.92	0.001
Error	4	0.2289			
Total	7	48.8385			

Table 4.25 Model summary for Contact Angle versus Cu, Ni

S	R-sq.	R-sq. (adj)	R-sq. (pred)
0.239191	99.53%	99.18%	98.13%

Table 4.26 Coded coefficients for Contact Angle versus Cu, Ni

Term	Effect	Coef	SE Coef	T-Value	p-Value	VIF
Constant		56.025	0.846	66.25	0	
Cu	-30.1	-15.05	1.07	-14.07	0	10
Ni	-32.42	-16.21	1.07	-15.15	0	10
Cu*Ni	24.04	12.02	1.35	8.88	0.001	19

Regression Equation in Uncoded Units is given by

$$Contact\ Angle = 56.025 - 15.05\ Cu - 16.21\ Ni + 12.02\ Cu * Ni \tag{4.7}$$

4.3.4   Factorial Regression: Hardness versus Cu, Ni

Factorial regression of hardness versus Cu and Ni were conducted. The analysis of variance is shown in the table 4.27. The model summary is tabulated in the table 4.28. The coded coefficients details are shown in the table 4.29.

Table 4.27 Analysis of variance for Hardness versus Cu, Ni

Source	DF	Adj SS	Adj MS	F-Value	P-Value
Model	3	89.9422	29.9807	1593.66	0
Linear	2	7.8721	3.9361	209.23	0
Cu	1	5.0702	5.0702	269.51	0
Ni	1	1.682	1.682	89.41	0.001
2-Way Interactions	1	14.824	14.824	787.99	0
Cu*Ni	1	14.824	14.824	787.99	0
Error	4	0.0753			
Total	7	90.0175			

Table4.28 Model summary for Hardness versus Cu, Ni

S	R-sq.	R-sq. (adj)	R-sq. (pred)
0.137159	99.92%	99.85%	99.67%

Table 4.29 Coded coefficients for Hardness versus Cu, Ni

Term	Effect	Coef	SE Coef	T-Value	p-Value	VIF
Constant		10.24	0.485	21.12	0	
Cu	-20.14	-10.07	0.613	-16.42	0	10
Ni	-11.6	-5.8	0.613	-9.46	0.001	10
Cu*Ni	43.56	21.78	0.776	28.07	0	19

Regression Equation in Uncoded Units is given by

$$Hardness = 10.24 - 10.07\ Cu - 5.8\ Ni + 21.78\ Cu * Ni \qquad (4.8)$$

4.3.5 Response Optimization: Hardness, Contact Angle, Melting Temperature

The optimized response from the analysis is shown in the table 4.30 and table 4.31. The prediction of the optimized composition is shown in the table 4.32. It can be found that the composition of Cu is 1% and of Ni is 1% by wt.

Table 4.30 Parameters: Hardness, Contact Angle, Melting Temp(C)

Response	Goal	Lower	Target	Upper	Weight	Importance
Hardness	Maximum	7.6	16.2		3	3
Contact Angle	Minimum		36.75	43.58	2	2
Melting temperature	Minimum		232.2	240.34	1	1

Table 4.31 Solutions

Solution	Cu	Ni	Hardness fit	Contact Angle fit	Melting Temperature fit	Composite Desirability
1	1	1	16.15	36.785	232.325	0.985358

Table 4.32 Multiple response prediction

Variable	Setting
Cu	1
Ni	1

Table 4.33 Best fit solution

Response	Fit	SE Fit	95%CI	95% PI
Hardness	16.15	0.097	(15.8807, 16.4193)	(15.6836, 16.6164)
Contact Angle	36.785	0.169	(36.315, 37.255)	(35.972, 37.598)
Melting temperature	232.325	0.134	(231.952, 232.698)	(231.679, 232.971)

4.3.6 Main effect plots

The mean response of the level factors can be represented in the main effect plots. This is done by connections made by the lines. It can be interpreted that there is no main effect if horizontal line is present in the diagram. Little deflection from the horizontal direction indicates that it will significantly affect the response. Lines with higher slope give the information that the magnitude of the main effect is higher. The effect can be defined as the variations in melting temperature, hardness and the contact angle when the factor changes from one level to another level. Calculations are done at minimum and maximum values of each factor (Bharath, 2019). The information about the direction of the effect (i.e. Increase or decrease in the average response value) is obtained from the sign of the main effect plot. The strength of the effect is obtained from the magnitude. The main effect diagrams give vital information about the information about the factor influence in the properties like melting temperature, hardness and the contact angle of SCN110. The main effect plots for melting temperature, hardness and contact angle is given in the figure 4.7, figure 4.8 and figure 4.9.
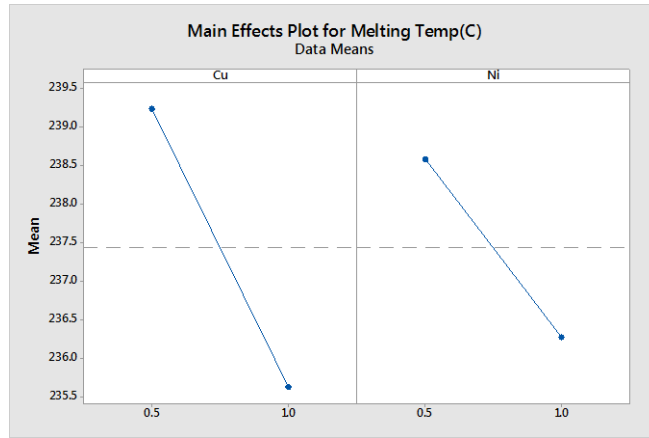
Figure 4.8 Mean effects plot for melting temperature
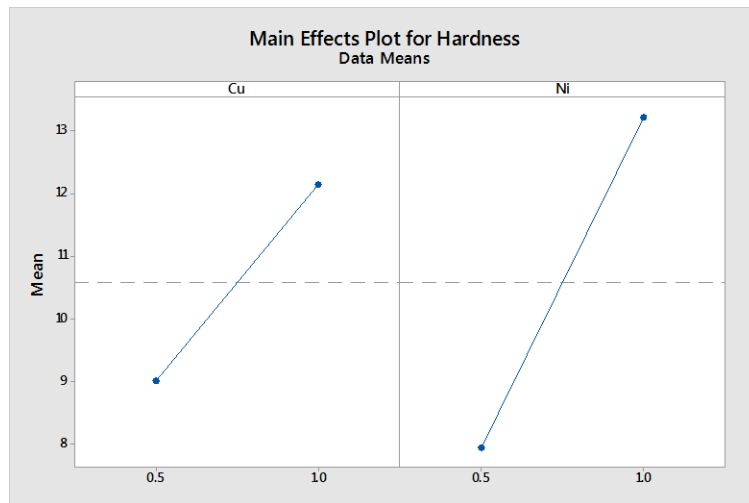
Figure 4.9 Mean effects plot for Hardness
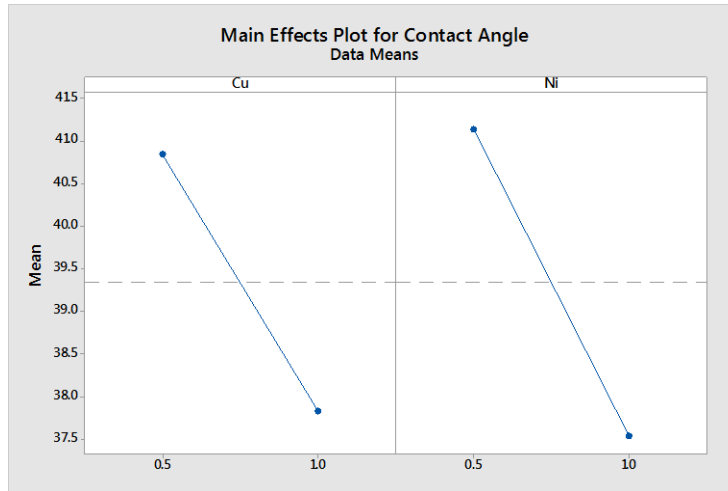
Figure 4.10 Mean effects plot for contact angle

4.3.7 Interaction plots

The behaviour of one variable which is depending on the value of another variable is better understood by interaction plots. An interaction plot displays the levels of one variable on the X axis and has a separate line for the means of each level of the other variable. Y axis is the dependent variable. The interaction effects are analysed in the regression analysis, ANOVA and DOE. The influence of one factor and a continuous response with the value of the second factor can be identified from the interaction plots. The lines in the diagram can be used to interpret how the relation between the factor and the response are affected. Parallel lines denote that there is no interaction. Non-parallel lines in the diagram interprets that there is interaction occurring. The strength of the interaction is proportional to number of non-parallel lines. Interaction plot for hardness, contact angle and melting temperature is shown in the figure 4.10, figure 4.11 and figure 4.12. It can be interpreted that the influence of these factors are present.

66
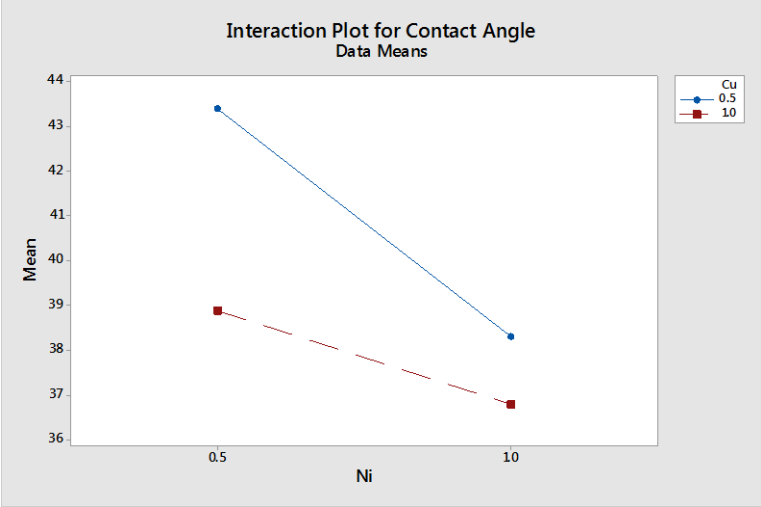
Figure 4.11 Interaction plot for contact angle
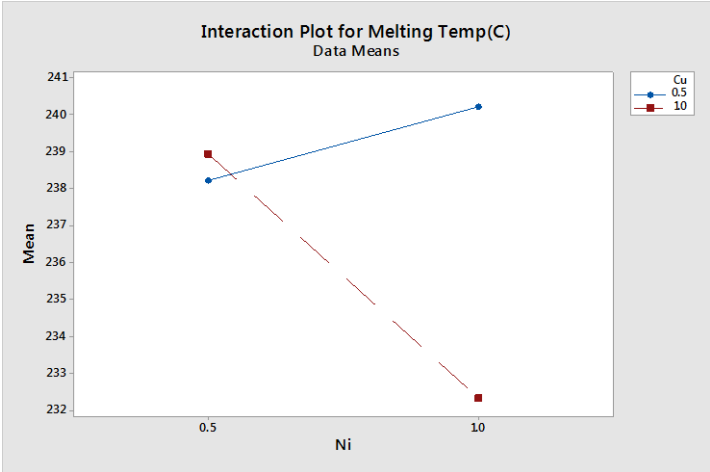
Figure 4.12 Interaction plot for melting temperature
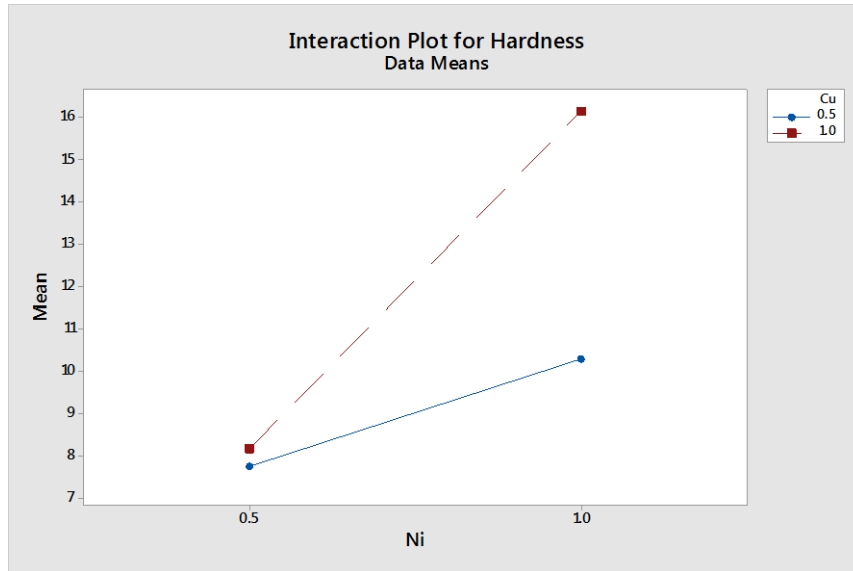
Figure 4.13 Interaction plot for Hardness

The present section deals with design of experiments (DoE) checks about the use of Sn, Cu and Ni to make a new lead free solder alloy. By design experiments it has been found that, the selected parameters are the most impacting factors for response. The ANOVA evidently shows with its P- values having less than 0.05 that Cu and Ni composition in the alloy is having significant impact in the Melting temperature, Contact Angle and Hardness. The R square values of the regression equation is calculated to be more than 95% which denotes that model is best and convey us that there are no other factors impacting the factors. The same can be seen graphically in the Mean effects plot. The Interaction plot shows the interaction between the Cu & Ni with the factors. From the results of Design of Experiments we can infer that Cu-1 and Ni – 1% by qt. is the best optimized composition for the new solder alloy. Therefore Sn-1Cu-1Ni will be an optimum composition of the new lead free solder alloy.

4.4 CHARACTERISTICS AND PROPERTIES OF SCN110 SOLDER ALLOY

Table 4.34 Chemical composition required for SCN110

Solder alloy	Sn (%)	Cu (%)	Ni (%)
SCN110	98	1	1

4.4.1 Properties of SCN110

4.4.1.1 Chemical Composition

Chemical compositions of the alloys were analyzed using ICP-OES. The required composition is shown in table 4.34. The results of the analysis are shown in the table 4.35. Composition results of all the five alloy samples are listed. From this list of alloys, one alloy is selected for further investigations.

Table 4.35 Chemical Composition results

Solder alloy	Sn (%)	Cu (%)	Ni (%)
SCN110 Sample 1	97.9034	0.9897	1.0976
SCN110 Sample 2	97.9501	0.9764	1.0674
SCN110 Sample 3	97.8954	1.1098	0.9844
SCN110 Sample 4	97.9976	0.9764	0.9657
SCN110 Sample 5	97.9932	0.9867	0.9853

4.4.1.2 Melting Temperature

Melting temperature Analysis for SCN110 was conducted using Thermo Gravimetric and Differential Thermal analysis (TG-DTA). The addition of the Ni into the Sn-Cu adds the nucleation of the phase and as a result the alloy can solidify directly as a eutectic. This

happens without Sn dendrites getting primary precipitated (. The results are given in the
table 4.36

Table 4.36 Melting temperature results

Solder alloy	Melting Temperature (°C)
SCN110 Sample 1	232.45
SCN110 Sample 2	232.35
SCN110 Sample 3	232.67
SCN110 Sample 4	232.66
SCN110 Sample 5	232.54
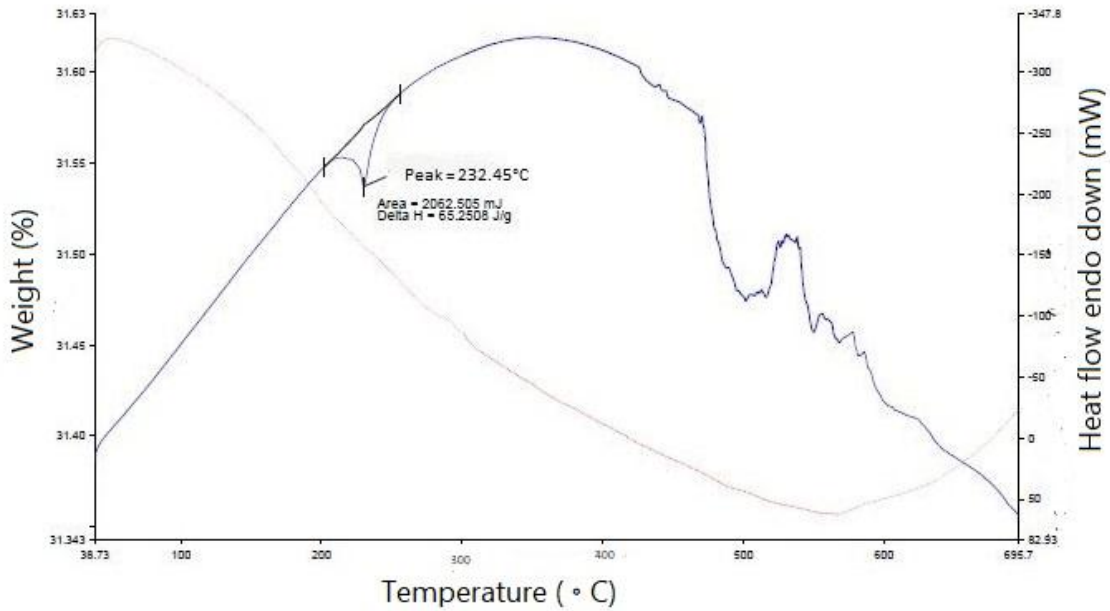
Fig, 4.14a TGA results of SCN110
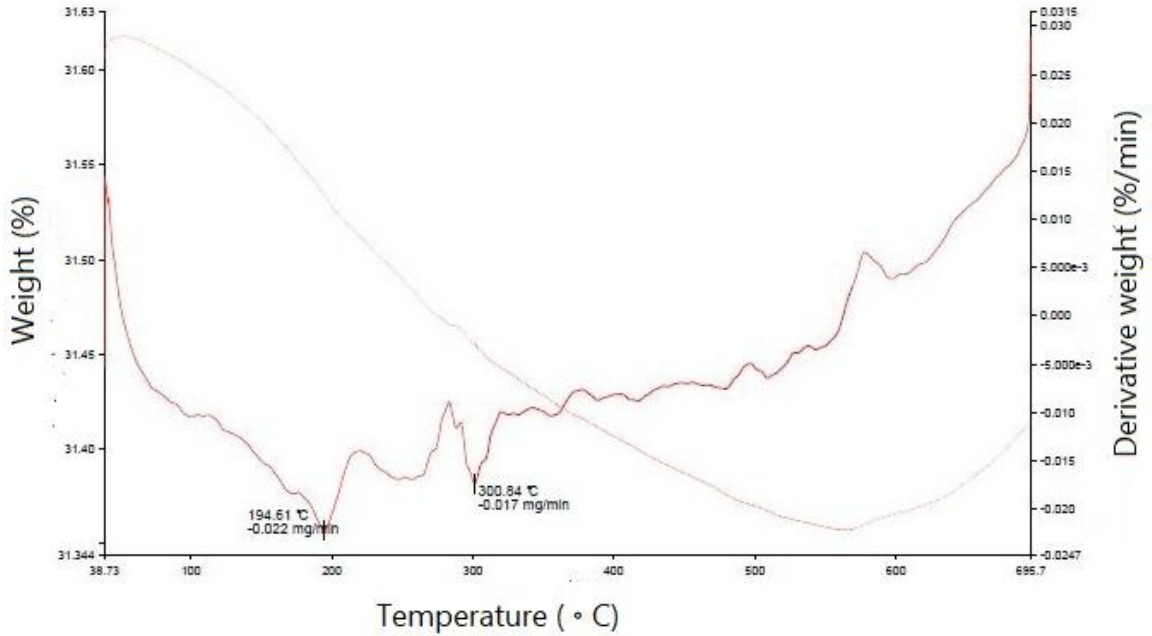
Fig. 4.14b DTA results of SCN110

4.4.1.3 Contact angle and hardness

Contact angle measured SCN110 are shown in the table 4.37. Solder wettability is found to be enhanced with the presence of Ni in SCN110. The presence of Ni in alloy strengthens the solder alloy. Contact angle of SCN110 is in between 30° and 40° (36.75±0.03). Therefore its wetting characteristics are good. Hardness values measured for are shown in the table 4.38. Good hardness values (16.13±0.06) are obtained for SCN110 solder alloys.

Table 4.37 Contact angle measurement results

Solder alloy	Contact angle (°C)
SCN110 Sample 1	36.82
SCN110 Sample 2	36.76

SCN110 Sample 3	36.75
SCN110 Sample 4	36.75
SCN110 Sample 5	36.77
SCN110 Sample 6	36.8
SCN110 Sample 7	36.75
SCN110 Sample 8	36.68
SCN110 Sample 9	36.75
SCN110 Sample 10	36.7

Figure 4.15 Contact angle measurement of SCN110.

Table 4.38 Hardness measurement results

Solder alloy	Hardness (Hv)
SCN110 Sample 1	16.1
SCN110 Sample 2	16
SCN110 Sample 3	16.2
SCN110 Sample 4	16.1
SCN110 Sample 5	16.1
SCN110 Sample 6	16.1

SCN110 Sample 7	16.2
SCN110 Sample 8	16.2
SCN110 Sample 9	16.1
SCN110 Sample 10	16.2

4.5 MICROSTRUCTURE OF SCB305 AND SCN110

Scanning electron micrographs provides the detailed and accurate microstructure of the solder alloys. The surface details of the samples were analysed by field-emission scanning electron microscopy (FE-SEM, Carl Zeiss Sigma). The micrographs of SCB305 and SCN110 are shown in figure 4.13 and figure 4.14. Improvement in the solder microstructure is found due to the presence of Ni. Hypoeutectic binary composition of Sn-Cu is found to be shifted to ternary eutectic due to the presence of Ni thereby enhancing the fluidity of the solder. It also reduces the freezing range (Fan Yang et al., 2016). The weak irregular binary eutectic becomes strong ternary eutectic. Ni additions to SnCu alloy can enhance fluidity, which can be a beneficial property in wave soldering (Henshall et al., 2008). A complex compound $(CuNi)_6Sn_5$ is formed as the added Ni substitutes for Cu in the Cu_6Sn_5 particles. A major effect on the concentration gradient within the layer can be observed due to the small amount addition of Ni. The Cu dissolution will get a noteworthy slow down due to this gradient. Cu_3Sn intermetallic growth gets slow down with addition of Ni in the SCN110 alloy. The undercooling behaviour is greatly influenced by the addition of Bi. The presence of Bi refines the microstructure (Fan Yang et al., 2016). The β-Sn dendrites growth rate is restrained with presence of Bi (Fan Yang et al., 2016). When excess Bi was added, a solidification crack

was observed. It may be due to the increasing nature of the range of melting temperature between liquidus and solidus (El-Daly et al., 2015). Clusters of Bi particle are observed in the microstructure. Due to the presence of Bi in the Sn-Cu, the microstructure change is noted from great number of β-Sn surrounded by eutectic region to dark gray Cu_6Sn_5 particles.
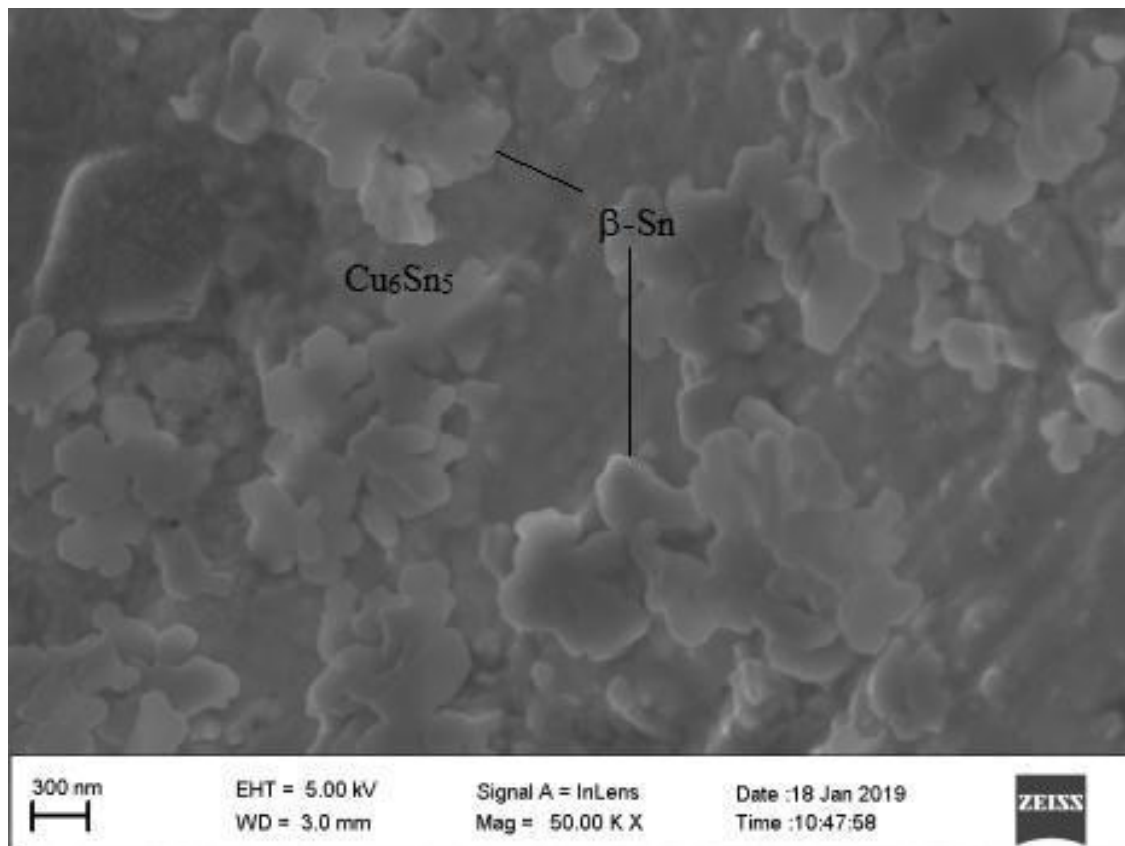
Figure 4.16 FE-SEM image of SCB305
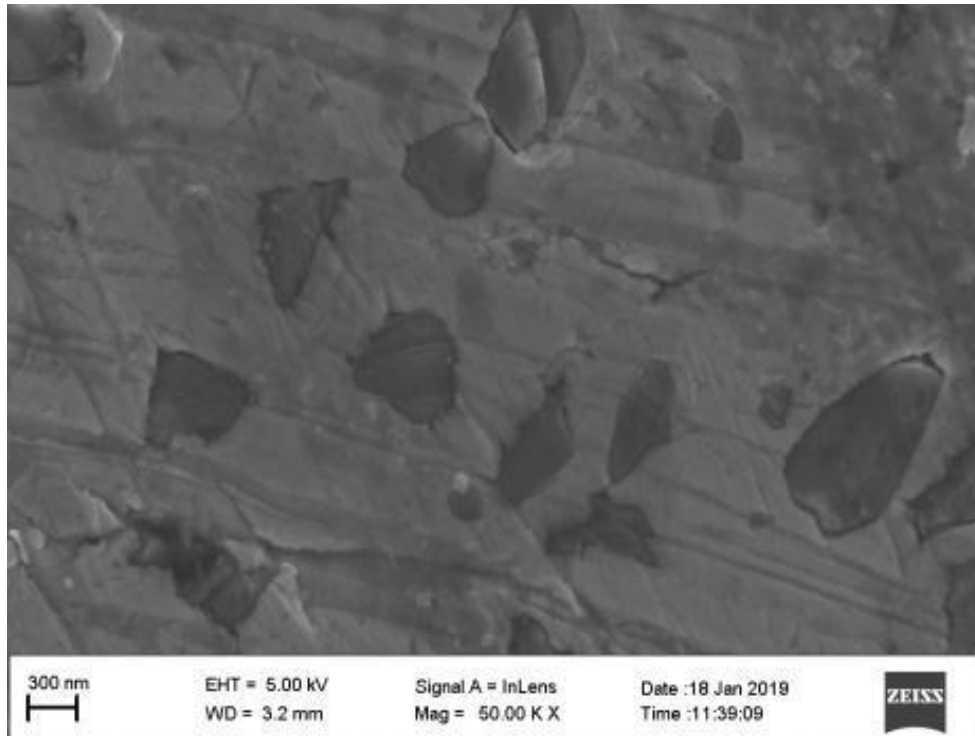
Figure 4.17 FE-SEM image of SCN110

4.6 COMPARISON OF SCB305 AND SCN110 WITH SAC305 AND SAC405

The properties of SCB305 and SCN110 are compared with SAC305 and SAC40. SAC305 and SAC405 are two widely accepted lead free solder alloys. The melting temperature, hardness, contact angle and cost of the four alloys are shown in the table 4.39. The graphical comparison of the same is also shown in the figures 4.15 to 4.18.

Table 4.39 Properties of SCB305, SCN110, SAC305 and SAC405

Solder alloy	Melting Temperature (°C)	Hardness (Hv)	Contact angle (°)	Cost ($/Kg)
SCB305	231.15	19.8	28.74	23.05
SCN110	232.5	16.1	36.75	20.65
SAC305	219.5	20.8	26.7	36.63
SAC405	220	20.21	29	41.89
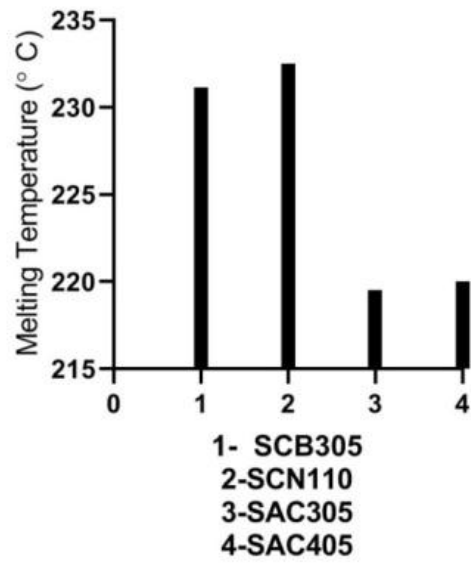
Figure 4.18 Melting temperature comparisons of SCB305 and SCN110 with SAC305 and
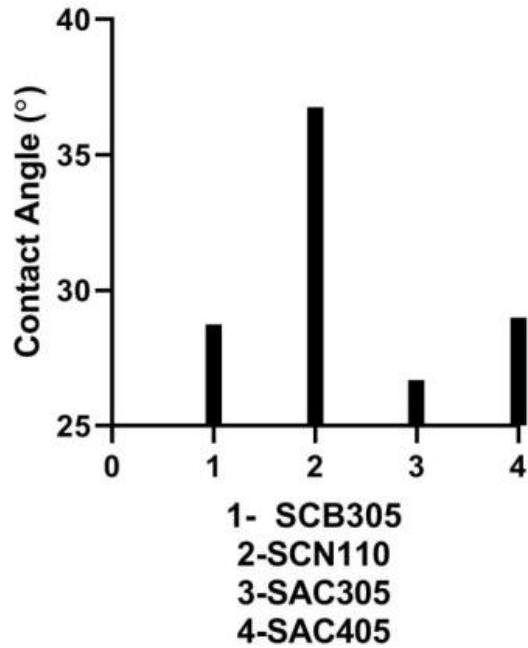
SAC405

Figure 4.19 Contact angle comparisons of SCB305 and SCN110 with SAC305 and
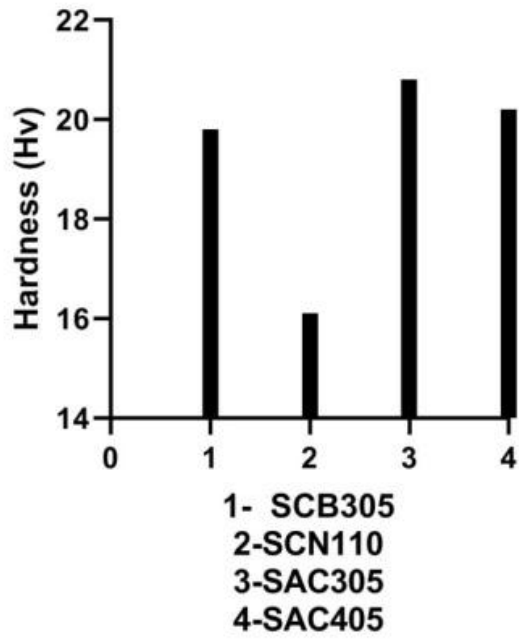
SAC405

Figure 4.20 Hardness comparisons of SCB305 and SCN110 with SAC305 and SAC405
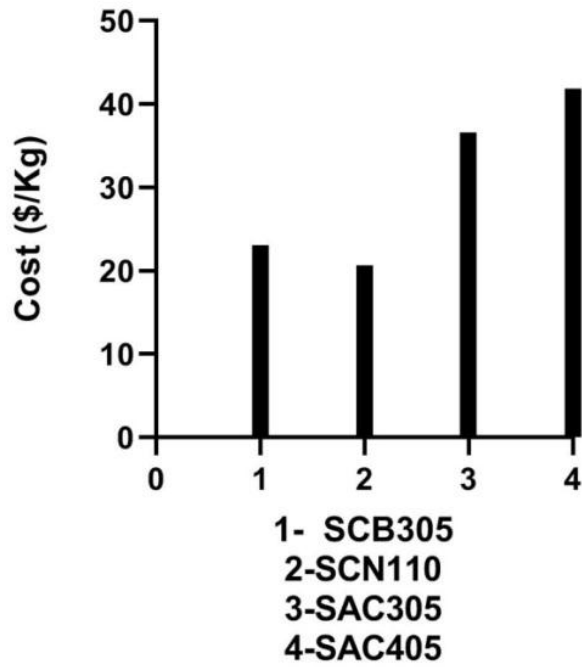
Figure 4.21 Cost comparisons of SCB305 and SCN110 with SAC305 and SAC405

Two novel lead-free solder alloys, one Sn-0.5Cu-3Bi (SCB305) and Sn-1Cu-1Ni (SCN110) are successfully developed. DoE was conducted at the initial stage. Melting temperature, hardness and contact angle of SCB305 are 231.15°C, 19.8Hv and 28.74° respectively. Melting temperature, hardness and contact angle of SCN 110 are 232.5°C, 16.1Hv and 36.75° respectively. All these properties were comparable with the existing SAC305 and SAC405 alloys. The cost of SCB305 and SCN110 are $23.05/Kg and $20.65/Kg respectively. Details of the cost of the alloys are shown in annexure I. The cost of SAC305 and SAC405 are $36.63/Kg and $41.89/Kg respectively. Cost wise comparison also suggests that new alloys are better. The patent cost of the SAC alloys will again make it a costlier alloy.

CHAPTER 5

EFFECT OF ADDITION OF Ag INTO Sn-0.5Cu-3Bi (SCB 305)

In the previous chapter, new lead free solder alloy SCB 305 (0.5% Cu, 3% Bi and rest Sn by wt.) is developed. In this chapter, experimental investigation on the effect of silver (Ag) addition on the melting behavior, microstructure, and microhardness into Sn-0.5Cu-3Bi is carried out. The aim of this investigation is to verify whether the addition of Ag is improving the property of the alloy.

5.1   EXPERIMENTAL PROCEDURE

5.1.1   Sample preparation

Solder alloy specimens were produced from pure metals which were in the powder form. The composition and assigned codes are provided in the table 5.1. Pure metals of Sn, Cu, Bi and Ag in the form of powder are weighed in proper weight proportions and were melted in induction furnace at more than 1000°C for 45 minutes. Then these were transferred to cylindrical moulds. Five samples were made using the above procedure. The samples were quenched and were kept at room temperature for one day.   The first sample was made using Sn, Cu and Bi according to the composition shown in the Table 1. In the next four samples Ag was added in four different proportions (0.25, 0.5, 0.75, and 1 % by wt.). Thus samples were obtained in the form of disc shapes. Finally these samples were undergone visual inspection to ensure that the surface of these samples were free from damages. To check the variation above 1% by wt., 1.25, 1.5 and 1.5 % by wt. were also analyzed.

79

Table 5.1 Composition of the solder alloy samples required

Solder Alloy	Sn (%)	Cu (%)	Bi (%)	Ag (%)
Sn-0.5Cu-3Bi	96.5	0.5	3	0
Sn-0.5Cu-3Bi -0.25Ag	96.25	0.5	3	0.25
Sn-0.5Cu-3Bi -0.5Ag	96	0.5	3	0.5
Sn-0.5Cu-3Bi -0.75Ag	95.75	0.5	3	0.75
Sn-0.5Cu-3Bi -1Ag	95.5	0.5	3	1

5.1.2 Melting temperature analysis

Melting temperature analysis of all the five samples (one sample of Sn-Cu-Bi and four samples of Sn-Cu-Bi-xAg) were conducted using Thermo Gravimetric and Differential Thermal analysis (TG-DTA). Thermo Gravimetric analysis (TGA) measured the weight loss or gain as a function of temperature ,the TGA trace appear as steps, it can be deal with the derivative of TGA with respect to time or temperature. Differential thermal analysis (DTA) is a technique for recording the difference in temperature between a substance and a reference material as a function of time or temperature as the two specimens are subjected to identical temperature regimes in an environment heated or cooled at a controlled rate.

5.1.3 Hardness test

Hardness tests were performed using HMV-G micro Vickers hardness tester. Each Hv value was the average of ten different readings which were taken at random points on the surface of the sample. For hardness tests to be performed on the sample, the surface

should be smooth. Sample preparation was done using grinding by taking different grades of SiC papers. Then the samples were polished. The surfaces of the alloys were analysed in Axio vertical A1 metallurgical microscope before and after the microhardness test.

5.1.4   Wettability studies

Capacity of molten solder to react with the bottom substrate is referred to as wetting. It forms a certain amount of intermetallic compound that acts as an adhesion layer to join the solder and the substrate. The reaction between the solder and substrate is important as it may affect the micro structure. It will also affect the mechanical strength of the solder joint. Here the molten sample is spread on the Copper substrate. Then the contact angle is measured. Generally if the wetting or contact angle lies between 0° and 90° the system is said to be wet. If the wetting or contact angle is between 90° and 180° the system is considered to be non-wetting (Sharif and Chan, 2004).

5.1.5   Microstructure analysis

All the five samples were ground with four grades of SiC papers and then mechanically polished with a diamond suspension. Chemical etching was done on the alloys using 95% ethanol solution/5% hydrochloric acid. The surface details of the samples were analysed by field-emission scanning electron microscopy (FE-SEM, Carl Zeiss Sigma).All the images were taken at a magnification starting from 5K X- 50 KX, scale=1μm, Electron High Tension(EHT) = 5.00 Kv, Working Distance (WD) = 3.2 mm

5.2   RESULTS OF THE ANALYSIS

5.2.1   Chemical composition

Five alloy samples were made with different composition. Chemical compositions of the alloys were analyzed using ICP-OES. The results of the analysis are shown in the table 5.2. Analysis was conducted till 1.75 % by wt. of silver. The results of the analysis were matching with the predicted amount of composition.

Table 5.2 Chemical composition of the samples

Solder Alloy	Chemical Composition Result			
	Sn (%)	Cu (%)	Bi (%)	Ag (%)
Sn-0.5Cu-3Bi	96.5911	0.4901	2.9187	0
Sn-0.5Cu-3Bi -0.25Ag	96.3417	0.4832	2.9272	0.2478
Sn-0.5Cu-3Bi -0.5Ag	95.9127	0.5132	3.0649	0.5091
Sn-0.5Cu-3Bi -0.75Ag	95.8392	0.5071	2.9048	0.7488
Sn-0.5Cu-3Bi -1Ag	**95.5578**	**0.4973**	**2.9274**	**1.0174**
Sn-0.5Cu-3Bi -1.25Ag	95.1645	0.4901	3.0876	1.2478
Sn-0.5Cu-3Bi -1.5Ag	94.8767	0.4967	2.9867	1.4897
Sn-0.5Cu-3Bi -1.75Ag	94.7647	0.5099	2.9711	1.7443

5.2.2 Melting Temperature

The soldering temperature depends on the melting temperature of the soldering alloy. Therefore the melting temperature is considered as a critical solder characteristic. A higher soldering temperature is not recommended because the higher temperature may lead to the damage of the electronic package. The melting points of all the five samples were tested using TGA analysis. The results were noted down and a comparison is shown in the figure 5.1. It can be seen that the melting temperature of Sn-Cu-Bi alloy is 231.15° C. The melting temperature of Sn-Cu-Bi-xAg (x= 0.25, 0.5, 0.75,1 wt.%) are 230.13° C, 229.34° C, 228.92° C, 226.93° C respectively. So it can be concluded that with the addition of Ag into Sn-Cu-Bi, the melting temperature is decreasing. The Ag added in to the Sn-0.5Cu-3Bi is found to be uniformly distributed in the solder matrix. Melting temperatures of a single material are the characteristic properties that are subject on the interatomic distance and the root mean vibration amplitude. The formation of Ag_3Sn in the matrix has altered the above properties which resulted in the decrease of melting temperature on addition of Ag incrementally. The reinforcement addition could alter the surface instability and the variation in the physical properties and the grain boundary characteristics. The degree of undercooling is the one of the key factors that affects the development and growth of intermetallic compounds. The undercooling of Sn-0.5Cu-3Bi solder material is meaningfully reduced with the addition of Ag. In other words the melting temperature is decreasing with the addition of Ag into Sn-0.5Cu-3Bi. Melting temperature results are shown in table 5.3

Table 5.3 Melting temperature of Sn-0.5Cu-Ni-xAg

Solder Alloy	Melting Temperature (°C)
Sn-0.5Cu-3Bi	231.15
Sn-0.5Cu-3Bi -0.25Ag	230.13
Sn-0.5Cu-3Bi -0.5Ag	229.34
Sn-0.5Cu-3Bi -0.75Ag	228.92
Sn-0.5Cu-3Bi -1Ag	**226.93**
Sn-0.5Cu-3Bi -1.25Ag	226.65
Sn-0.5Cu-3Bi -1.5Ag	226.98
Sn-0.5Cu-3Bi -1.75Ag	227.18
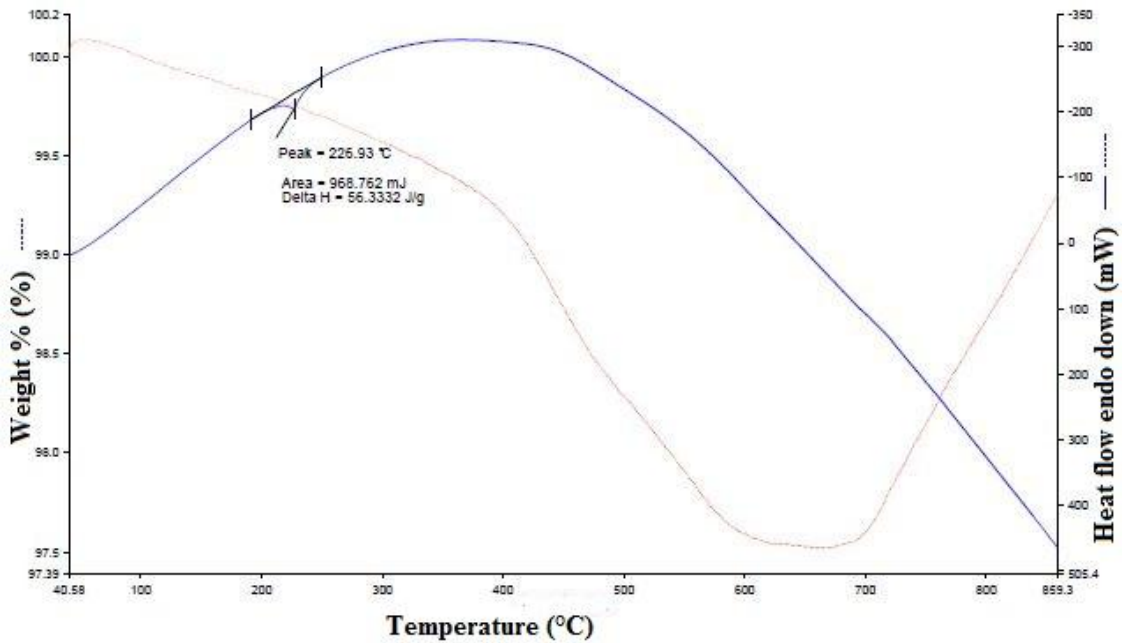
Figure 5.1 TGA graph of Sn-0.5Cu-3Bi-1Ag
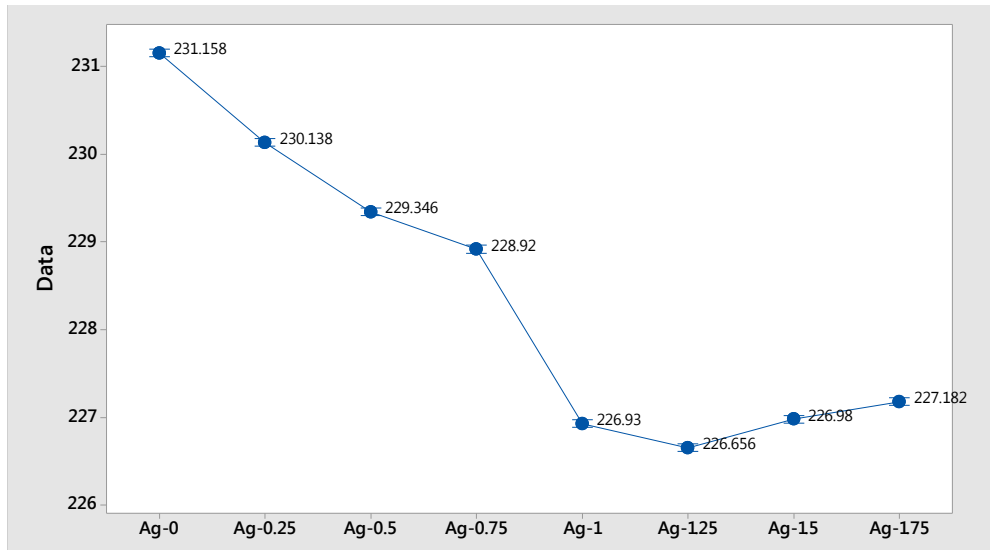
Fig. 5.2 Comparison of melting temperatures of the samples

5.2.3 Wettability (Contact angle)

Contact angle as a function of Ag addition to the Sn-Cu-Bi solder is shown in the figure 5.2. It can be seen that the contact angle of Sn-Cu-Bi alloy is 28.74°. The results are shown in table 5.4. The contact angle of Sn-Cu-Bi-xAg (x= 0.25, 0.5, 0.75,1 wt%) are 27.53°, 26.44°, 25.12° and 24.87° respectively. Therefore, the contact angle is getting reduced as the Ag is added. The effect of the Ag in the molten solder is the reason for these improvements. It acts as an agent to bring down the surface tension of the alloy. It results in the upsurge in the wettability between Cu substrate. The phenomenon could be due to the decreased surface tensions of the molten solder in the presence of Ag. In this the liquid-solid and liquid-vapor surface tensions are lessened. The higher Ag concentrations reduced the viscosity of the molten solder, which is resulting in the decline in the contact angle.

Table 5.4 Contact angle of Sn-0.5Cu-Ni-xAg

Solder Alloy	Contact angle (°)
Sn-0.5Cu-3Bi	28.74
Sn-0.5Cu-3Bi -0.25Ag	27.53
Sn-0.5Cu-3Bi -0.5Ag	26.44
Sn-0.5Cu-3Bi -0.75Ag	25.12
Sn-0.5Cu-3Bi -1Ag	**24.87**
Sn-0.5Cu-3Bi -1.25Ag	25.34
Sn-0.5Cu-3Bi -1.5Ag	27.56
Sn-0.5Cu-3Bi -1.75Ag	27.45
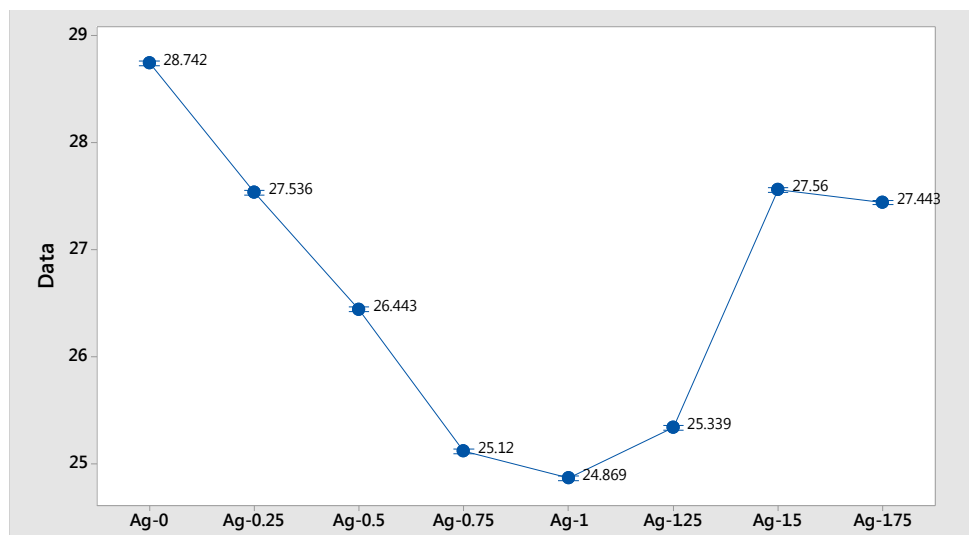
Fig. 5.3 Comparison of contact angles of the samples

5.2.4 Microhardness test

The abrasion behavior and wear of a solder material can be easily analysed using the microhardness property values. The fitness of these alloys for various applications can also be discovered using this analysis. All the five samples were undergone microhardness analysis. The analysis was done to know the effect of addition of Ag into the Sn-Cu-Bi alloy. The results were noted down and the comparison is shown in figure 5.3.The results are tabulated in table 5.5. It can be found that the hardness value increases with the addition of Ag into the Sn-0.5Cu-3Bi alloy. The hardness value of Sn-Cu-Bi alloy is found to be 19.8 Hv, and when 1% of Ag is added to this alloy, hardness value is found to be increased to 24.2 Hv. A comparison of microhardness value of these five alloys with SAC305 and SAC405 were also conducted. The microhardness property values of SAC305 and SAC 405 were taken as 13.47Hv and 13.98 Hv (Yu and Abdullah, 2011). It can be analysed that these five alloys possess higher hardness value when compared to SAC305, SAC405.

The presence of Ag in the solder matrix holds the grain boundaries, about to happen their sliding and allegedly strengthening the microhardness of the composite solder according to the dispersion strengthening mechanism. There is a gain in strength as the grain size decreases. In other words, the hardness of the Sn-0.5Cu-3Bi is found to be increasing with the addition of Ag.

Table 5.5Hardness of Sn-0.5Cu-Ni-xAg

Solder Alloy	Hardness (Hv)
Sn-0.5Cu-3Bi	19.8
Sn-0.5Cu-3Bi -0.25Ag	20.7
Sn-0.5Cu-3Bi -0.5Ag	21.8
Sn-0.5Cu-3Bi -0.75Ag	22.76
Sn-0.5Cu-3Bi -1Ag	**24.2**
Sn-0.5Cu-3Bi -1.25Ag	24.1
Sn-0.5Cu-3Bi -1.5Ag	23.1
Sn-0.5Cu-3Bi -1.75Ag	23.3
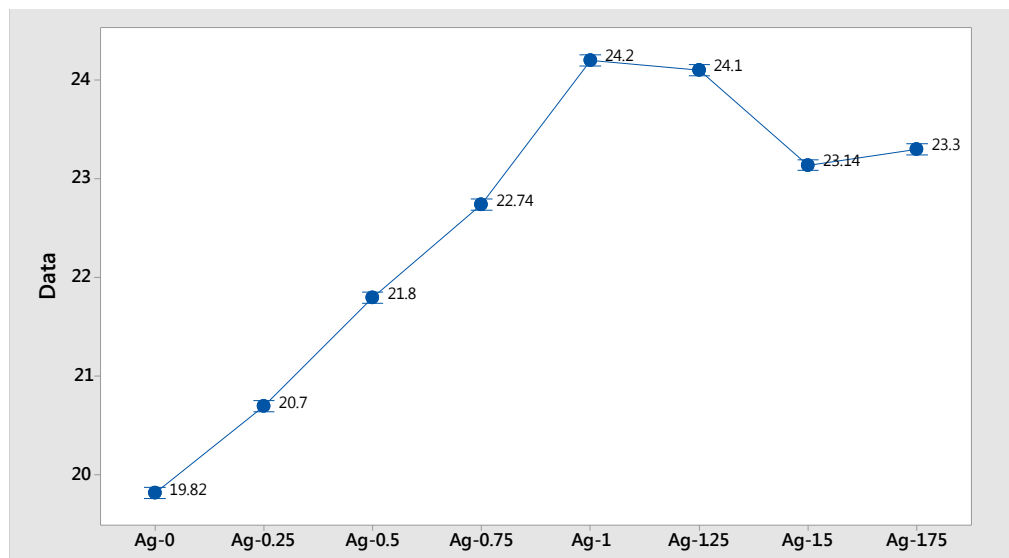
Fig. 5.4 Comparison of hardness values of the samples

5.2.5 Shear strength

Material's ability to resist forces that can cause the internal structure of the material to slide against itself is termed as shear strength. Shear strength a test of the samples with different amount of Ag is conducted using the method explained in the above section. The results of the analysis are noted and are given in the table 5.6. The variation of the shear strength is shown in the figure 5.4. The dispersion hardening with the addition may be a reason for the increase in the shear strength. With the addition of Ag, the density of the alloy is also found to be increasing slightly. The ultimate strength of Sn-0.5Cu-3Bi is found to be increased by 19.3% with the addition of 1% by wt. Ag.
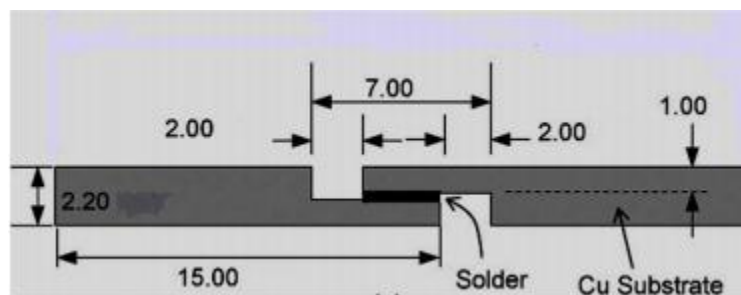
Figure 5.5 Geometry of shear strength specimen

Table 5.6 Shear strength results of the alloys

Solder Alloy	Ultimate Shear stress (Mpa)
Sn-0.5Cu-3Bi	23.4
Sn-0.5Cu-3Bi -0.25Ag	26.5
Sn-0.5Cu-3Bi -0.5Ag	25.4
Sn-0.5Cu-3Bi -0.75Ag	26.4
Sn-0.5Cu-3Bi -1Ag	**28**
Sn-0.5Cu-3Bi -1.25Ag	27.6
Sn-0.5Cu-3Bi -1.5Ag	27.3
Sn-0.5Cu-3Bi -1.75Ag	27.8
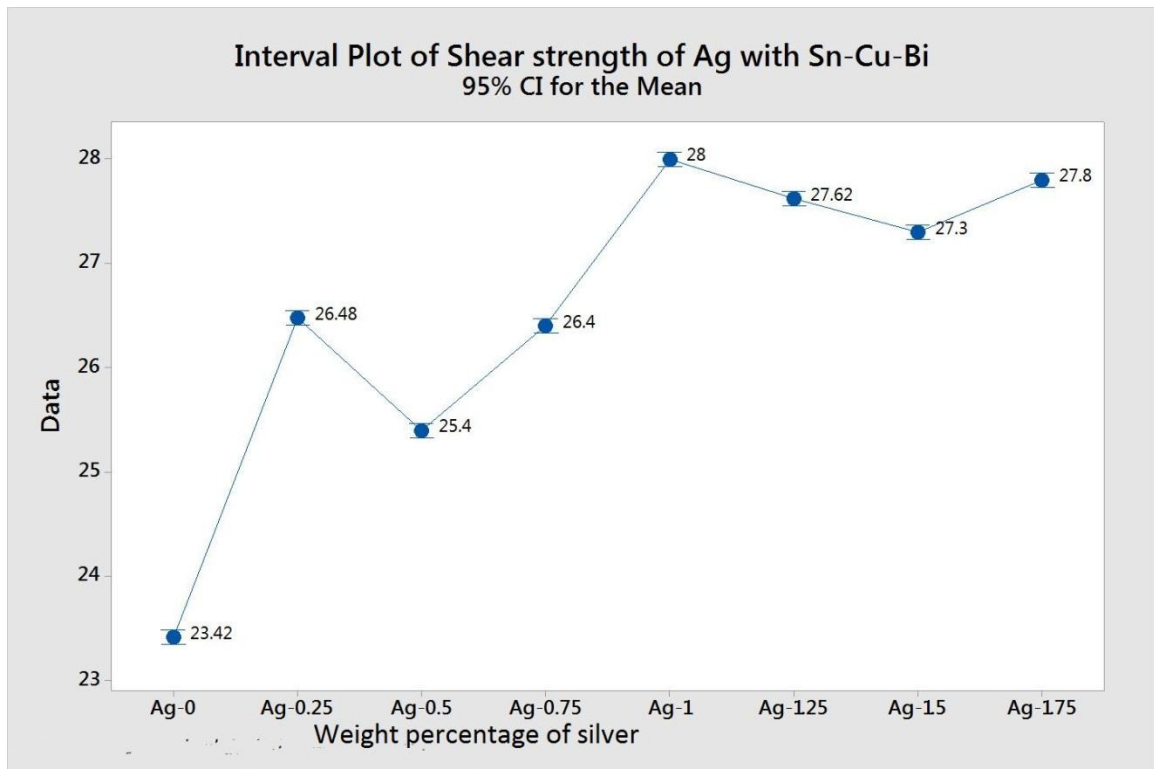
Fig. 5.6 Variation of ultimate shear strength with the addition of Ag.

Surface of Sn-0.5Cu-3Bi-1Ag with concurrent visual display by secondary electron emission mode of scanning electron microscopy exposes the presence of Sn, Cu, Bi, Ag as shown in the figure 5.5. The elemental mapping of the surface of the specimen is also obtained using the analysis.
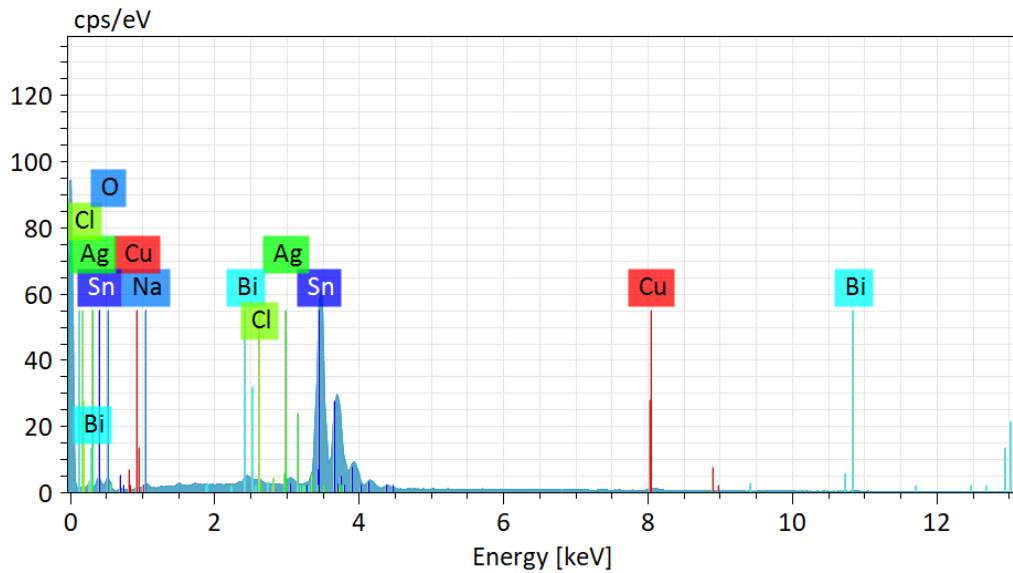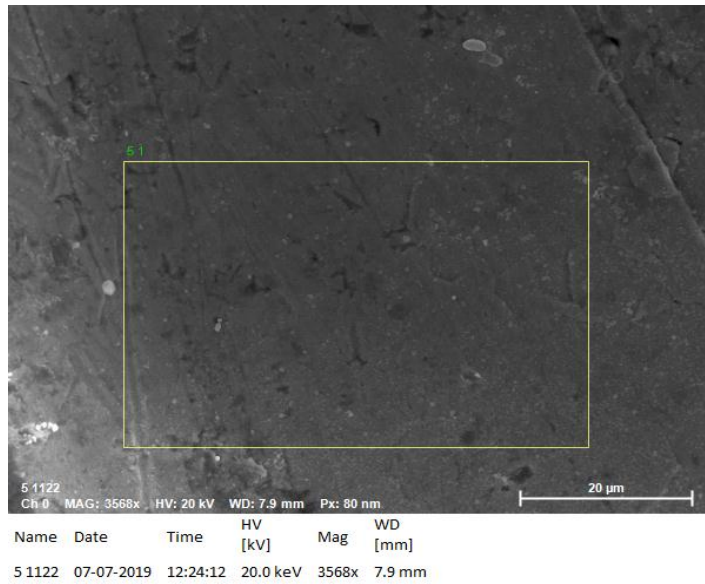
Fig. 5.7 EDS analysis results of Sn-0.5Cu-3Bi-1Ag

5.2.6 Impact toughness

Impact toughness is a fundamental material property required to measure the performance of solder alloys. The impact toughness is directly proportional to the energy absorbed by the alloy. The crashworthiness of the solder alloy is an important property. Impact toughness tests for all the samples with different amount of Ag are conducted using Charpy impact test explained in the previous chapter. The energy absorbed by the test specimen gives idea about the impact toughness. The results obtained are given in the table 5.7 and figure 5.6. The samples which are able to absorb more impact energy during the conduction of impact test will be considered as materials having more impact toughness. The microstructure also will have close relation with the impact toughness. Charpy test is the apt test for determining the impact toughness of the solder alloy. Even if we are using large test specimens for the test when compared to the solder joints, the strain rate experiencing in the both cases are matching. The impact toughness of Sn-0.5Cu-3Bi is found to be increased by 8.6% with the addition of 1% by wt. Ag.

Table 5.7 Impact toughness test results of the alloys

Solder Alloy	Impact Toughness (J)
Sn-0.5Cu-3Bi	10.4
Sn-0.5Cu-3Bi -0.25Ag	10.7
Sn-0.5Cu-3Bi -0.5Ag	10.9
Sn-0.5Cu-3Bi -0.75Ag	11
Sn-0.5Cu-3Bi -1Ag	**11.3**
Sn-0.5Cu-3Bi -1.25Ag	11.6
Sn-0.5Cu-3Bi -1.5Ag	11.7
Sn-0.5Cu-3Bi -1.75Ag	11.9
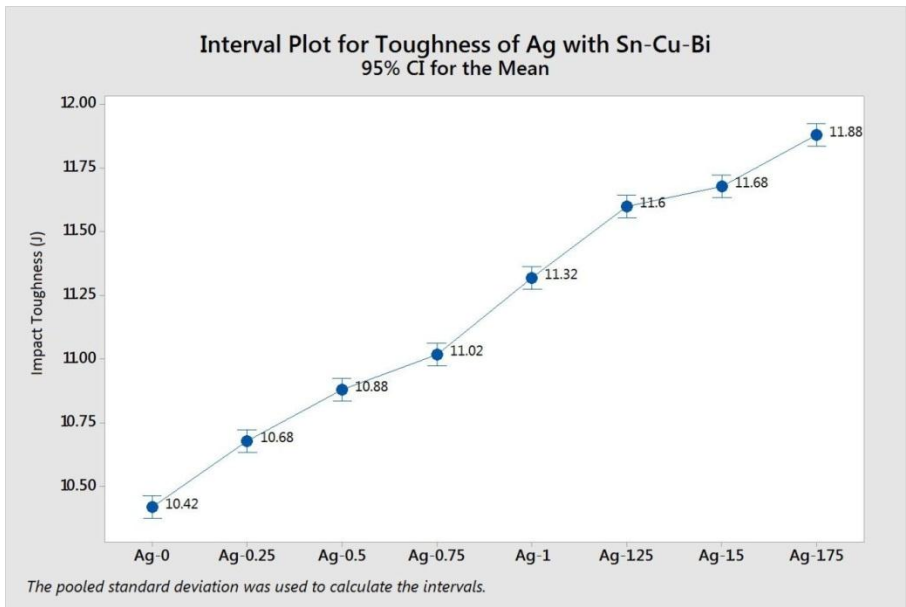
Fig. 5.8 Variation of Impact toughness with the addition of Ag
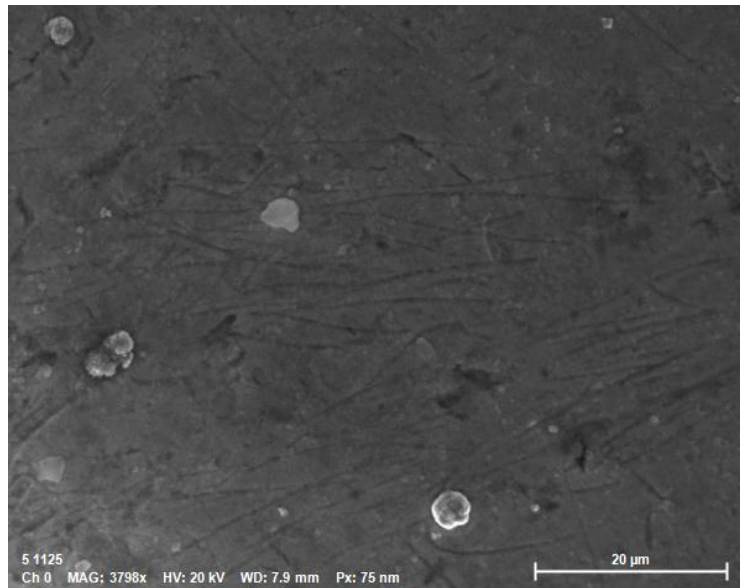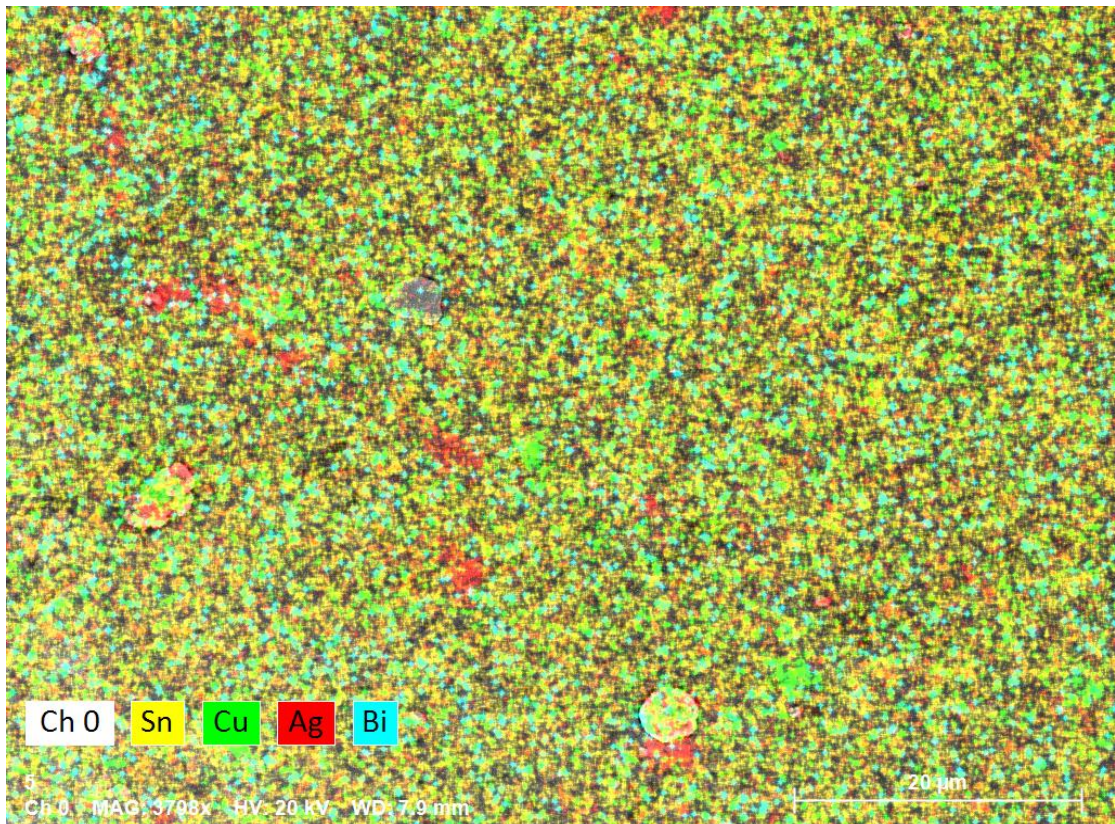
Fig. 5.9 Element mapping of Sn-0.5Cu-3Bi-1Ag

94

5.2.7 Microstructure evaluation

SEM micrographs will give the detailed and accurate configuration of the solder alloys. The surface details of the samples were analysed by field-emission scanning electron microscopy (FE-SEM, Carl Zeiss Sigma). The micrographs of four alloys are shown in figure 5.8. The FE SEM image of Sn-0.5Cu-3Bi-1Ag is shown in the figure 5.9. The microstructure analysis of alloys has as far as the knowledge the coarse β Sn grains. Ag_3Sn, Cu_6Sn_5 and tin in the alloys are found in the eutectic region. With the addition of Ag, the β-Sn grains refine in a better way. Eutectic bands become narrower rather. Ag is found to be homogeneously distributed in the surface of the solder matrix as observed from the microstructure evaluation. The mechanical properties are changed due to the different microstructure of the alloys; mainly the change is size of β-Sn grains and IMC particles. Some intermetallics become coarse with the increasing of Ag content. The slipping of dislocation is prevented by the refined grain boundary and the homogeneous dispersion of Cu_6Sn_5. α phase Cu and β phase Ag are also seen in the evaluation. The formation of Ag_3Sn in the matrix has altered the above properties which resulted in the decrease of melting temperature on addition of Ag incrementally. The reinforcement addition could modify the surface instability and the variation in the physical properties and the grain boundary characteristics.
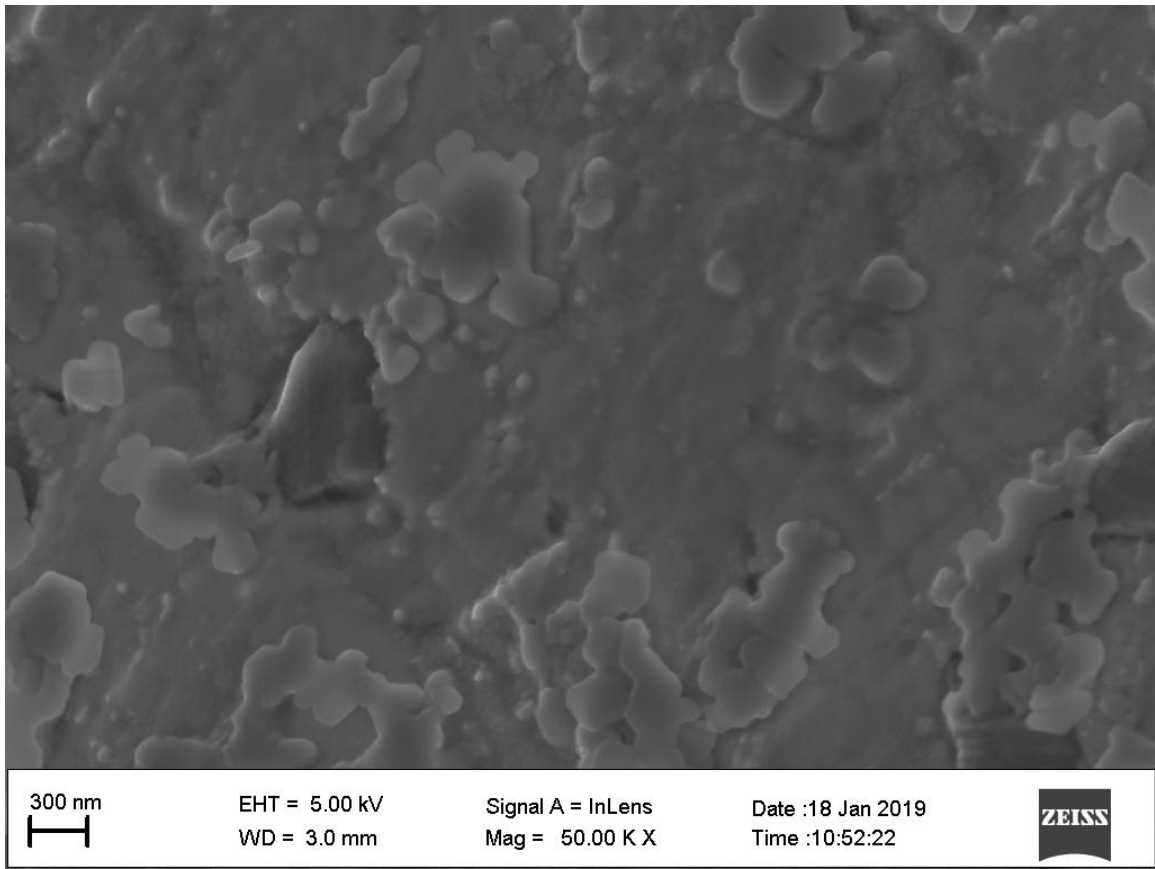
Fig. 5.10 FE SEM image of Sn-0.5Cu-3Bi-1Ag at 50 K

The effect of Ag addition into Sn-0.5Cu-3Bi solder alloy on the microstructure and mechanical properties has been investigated. The addition of Ag resulted in decrease of melting temperature of the solder alloy on increasing concentration. The formation of Ag_3Sn in the matrix has altered the properties which resulted in the decrease of melting temperature on addition of Ag incrementally. The addition of Ag resulted in increase of the microhardness of the solder alloy. The presence of Ag in the solder matrix holds the grain boundaries, about to happen their sliding and allegedly strengthening the microhardness of the composite solder according to the dispersion strengthening mechanism. There is a gain in strength as the grain size decreases. In other words, the hardness of the Sn-0.5Cu-3Bi is found to be increasing with the addition of Ag. Contact

angle is found to be decreasing with the addition of Ag. The addition of Ag can decrease surface tension of the given alloys. The improvement of the wetting behaviour has been observed due to the Ag addition. The improvement on wettability of Sn-Cu-Bi solders can be examined through the outcome of adding Ag to impact the surface tension. The microstructure observations revealed that the Ag was uniformly distributed on the surface of the solder matrix. The mechanical properties are changed due to the different microstructure of the alloys; mainly the change is size of β-Sn grains and IMC particles. Some intermetallic becomes coarse with the increasing of Ag content. The reinforcement addition could modify the surface instability and the variation in the physical properties and the grain boundary characteristics.

The recommended content of the Ag to be added into the Sn-0.5Cu-3Bi solder alloy is 1.0 % by wt. This alloy shows significant increase of mechanical properties and wettability. By analysing the properties it can be considered as a probable substitute to lead–tin alloy. It can be used in the electronic packages in the automobiles where the temperature is relatively high.

CHAPTER 6

EFFECT OF ADDITION OF Ag INTO Sn-1Cu-1Ni (SCN 110)

In chapter 4, new lead free solder alloy- SCN110 is developed. In this chapter, investigation on the effect of silver (Ag) addition on the melting behaviour, microstructure, and microhardness of Ternary lead free solder alloy Sn-1Cu-1Ni is done. The aim of this chapter is to verify whether the addition of Ag into SCN110 improves its property.

6.1   EXPERIMENTAL PROCEDURE

6.1.1   Sample preparation

The most commonly followed method for the preparation of the solder alloys is powder metallurgy. The elements in the composition will be in the form of powder. The constituent elements are melted into the required shape at enhanced temperatures. Sn, Cu, Ni and Ag were made available in the form of powder and are allowed to melt at enhanced temperature of about 1100°C for 45 minutes. This molten material is then transferred into specially designed cylindrical moulds. All these five alloys with variation in the composition of Ag are allowed to quench and were kept in the room temperature for 2 days. Visual analysis of these alloys was conducted for the initial acceptance. These alloys were undergone chemical composition analysis.

6.1.2   Melting temperature analysis

Higher melting temperature of the solder alloy is considered as a bad property citing the fact that the electronic package will fail at higher temperatures. Melting temperature analysis of all the five samples were conducted using Thermo Gravimetric and

Differential Thermal analysis (TG-DTA). Thermo Gravimetric analysis (TGA) measured the weight loss or gain as a function of temperature ,the TGA trace appear as steps, it can be deal with the derivative of TGA with respect to time or temperature. Differential thermal analysis (DTA) is a technique for recording the difference in temperature between a substance and a reference material as a function of time or temperature as the two specimens are subjected to identical temperature regimes in an environment heated or cooled at a controlled rate.

6.1.3   Microhardness measurement and Wetting analysis

Abrasion and wear characteristics of a material can be assessed using hardness analysis. Hardness tests were performed using hardness testing machine. Each Hv value was the average of fifteen different readings which were noted down at random points on the surface of the sample. Sample preparation was done using grinding by taking different grades of SiC papers. Then the samples were polished. The surfaces of the alloys were analyzed in Axio Vertical A1 metallurgical microscope before and after the microhardness test.

Wetting can defined as the ability of the molten solder alloy to react with the bottom substrate. Intermetallic compounds (IMC) are formed which act as the adhesion layer to join the solder and the substrate. The molten sample of the five alloys was spread over the Cu substrate. Then the contact angle is measured. Generally if the wetting or contact angle lies between 0° and 90° the system is said to be wet. If the wetting or contact angle is between 90° and 180° the system is considered to be non-wetting.

6.1.4 Microstructure analysis

Four grades of SiC papers were used for grinding the five alloy samples which is followed by the mechanical polishing with a diamond suspension. 95% ethanol solution/5% HCl is used for chemical etching. . The surface details of the samples were analysed by field-emission scanning electron microscopy (FE-SEM, Carl Zeiss Sigma). All the images were taken at a magnification of 5.00 KX-50KX, scale=1μm, Electron High Tension (EHT) = 5.00 Kv, Working Distance (WD) = 3.2 mm

6.2 RESULTS

6.2.1 Chemical Composition

Five alloy samples were made with different composition. Chemical compositions of the alloys were analysed using ICP-OES. The required chemical composition for the alloys is given in table 6.1The results of the analysis are shown in the table 6.2

Table 6.1 The composition of the alloys required

Solder Alloy	Composition required (%by wt.)			
	Sn	Cu	Ni	Ag
Sn-0.5Cu-1Ni	98	1	1	0
Sn-0.5Cu-1Ni-0.25Ag	97.75	1	1	0.25
Sn-0.5Cu-1Ni -0.5Ag	97.5	1	1	0.5
Sn-0.5Cu-1Nii -0.75Ag	97.25	1	1	0.75
Sn-0.5Cu-1Ni -1Ag	97	1	1	1

Table 6.2 Chemical composition analysis Results

Solder Alloy	Chemical Composition results (% by wt.)			
	Sn	Cu	Ni	Ag
Sn-1Cu-1Ni	97.9622	1.018	0.9987	0
Sn-1Cu-1Ni-0.25Ag	97.6236	0.9987	1.0456	0.2321
Sn-1Cu-1Ni -0.5Ag	97.4534	1.0534	0.9875	0.4857
Sn-1Cu-1Ni -0.75Ag	97.2445	1.0134	0.9523	0.7798
Sn-1Cu-1Ni -1Ag	**96.975**	**0.9895**	**0.9675**	**1.058**
Sn-1Cu-1Ni -1.25Ag	96.6945	1.0634	0.9843	1.2478
Sn-1Cu-1Ni -1.5Ag	96.3288	0.9911	1.0745	1.5056
Sn-1Cu-1Ni -1.75Ag	96.1095	1.0634	0.9819	1.7452

6.2.2   Melting Temperature

The melting points of all the five samples were tested using TGA analysis. The results were noted down and a comparison is shown in the figure 6.1. The results are shown in table 6.3 It can be seen that the melting temperature of Sn-Cu-Ni alloy is 232.2 ° C. The melting temperature of Sn-Cu-Ni-xAg (x= 0.25, 0.5, 0.75,1 wt. %) are 231.2° C, 230.1° C, 229.4° C, 228.7° C respectively. So it can be concluded that with the addition of Ag into Sn-Cu-Ni, the melting temperature is decreasing by a maximum of 4 degrees. The distance between the adjacent atoms and the root mean vibration amplitude determines the melting temperature property. Ag_3Sn formed in the matrix has changed the melting point characteristics which resulted in the slight decrease of the melting temperature. The undercooling of Sn-Cu-Ni solder material is found to be decreasing slightly with the addition of Ag

Table 6.3 Melting temperature of Sn-1Cu-1Ni-xAg

Solder Alloy	Melting Temperature (°C)
Sn-1Cu-1Ni	232.2
Sn-1Cu-1Ni-0.25Ag	231.2
Sn-1Cu-1Ni -0.5Ag	230.1
Sn-1Cu-1Ni -0.75Ag	229.4
Sn-1Cu-1Ni -1Ag	228.4
Sn-1Cu-1Ni -1.25Ag	228.6
Sn-1Cu-1Ni -1.5Ag	228.5
Sn-1Cu-1Ni -1.75Ag	228.3
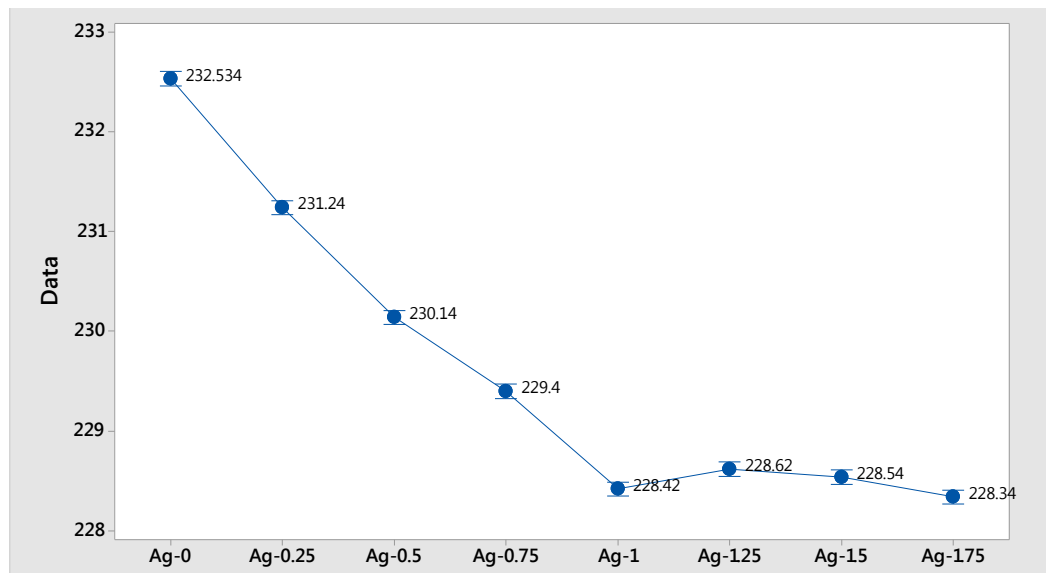
Fig. 6.1 Melting temperature variation of Sn-1Cu-1Ni-xAg
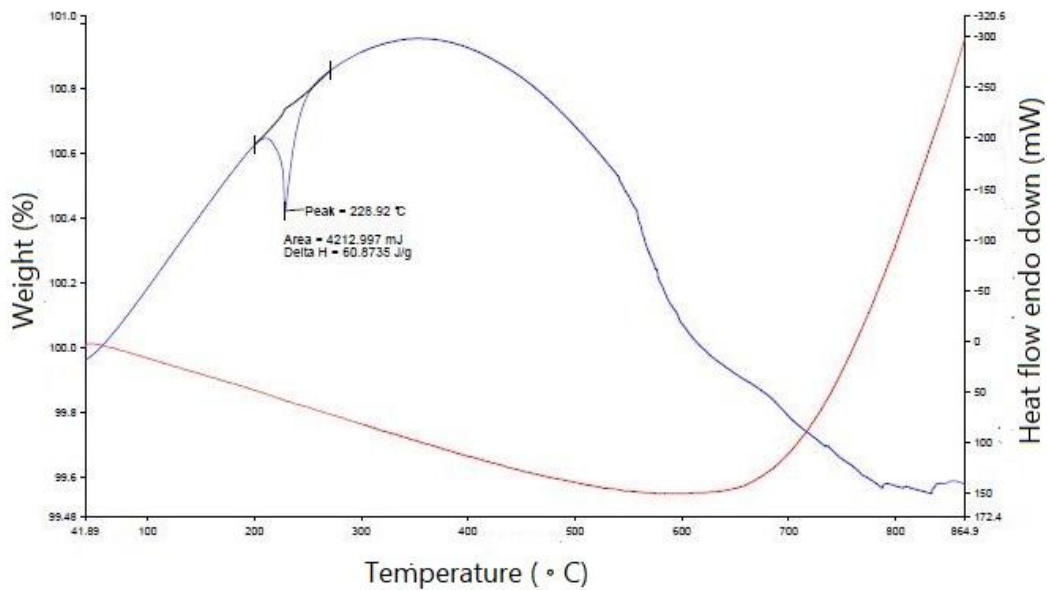
Figure 6.2 TGA plot for Sn-1Cu-1Ni-1Ag sample

6.2.3 Hardness and Wetting

Hardness value and contact angle measured are tabulated in the table 6.4. Contact angle as a function of Ag addition to the Sn-Cu-Ni solder is shown in the figure 6.3. It can be seen that the contact angle of Sn-Cu-Ni alloy is 36.75°. The contact angle of Sn-Cu-Ni-xAg (x= 0.25, 0.5, 0.75,1 wt. %) are 27.54°, 26.44°, 24.12° and 22.87° respectively .Therefore, the contact angle is getting reduced as the Ag is added.

It can be seen that the hardness value increases with the addition of Ag into the Sn-1Cu-1Ni alloy. The hardness value of Sn-Cu-Ni alloy is found to be 16.1 Hv, and when 1% of Ag is added to this alloy, hardness value is found to be increased to 19.2 Hv. A comparison of microhardness value of these five alloys with SAC305 and SAC405 were also conducted. The microhardness property values of SAC305 and SAC 405 were taken as 13.47Hv and 13.98 Hv. Comparison of variation of hardness of the alloy with percentage of Ag addition is shown in figure 6.2.

103

Table 6.4 Contact angle and hardness of Sn-1Cu-1Ni-xAg

Solder Alloy	Contact angle (°)	Hardness (Hv)
Sn-1Cu-1Ni	36.75	16.1
Sn-1Cu-1Ni-0.25Ag	27.54	16.3
Sn-1Cu-1Ni -0.5Ag	26.44	17.5
Sn-1Cu-1Ni -0.75Ag	24.12	18.7
Sn-1Cu-1Ni -1Ag	**22.87**	**19.2**
Sn-1Cu-1Ni -1.25Ag	24.56	19.4
Sn-1Cu-1Ni -1.5Ag	24.67	19.1
Sn-1Cu-1Ni -1.75Ag	25.06	19.4
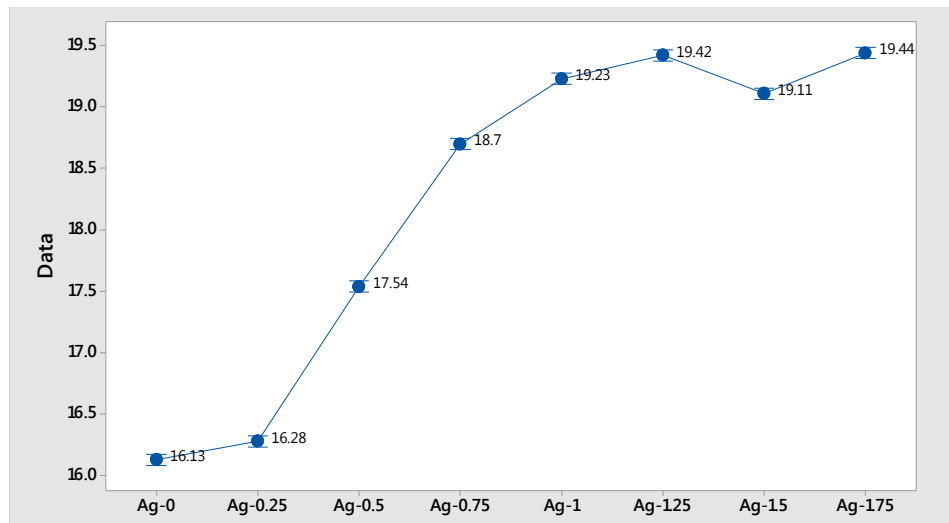
Fig. 6.3 Hardness variations of Sn-1Cu-1Ni-xAg
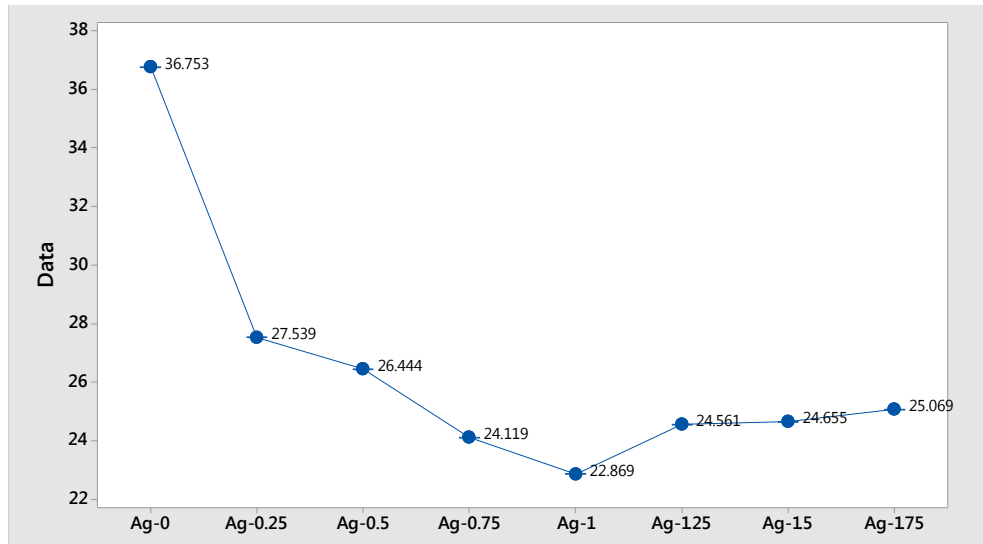
Fig. 6.4 Contact angle variation of Sn-1Cu-1Ni-xAg

6.2.4 Shear strength

Shear strength tests of the samples with different amount of Ag are conducted using the method explained in the above section. The results of the analysis are noted and are given in the table 6.5. Following strengthening mechanisms can be identified as the reason for improvement in the mechanical properties. Geometrically similar dislocations generated which accommodate the elastic modulus and thermal modulus mismatch. The results obtained are shown in the figure 6.4. The dispersion hardening with the addition may be a reason for the increase in the shear strength. With the addition of Ag, the density of the alloy is also found to be increasing slightly. The ultimate shear stress of Sn-1Cu-1Ni is found to be increased by 8.3% by wt. with 1% addition of Ag.

Table 6.5 Shear strength results of the alloys

Solder Alloy	Ultimate Shear stress (MPa)
Sn-1Cu-1Ni	27.4
Sn-1Cu-1Ni-0.25Ag	27.2
Sn-1Cu-1Ni -0.5Ag	28.3
Sn-1Cu-1Ni -0.75Ag	29.2
Sn-1Cu-1Ni -1Ag	**29.7**
Sn-1Cu-1Ni -1.25Ag	29.5
Sn-1Cu-1Ni -1.5Ag	29.9
Sn-1Cu-1Ni -1.75Ag	29.5
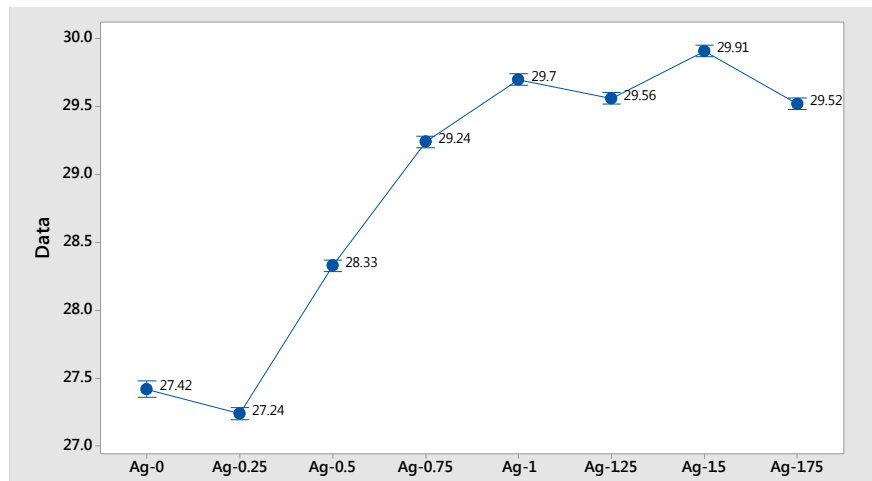
Fig. 6.5 Variation of shear strength of the alloys.

6.2.5 Impact toughness

Impact toughness tests for all the samples with different amount of Ag are conducted using Charpy impact test explained in the previous section. The energy absorbed by the

test specimen gives idea about the impact toughness. The results obtained are given in the table 6.6. The results obtained are shown in the figure 6.5.The samples which are able to absorb more impact energy during the conduction of impact test will be considered as materials having more impact toughness. The microstructure also will have close relation with the impact toughness. Charpy test is the apt test for determining the impact toughness of the solder alloy. Even if we are using large test specimens for the test when compared to the solder joints, the strain rate experiencing in the both cases are matching. The impact toughness of Sn-1Cu-1Ni is found to be increased by 3.1% with the addition of 1% by wt. Ag.

Table 6.6 Impact toughness test results of the alloys

Solder Alloy	Impact Toughness (J)
Sn-1Cu-1Ni	9.4
Sn-1Cu-1Ni-0.25Ag	9.7
Sn-1Cu-1Ni -0.5Ag	9.8
Sn-1Cu-1Ni -0.75Ag	9.9
Sn-1Cu-1Ni -1Ag	**10.1**
Sn-1Cu-1Ni -1.25Ag	10.1
Sn-1Cu-1Ni -1.5Ag	9.9
Sn-1Cu-1Ni -1.75Ag	9.7
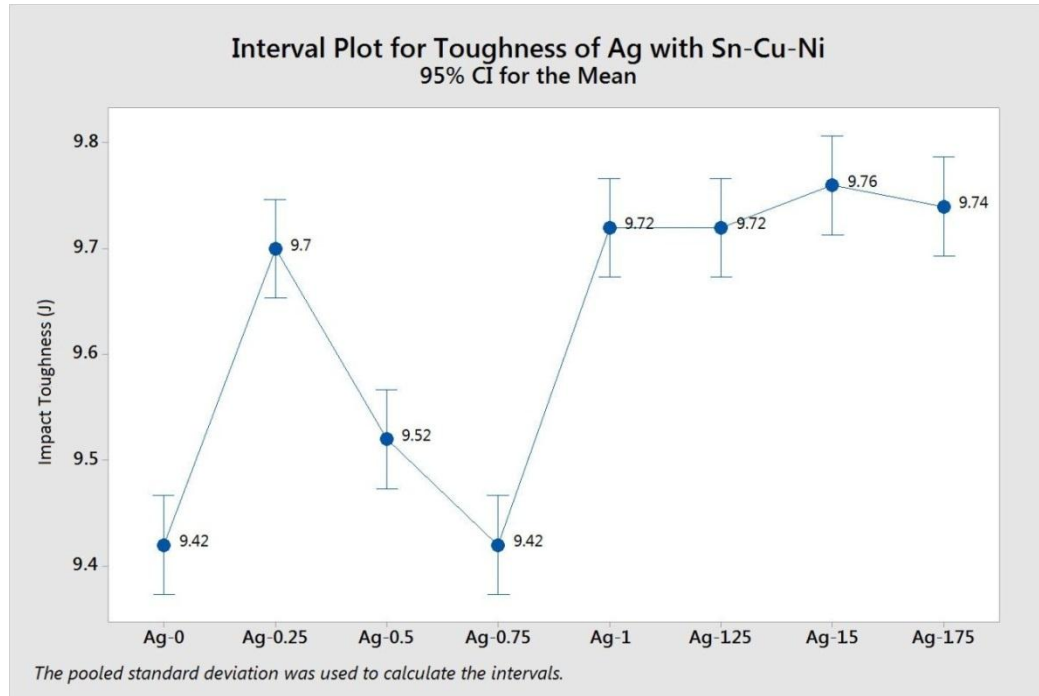
Fig. 6.6 Impact toughness test results

6.2.6 Microstructure analysis

The microstructure analysis of alloys has as far as the knowledge the coarse β Sn grains. Ag_3Sn, Cu_6Sn_5 and tin in the alloys are found in the eutectic region. The refinement of β-Sn grains is happened in a good manner due to the addition of particle of Ag. Ag is found to be uniformly distributed on the solder matrix which can be observed from the microstructure analysis. Eutectic bands are found to be becoming narrow. The refined grain boundary is the reason for the slipping of the dislocation prevention. Another reason is the Cu_6Cu_5 dispersion at the grain boundary of β-Sn dendrites in a uniform fashion. Evaluation also revealed the α phase Cu and β phase Ag. The FE-SEM image of Sn-Cu-Ni when 1% by wt. Ag added is shown in the figure 6.6.
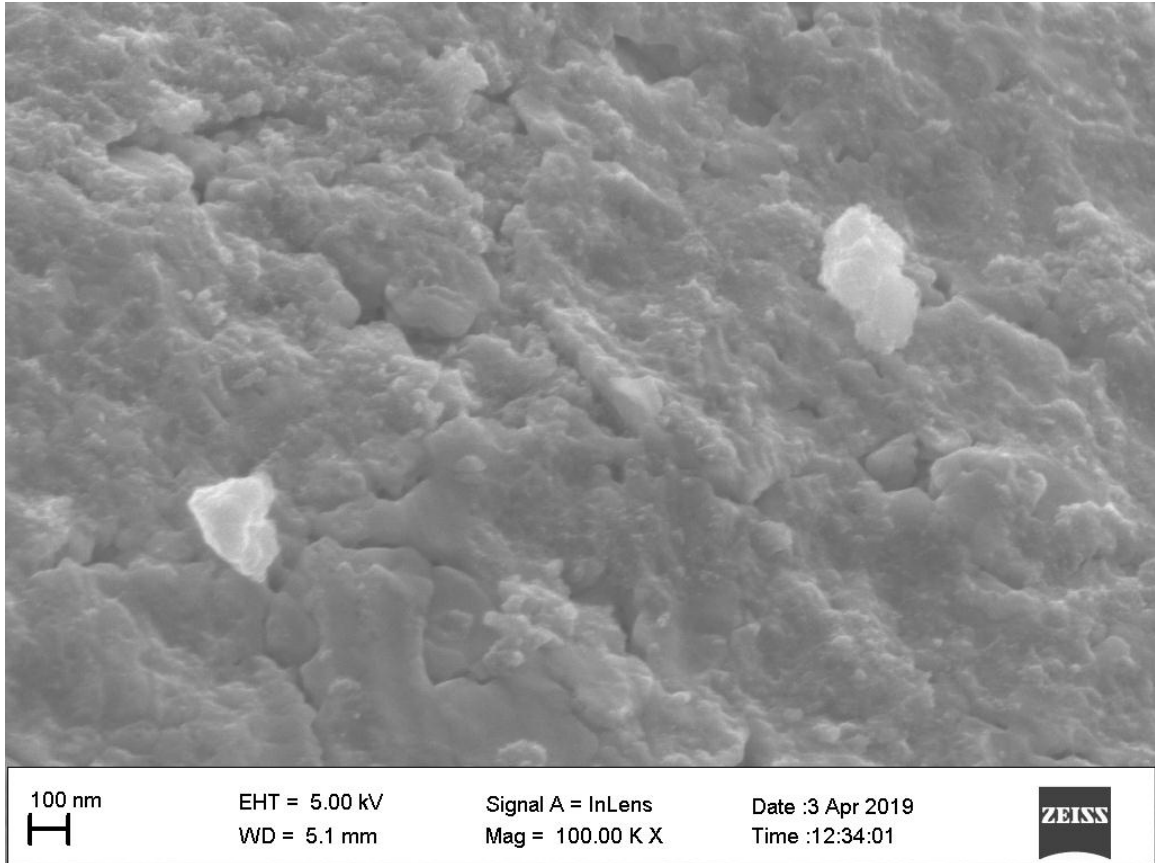
Fig. 6.7 Microstructure of the alloy at 50K X

Effect of addition of Ag into SCN110 is investigated. Ag is added in 0.25, 0.5, 0.75, 1, 1.25, 1.5, and 1.75 % by wt. into the alloy. Melting temperature, hardness, contact angle, shear strength and impact toughness of these properties were analyzed. From the investigation, it is found that optimum amount of Ag that should be added is 1% by wt. Melting point decreased from 232.2°C to 228.4°C, hardness increased from 16.1 Hv to 19.2 Hv, and contact angle reduced from 36.75° to 22.87°. These are the basic mechanical properties that should be satisfied. Shear strength and impact toughness are found to be increased from 27.4MPa to 29.7MPa and 9.4 J to 10.1 J respectively. Microstructures of the alloys are also studied. Therefore with addition of 1% by wt. of

Ag, the properties of SCN110 are found to be enhanced. Sn-1Cu-1Ni-1Ag can be considered as a potential candidate for lead free solder alloy.

CHAPTER 7

INVESTIGATION ON CORROSION PROPERTIES OF

Sn-0.5Cu-3Bi-xAg

SAC305 and SAC405 are famous alloys which came as a replacement of Sn-Pb alloy. There is a threat in the usage of SAC in medical field. The medical devices fabricated using Sn-Cu-Ag has more chances of failure due to ECM (Electro Chemical migration). Continuous and slow decay of metals by the action of the surrounding medium like air, water or salt solution is known as corrosion .The corrosion resistance property of the solder alloy is another vital property which determines the life of the alloy. NaCl solution (3.5 % by wt.) is used for conducting the test. This is an accelerated test for 7 and 14 days which give information about the solder alloy. Sn-0.5-3Bi is a new solder alloy. The addition of Ag into the Sn-0.5Cu-3Bi has improved the properties. In this chapter, the corrosion characteristics of Sn-0.5Cu-3Bi-1Ag are analyzed. These results are compared with Sn-0.5Cu-3Bi and Sn-0.5Cu-3Bi-0.5Ag compositions. Weight loss method and current density measurements are the corrosion analysis techniques. Both the methods a can be equated with some conversion factors. Weight loss method is used in the present study. The specimens were prepared and immersed in 3.5% by wt. NaCl solution. This can be considered as an acceleration test. Weights of the specimen before and after immersion (after removing the corrosion products) with 7 days and 14 days were noted down. From this output, corrosion rate (CR) is calculated. The EDS analysis of the surface, FE-SEM analysis and the colour mapping were also done and reported. The results were compared with SAC305.

7.1 EXPERIMENTAL PROCEDURE

7.1.1 Specimen Preparation

The sample specimens were in the form of coupons whose dimensions are as per the figure 7.1. The samples were produced from pure metals (Sn, Cu, Bi and Ag) which were in the powder form. Five samples were prepared for each of the alloy composition - Sn-0.5Cu-3Bi-xAg (x = 0, 0.5, 1 % by wt.). The specimens were prepared using an induction furnace with Argon gas to avoid contaminations. The specimens were kept in room temperature for two days. The surface of the specimen was also undergone visual inspection to avoid any surface defects. The samples were polished thoroughly using SiC paper, washed and cleaned with deionized water and methanol. Sodium chloride powder (Merck) was dissolved in deionized water to make 3.5 wt.% NaCl solution. The solders materials were then immersed into the solution (corrosive) for 7 and 14 days. After immersion for the required period of time, the samples which are corroded were carefully extracted from their containers.
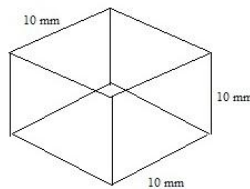
Fig. 7.1 Dimensions of the coupon used.

7.1.2 Weight loss method

In order to study the effect of corrosion on the specimens, there are two methods generally used. One is the weight loss method and the other one is current density method. In the former method, the specimens were immersed in the concerned liquid for some previously determined time. Weight of the sample before and after the procedure will be noted down. Based on this information, the corrosion rate can be found our using the following equation.

$$CR = \frac{w}{At} \qquad\qquad (7.1)$$

Where, CR – Corrosion rate

     w- Weight loss

     A – Area exposed

     t- Time of exposure

In weight loss method, the corrosion is expressed in terms of mdd (1mg/decimeter^2/1day). The SI unit is g/m^2/day. The area is added to the rate of corrosion equation; reason that, more surface exposure will lead to more dissolution. Thus the equation is normalized with area.

Weight loss method and current density method are same for measuring the corrosion characteristics. These two methods can be related by some conversion forms.

All the specimens were immersed in NaCl solution for 7 days and 14 days. The weight of the specimen before and after the immersion was noted. The corrosion media used in the experiment was 3.5 % by wt. NaCl solution. This was used to simulate the sea water. The weights of the specimens were noted down.

7.2 RESULTS AND DISCUSSIONS

7.2.1 Weight loss method results

The weight of the specimens before and after immersing for 7 days and 14 days are shown in the table 7.1. The weight loss of the specimen was noted down. Using the weight loss data, area of exposure of the specimen and the time of exposure (7 and 14 days), the corrosion rate (CR) is calculated in gmd ($g/m^2/day$). It is observed that the mean CR for Sn-Cu-Bi is 3.6386 gmd and 3.5643 gmd for 7 days and 14 days respectively. In the case of Sn-Cu-Bi-0.5Ag, 3.2643 gmd and 3.2464 are the mean CR values for 7 and 14 days respectively. The solder alloy in which more focus is given i.e. Sn-Cu-Bi-1Ag have 3.0929 gmd and 3.0726 gmd as the average CR values with the exposure of 7 and 14 days in order. The corrosion rate of a specific alloy remains almost same with 1 week and 2 weeks exposures. With the addition of Ag, the corrosion rate is found to be decreasing.

Table 7.1 The weight loss analysis results and the CR calculation results

Solder Alloy	Initial weight (gm)	Weight (7 Days) (gm)	Weight (14 days) (gm)	Corrosion rate (7 days) (gmd)	Corrosion rate (14 days) (gmd)
Sn-Cu-Bi-0Ag	7.3249	7.3149	7.3052	3.6386	3.5643
	7.3032	7.2929	7.2828		
	7.3103	7.3001	7.2902		
	7.2903	7.27996	7.2703		
	7.3201	7.31	7.3005		
Sn-Cu-Bi-0.5Ag	7.3351	7.3259	7.3169	3.2643	3.2464
	7.3162	7.3072	7.298		
	7.3051	7.2959	7.2869		
	7.3112	7.3021	7.2931		
	7.3213	7.3121	7.3031		
Sn-Cu-Bi-1Ag	7.3453	7.3366	7.3283	3.0929	3.0786
	7.3123	7.3037	7.2954		
	7.3053	7.2967	7.2878		
	7.3313	7.3226	7.3135		
	7.3233	7.3146	7.3063		

7.2.2   Microstructure analysis

Microstructure and EDS analysis results were collected. The EDS analysis results of the surface are shown in the figures 7.2-7.4. Results for the 7 days exposure and 14 days exposure are shown in each figure. Sn is the most electrochemically active element than the Ag_3Sn and Cu_6Sn_5. Therefore the first to be dissolved will be Sn.

The cathodic reaction happening can be shown as:

$$O_2 + 2H_2O + 4e^{-} \rightarrow 4OH^{-} \tag{7.1}$$

$$2H_2O + 2e^{-} \rightarrow H_2 + 2OH^{-} \tag{7.2}$$
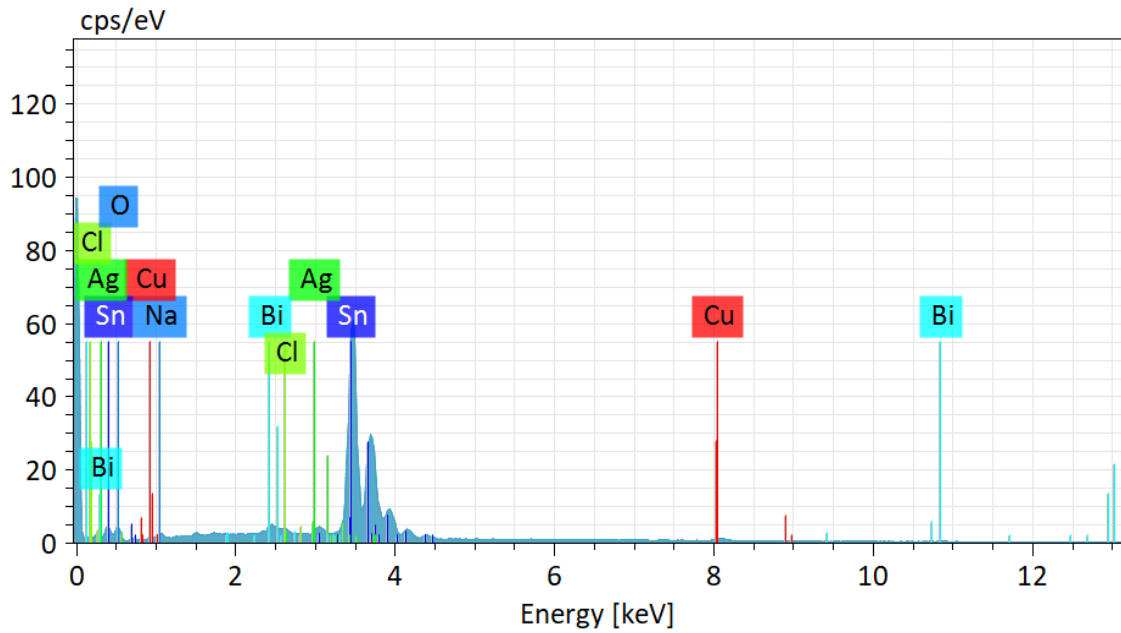
Fig. 7.2a EDS results of Sn-Cu-Bi samples immersed in 3.5% NaCl solution for 7 days
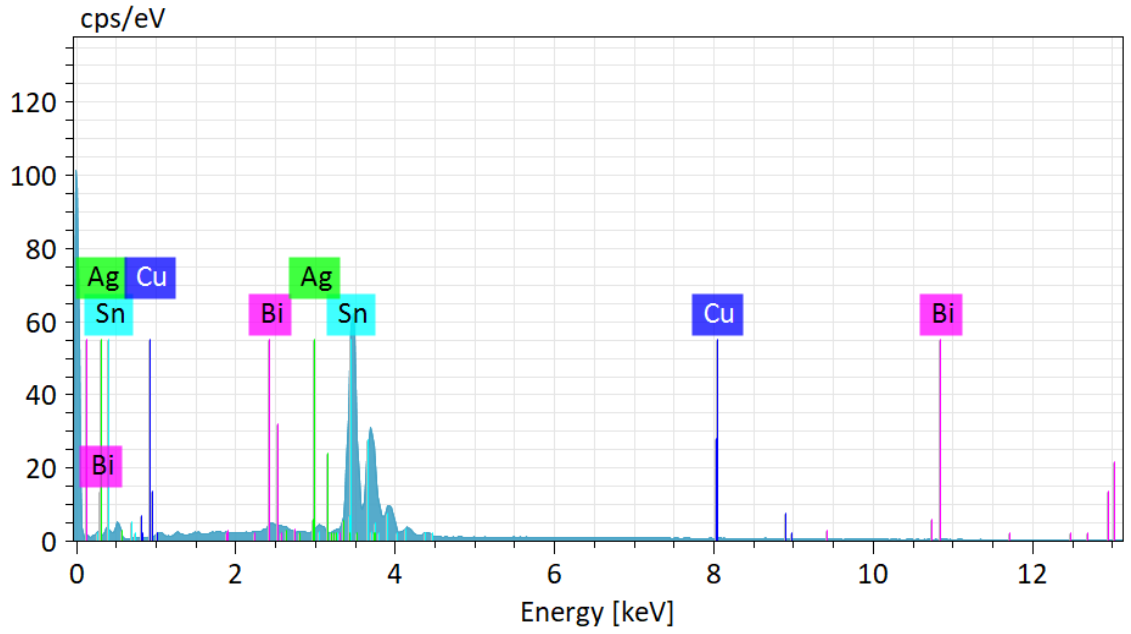
Fig. 7.2b EDS results of Sn-Cu-Bi samples immersed in 3.5% NaCl solution for 14 days
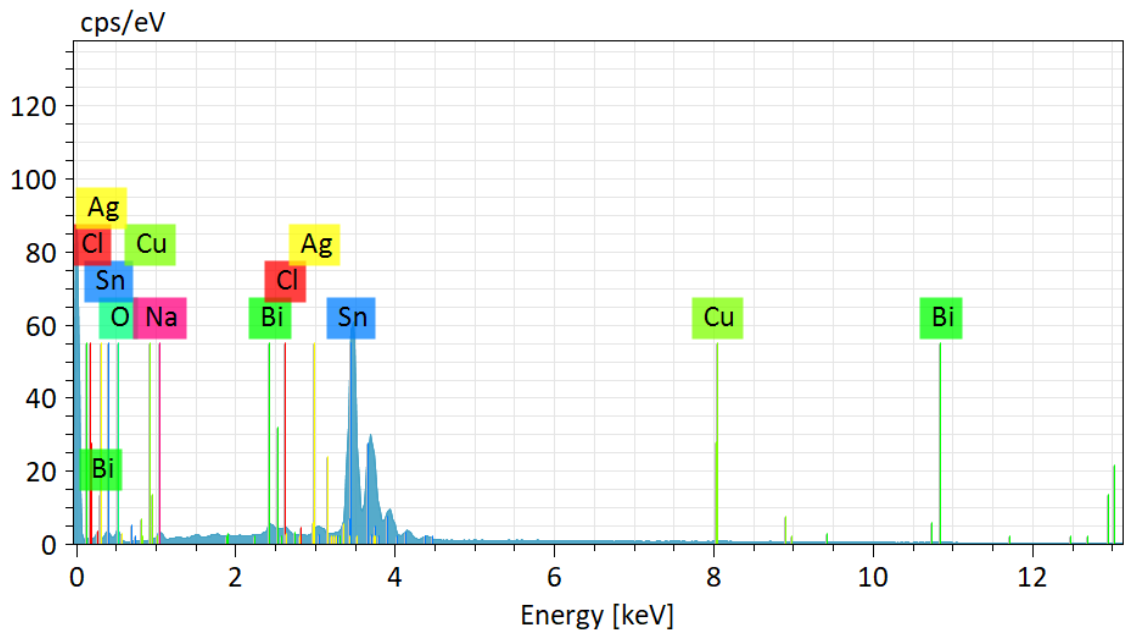
Fig. 7.3a EDS results of Sn-Cu-Bi-0.5Ag samples immersed in 3.5% NaCl solution for 7 days
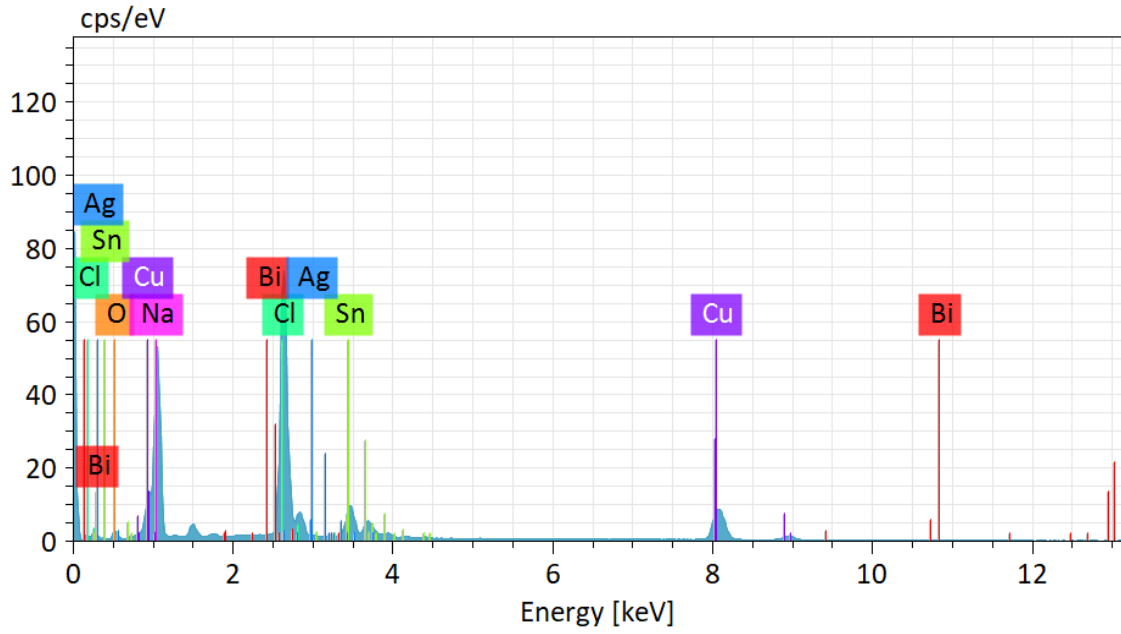
Fig. 7.3b EDS results of Sn-Cu-Bi-0.5Ag samples immersed in 3.5% NaCl solution for 14 days
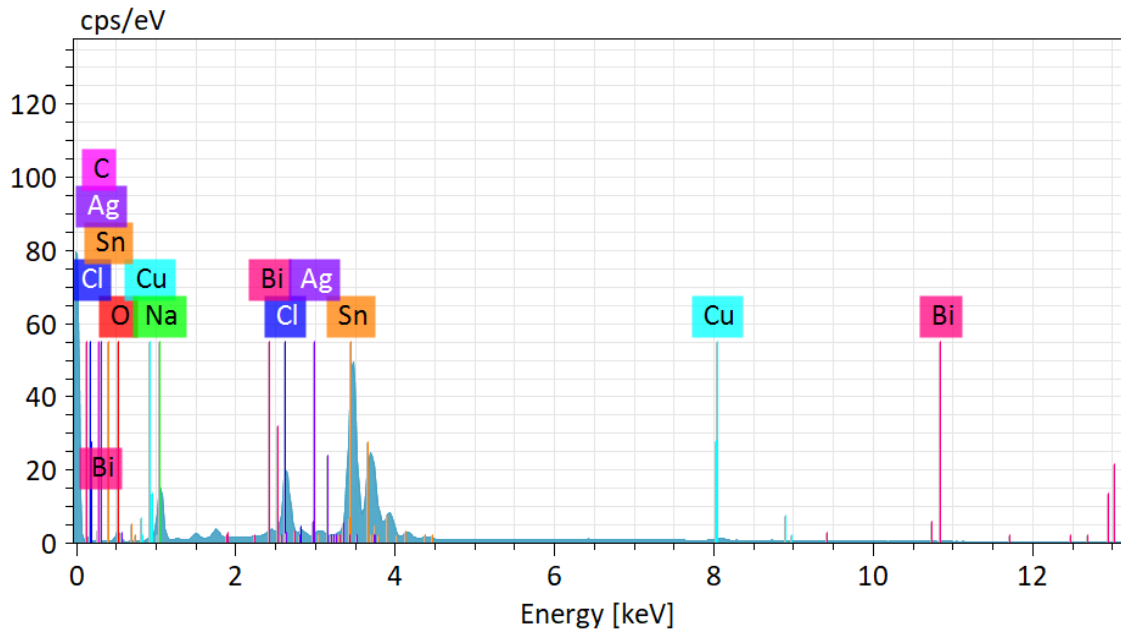
Fig. 7.4a EDS results of Sn-Cu-Bi-1Ag samples immersed in 3.5% NaCl solution for 7 days
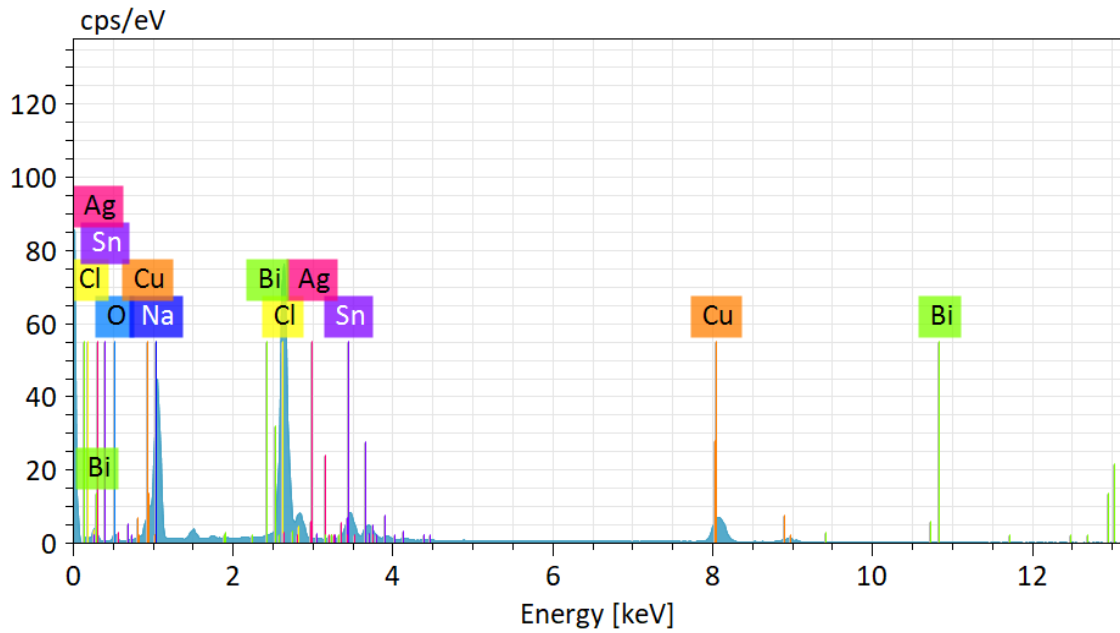
Fig. 7.4b EDS results of Sn-Cu-Bi-1Ag samples immersed in 3.5% NaCl solution for 14 days

The anodic reaction can be found as:

$$Sn + 2OH^- \rightarrow Sn(OH)_2 + 2e^- \tag{7.3}$$

$$Sn + 4H_2O \rightarrow Sn(OH)_4 + 4e^- + 4H^+ \tag{7.4}$$

$$Sn(OH)_2 + 2OH^- + 2e^- \rightarrow Sn(OH)_4 \tag{7.5}$$

$$Sn(OH)_2 + 2OH^- \rightarrow SnO + H_2O \tag{7.6}$$

$$Sn(OH)_4 \rightarrow SnO_2 + 2H_2O \tag{7.7}$$
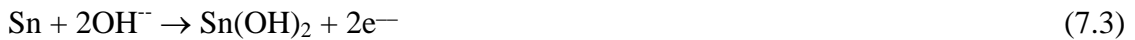
The FE-SEM images obtained at 50K X for Sn-Cu-Bi, Sn-Cu-Bi-0.5Ag and sn-Cu-Bi-1Ag resolution is given in the figure 7.5. The presence of dendrites can be easily

identified from the analysis. These dendrites are very different from the tin whiskers. The shape, mechanism of growth, direction of growth makes the dendrites differ from the tin whiskers. The growth mechanism of tin whiskers is unknown. Due to the migration of metallic ions from anode to cathode, the dendrites grows from cathode to anode direction (Meschter et al., 2014) .$Sn_3O(OH)_2Cl_2$ (tin oxide chloride hydroxide) are the main corrosion product identified which are in the form of shape similar to platelet with different orientations distributed on the surface (Lawson, 2007). Ag_3Sn, Cu_6Sn_5, SnO, SnO_2 can be found on the surface of the alloys. The reduction in the value of CR with the addition of Ag can be connected to the formation of Ag_3Sn and Cu_6Sn_5 which accelerates the resistance to the surface. The colour electron microscopy of Sn-0.5Cu-3Bi-1Ag for 7 days and 14 days exposure is given in the figure 7.6 and 7.8. The element wise colour mapping of the same has been provided in the figure 7.7 and 7.9.
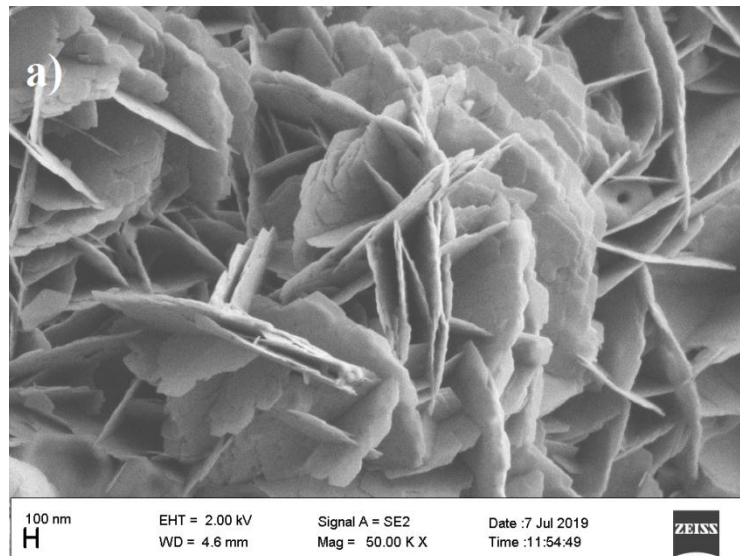
Fig. 7.5a FE SEM image of Sn-Cu-Bi immersed in 3.5% NaCl solution for 14 days
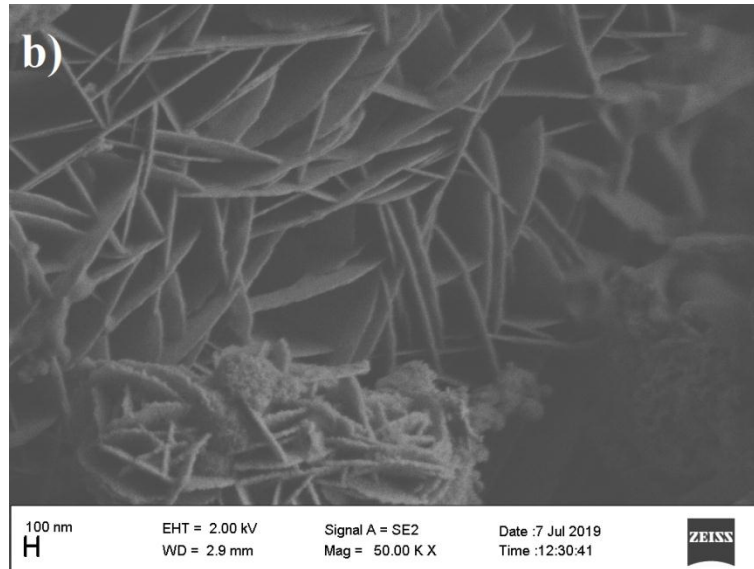
Fig. 7.5b FE SEM image of Sn-Cu-Bi-0.5Ag immersed in 3.5% NaCl solution for 14
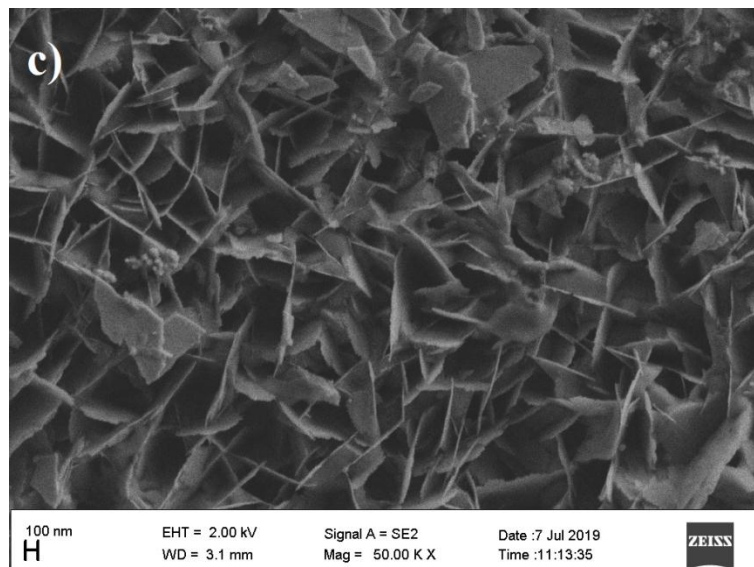
days

Fig. 7.5c FE SEM image of Sn-Cu-Bi-1Ag immersed in 3.5% NaCl solution for 14 days
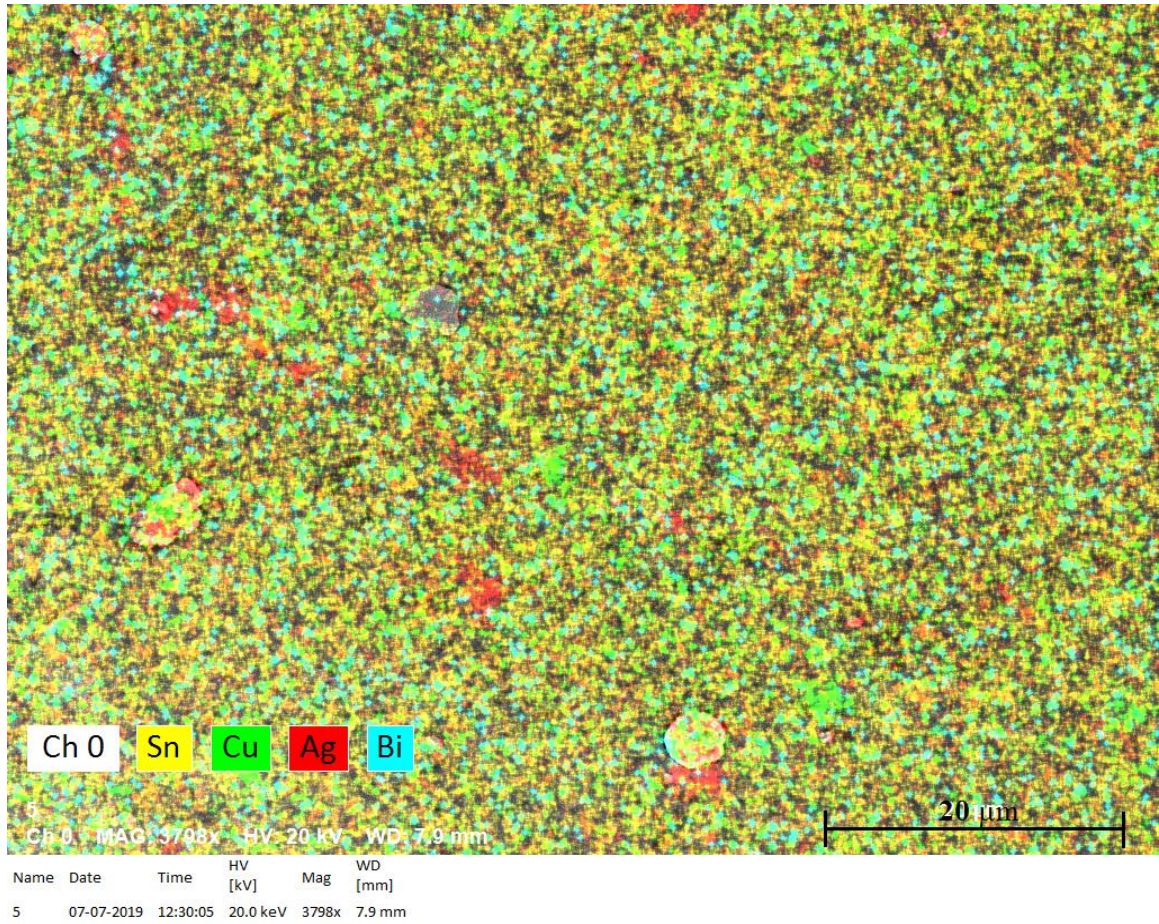
Fig. 7.6 Multicolour element mapping of Sn-Cu-Bi-1Ag immersed in 3.5% NaCl solution
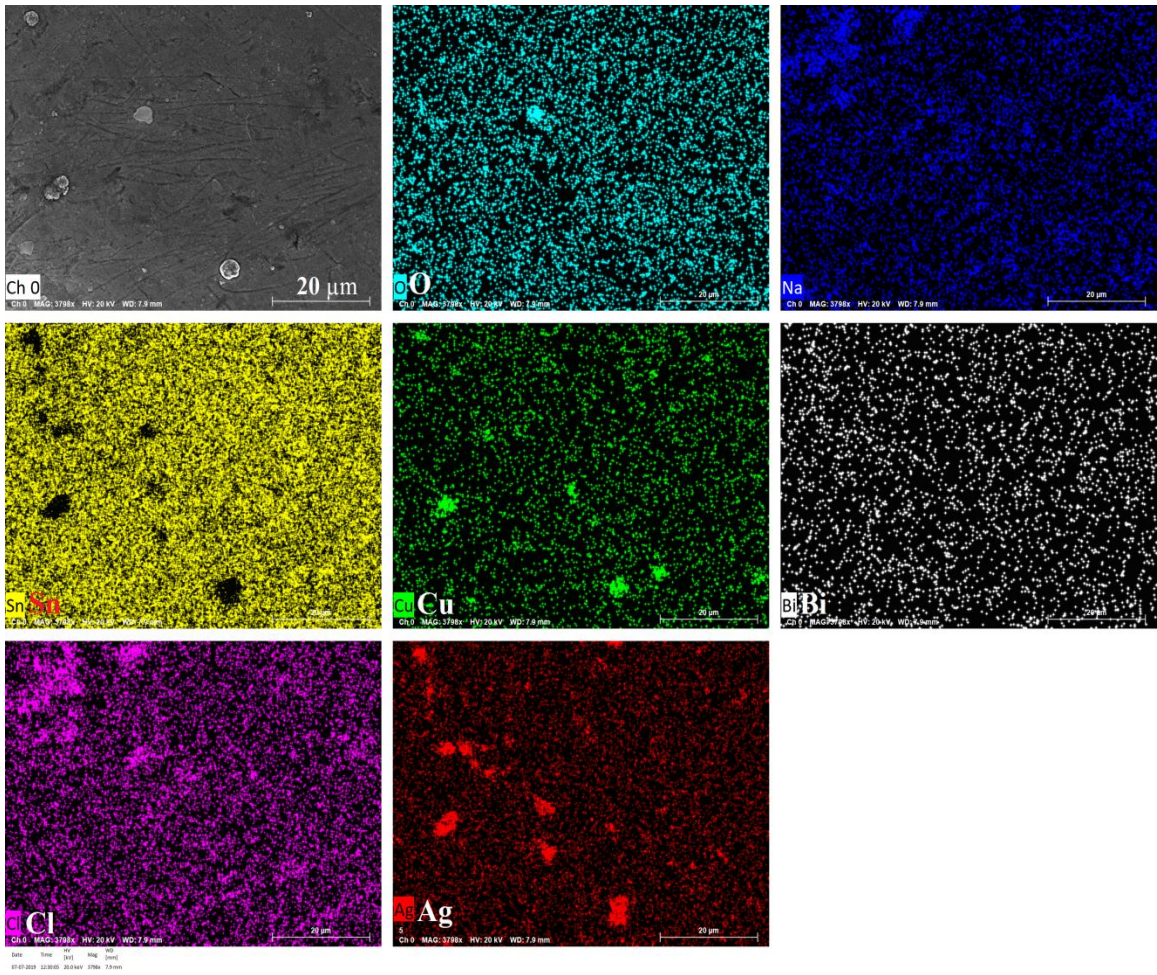
after 7 days

Fig. 7.7 Element wise colour mapping of Sn-Cu-Bi-1Ag immersed in 3.5% NaCl after 7 days
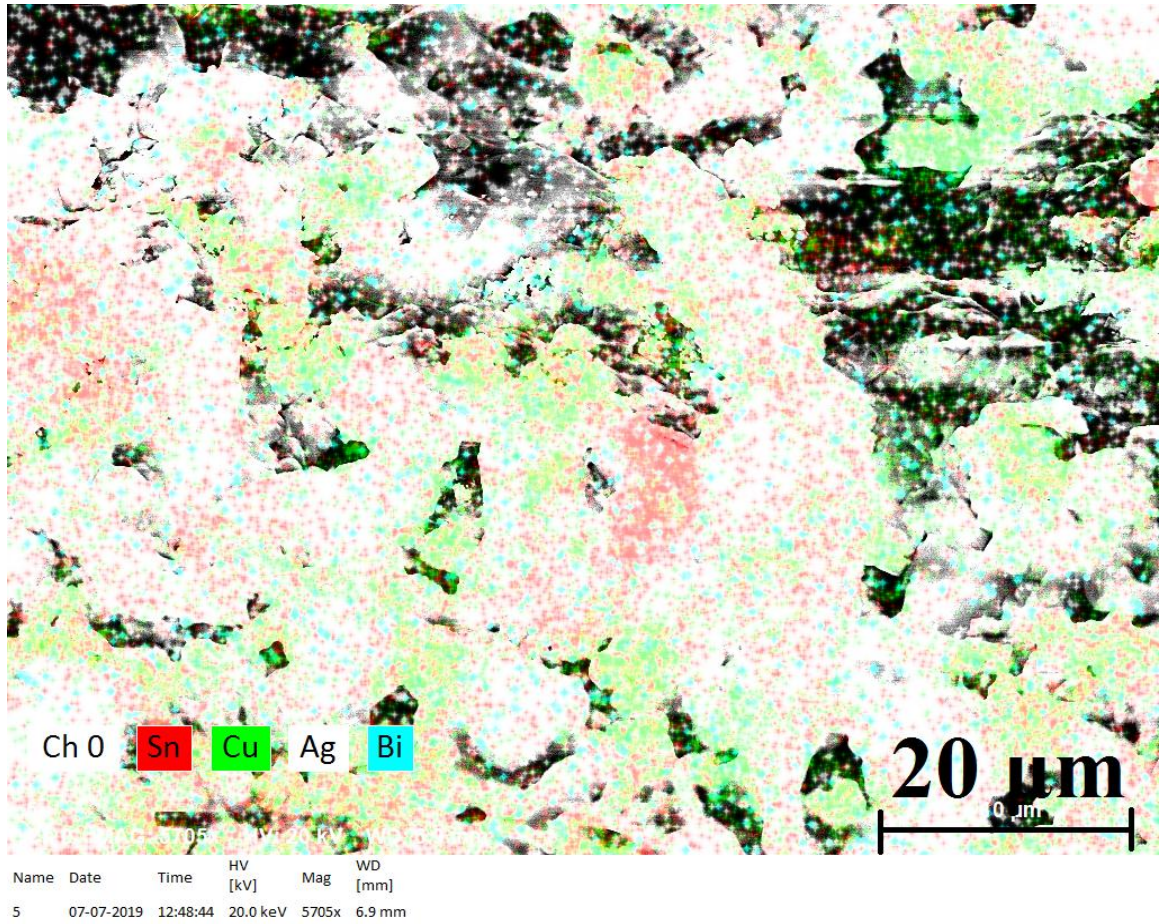
Fig. 7.8 Multicolour element mapping of Sn-Cu-Bi-1Ag immersed in 3.5% NaCl solution
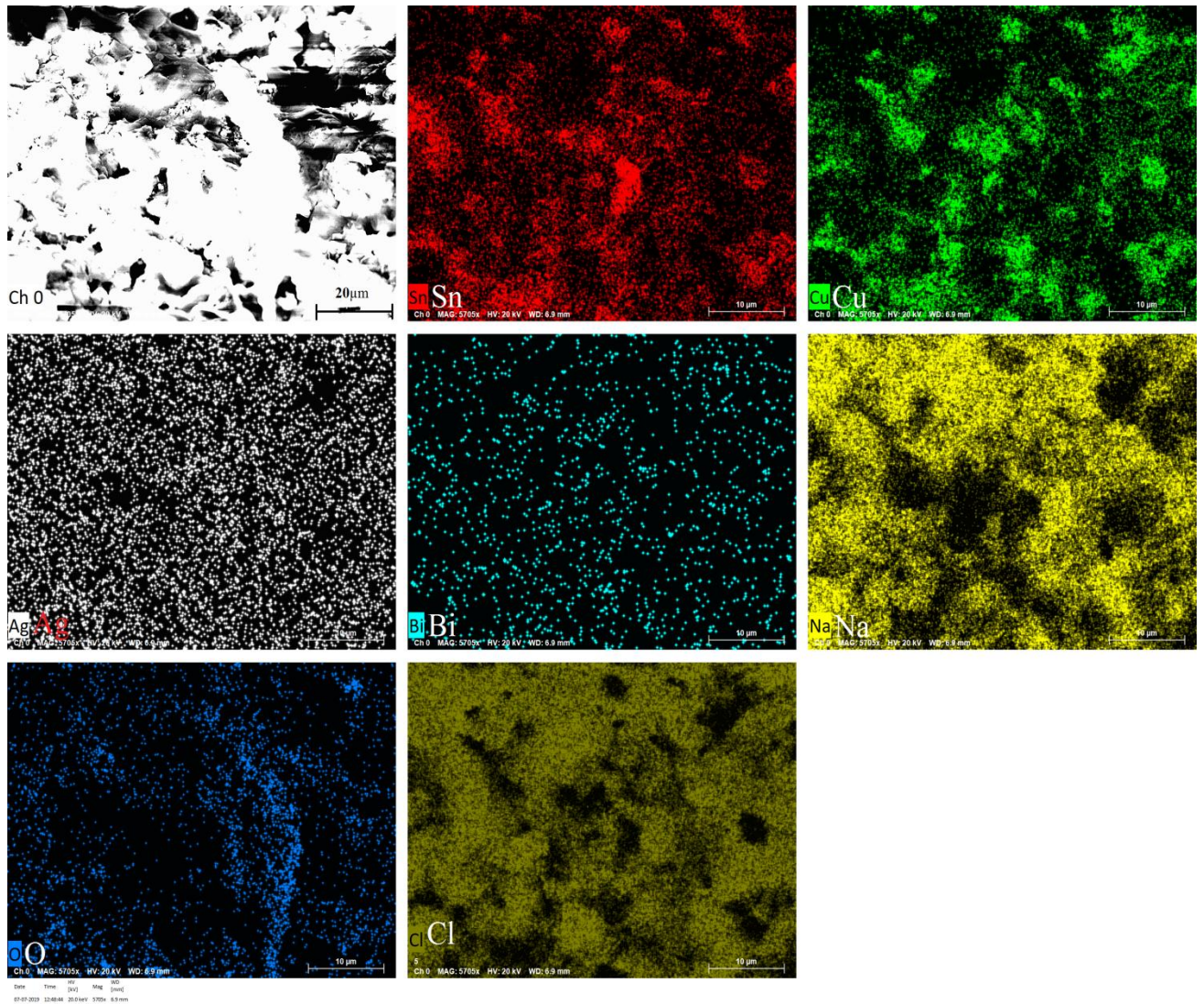
after 14 days

Fig. 7.9 Element wise colour mapping of Sn-Cu-Bi-1Ag immersed in 3.5% NaCl solution

after 14 days
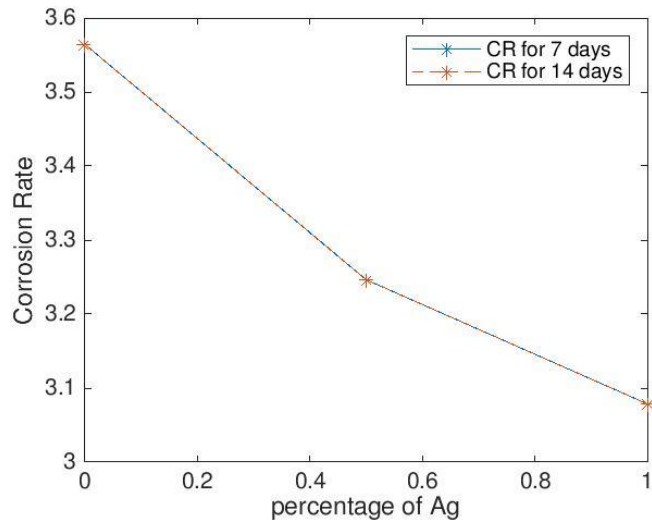
Fig. 7.10 Corrosion rate of the alloys for 7days and 14 days
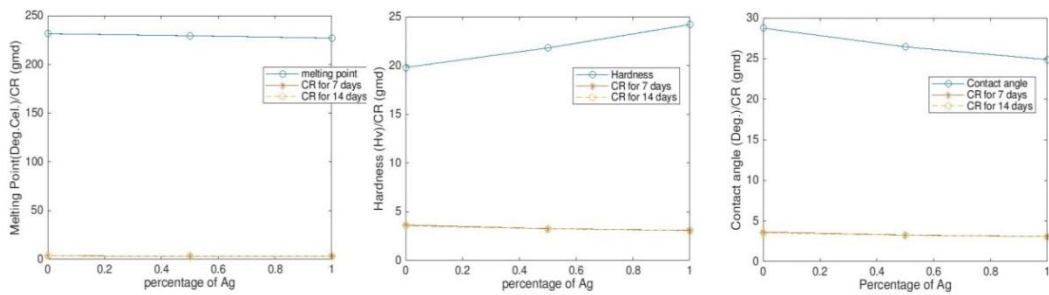
Fig. 7.11 Comparisons of properties of Sn-0.5Cu-3Bi-xAg and the corrosion rates.
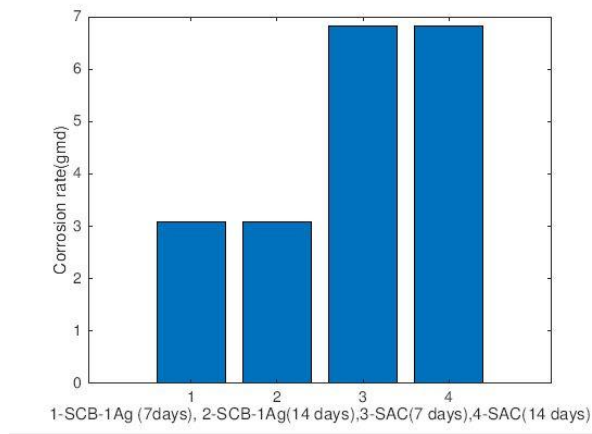
Fig. 7.12 Comparisons of Sn-0.5Cu-3Bi-1Ag and SAC305

Comparisons of properties of Sn-0.5Cu-3Bi-xAg and the corrosion rates is shown in the figure 7.11. The corrosion rates of Sn-0.5Cu-3Bi-1Ag are compared with SAC alloy and are shown in the figure 7.12. The corrosion rate is found to be lesser for Sn-0.5Cu-3Bi-1Ag. Therefore the new alloy is corrosion resistant. It was reported that Sn-phase rich outer layer and Pb-rich inner layer were found as the corrosion product of Sn-Pb solder alloy. The Pb-rich layer present is a threat to the resistance to corrosion (Dezhi et al., 2008). The addition of Ag into SCB305 alloy increased the mechanical properties and wetting characteristics. This chapter investigated experimentally the corrosion characteristics of Sn-0.5Cu-3Bi-xAg (x=0, 0.5, 1 % by wt.) in 3.5% by wt. NaCl solution for 7 days and 14 days by finding the weight loss. This can be considered as an accelerated corrosion test. With the addition of Ag into the alloy, the corrosion rate is found to be decreasing. For Sn-0.5Cu-3Bi-1Ag, corrosion rate is less when compared to x=0 and x = 0.5 %. Figure 7.10 shows the corrosion rate of the specimens for 1 week and 2 weeks. The corrosion rate decreases with increase in the Ag and corrosion rate is almost constant for 7 and 14 days. The comparison of corrosion rates and mechanical properties are shown in figure 11. It was reported that due to lower passivation current density, lead free solder joints displays much better resistance to corrosion than SAC solder alloy in 3.5 % Nacl Solution. Sn-Ag have more resistance than Sn-Cu-Ag and Sn-Cu (Dezhi et al., 2008). Figure 12 shows the comparison of corrosion rates of Sn-0.5Cu-3Bi-1Ag and SAC alloy for 7 days and 14 days. The present alloy is found to be having good properties.

It can be concluded that the Sn-0.5Cu-3Bi-1Ag is having good mechanical properties and corrosion resistant and can be considered as a potential candidate as a lead free solder alloy.

CHAPTER 8

INVESTIGATIONS ON THE CORROSION PROPERTIES OF

Sn-1Cu-1Ni-xAg

8.1 EXPERIMENTAL PROCEDURE

8.1.1 Specimen Preparation

The sample specimens were in the form of coupons (as shown in the figure 1) whose dimensions were 10 x 10 x 10 mm.. The samples were shaped from pure metals (Sn, Cu, Bi and Ag) which were in the powder form. Five samples were prepared for each of the alloy composition - Sn-0.5Cu-3Bi-xAg (x = 0, 0.25, 0.5, 0.75, 1 % by wt.). The specimens were prepared using an induction furnace with Argon gas to avoid contaminations. The specimens after solidification were kept in room temperature for two days. The surface of the specimen was also undertaken visual inspection to avoid any surface level defects. The samples were polished thoroughly using SiC paper, washed and cleaned with deionized water and methanol.

8.1.2 Weight loss method

In order to study the effect of corrosion on the specimens, there are two methods generally used. One is the weight loss method and the other one is current density method. In the former method, the specimens are immersed in the concerned liquid for some previously determined time. Weight of the sample before and after the procedure will be noted down. Based on this information, the corrosion rate can be found our using the following equation.

$$CR = \frac{w}{At} \tag{8.1}$$

Where, CR – Corrosion rate

w- Weight loss

A – Area exposed

t- Time of exposure

In weight loss method, the corrosion is expressed in terms of mdd ($1mg/decimeter^2/1day$). The SI unit is $g/m^2/day$. The area is added to the rate of corrosion equation; reason that, more surface exposure will lead to more dissolution. Thus the equation is normalized with area. All the specimens were immersed in NaCl solution for 7 days and 14 days. The weight of the specimen before and after the immersion was noted. The corrosion media used in the experiment was 3.5 % by wt. NaCl solution. This was used to simulate the sea water. The weights of the specimens were noted down.

8.1.3 Microstructure analysis

The surface details of the sample coupons after 7 days and 14 days were analysed by field-emission scanning electron microscopy (FE-SEM, Carl Zeiss Sigma).All the images were taken at a magnification of 10 K X and 25K X, scale=1μm, Electron High Tension (EHT) = 5.00 Kv, Working Distance (WD) = 3.2 mm. EDS analysis of the surface of the specimens were done. The element wise multi-colour mapping was also done.

8.2 RESULTS

8.2.1 Weight loss results

The weight of the specimens before and after immersing for 7 days and 14 days are shown in the table 8.1. The weight loss of the specimen was noted down. Using the weight loss data, area of exposure of the specimen and the time of exposure (7 and 14 days), the corrosion rate (CR) is calculated in gmd ($g/m^2/day$). The weight loss of all the five samples in each case was calculated. The corrosion rate is calculated in each case. The average of the corrosion rate of five samples in each case is calculated. Sn-1Cu-1Ni has a corrosion rate of 7.5429 gmd and 7.5327 gmd for 7 and 14 days respectively. Sn-1Cu-1Ni-0.5Ag has corrosion rates 6.3286 gmd and 6.2782 gmd for 7 days and 14 days respectively. Sn-1Cu-1Ni-1Ag has corrosion rates of 4.2571 gmd and 4.3015 gmd for 7 and 14 days respectively. The weight loss of all the samples, corrosion rates after 7 days and 14 days are shown in the table 1.

Table 8.1 Weight loss tabulation and the Corrosion Rate for 7 days and 14 days

Solder Alloy	Initial weight (gm)	Weight (7 Days) (gm)	Weight (14 days) (gm)	Corrosion rate (7 days) (gmd)	Corrosion rate (14 days) (gmd)
Sn-1Cu-1Ni	7.2872	7.2664	7.2455	7.5429	7.5327
	7.2763	7.2552	7.2342		
	7.2689	7.2478	7.2267		
	7.2802	7.2596	7.2374		
	7.2664	7.2444	7.2243		
Sn-1Cu-1Ni-0.5Ag	7.2985	7.2811	7.2637	6.3286	6.2782
	7.2856	7.2684	7.2506		
	7.3024	7.2841	7.2669		
	7.2821	7.2645	7.2471		
	7.3003	7.2822	7.2648		
Sn-1Cu-1Ni-1Ag	7.3098	7.2976	7.2855	4.2571	4.3015
	7.3203	7.3086	7.2960		
	7.3187	7.3068	7.2945		
	7.3167	7.3049	7.2928		
	7.3211	7.3091	7.2974		

8.2.2 Microstructure analysis

Microstructure and EDS analysis results were collected. The EDS analysis results of the surface are shown in the figures 8.1 and 8.2. Results for the 7days exposure and 14 days exposure are shown in each figure. Sn is the most electrochemically active element than the Ag_3Sn and Cu_6Sn_5. Therefore the first to be dissolved will be Sn.

The cathodic reaction happening can be shown as:

$$O_2 + 2H_2O + 4e^{-} \rightarrow 4OH^{-} \tag{8.2}$$

$$2H_2O + 2e^{-} \rightarrow H_2 + 2OH^{-} \tag{8.3}$$

The anodic reaction can be found as:

$$Sn + 2OH^{-} \rightarrow Sn(OH)_2 + 2e^{-} \tag{8.4}$$

$$Sn + 4H_2O \rightarrow Sn(OH)_4 + 4e^{-} + 4H^{+} \tag{8.5}$$

$$Sn(OH)_2 + 2OH^{-} + 2e^{-} \rightarrow Sn(OH)_4 \tag{8.6}$$

$$Sn(OH)_2 + 2OH^{-} \rightarrow SnO + H_2O \tag{8.7}$$

$$Sn(OH)_4 \rightarrow SnO_2 + 2H_2O \tag{8.8}$$
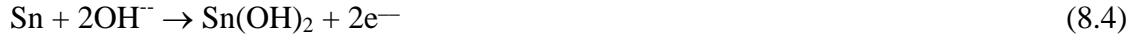
The EDS analysis results of the surface of Sn-1Cu-1Ni-0.5Ag and Sn-1Cu-1Ni-1Ag is shown in the figure 8.1 and figure 8.2. The FE-SEM results were shown in the figure 8.10 and 8.11. Dendrites formed can be very easily identified from the results. The mechanism of growth, shape, direction of growth is the characteristics which makes dendrites different from tin whiskers. Added that the growth mechanism of the tin whiskers is still unknown. The dendrite growth rate is influenced mainly by the alloying elements. The decreasing value of CR with the addition of Ag can be correlated to the formation of Ag_3Sn and Cu_6Sn_5 which accelerates the resistance to the surface. Usually dendrites grow from anode to cathode direction because of the migration of metallic ions from anode to cathode. The presence of Ag_3Sn, Cu_6Sn_5, SnO, and SnO_2 are also identified. Ag_3Sn is nobler than the β-Sn phase in the solder alloy due to the retaining of Ag_3Sn.

It was reported that the peak intensities of Tin reduced with immersion time enhancement. No evident changes in the gap of the pasty range and melting point of the lead free solder alloy SAC305 were also reported (Chuin et al., 2016). It was also reported in another study about passivation behavior of SAC305 .It was found that alloy in HCl is inferior when related with NaCl solution. SnO and SnO_2 were the oxide films formed for both the cases of HCl and NaCl although the solutions were different (Nurwahida et al. 2016). It was reported in another study that the fastest mean tie to failure considering electrochemical migration is SAC305. SAC 305 is reported to be a poor electric conductor in SBF medium considering electro chemical migration as a part

of four-probe results. In 3.5% wt. NaCl solution, lead free solutions showed good corrosion resistance than Sn-Pb alloy. This may be due to the lower corrosion current density and lower passivation current density. It was also reported that the corrosion resistance of Sn-Ag-Cu and Sn-Ag was almost same. The corrosion resistance of Sn-3.5Ag was reported to be better than the other two (Sarveswaran, 2017). The figure 8.7 shows the corrosion rate comparison of Sn-1Cu-1Ni-1Ag and SAC for 7days and 14 days. The corrosion rate of the alloy under present study is found to be low.
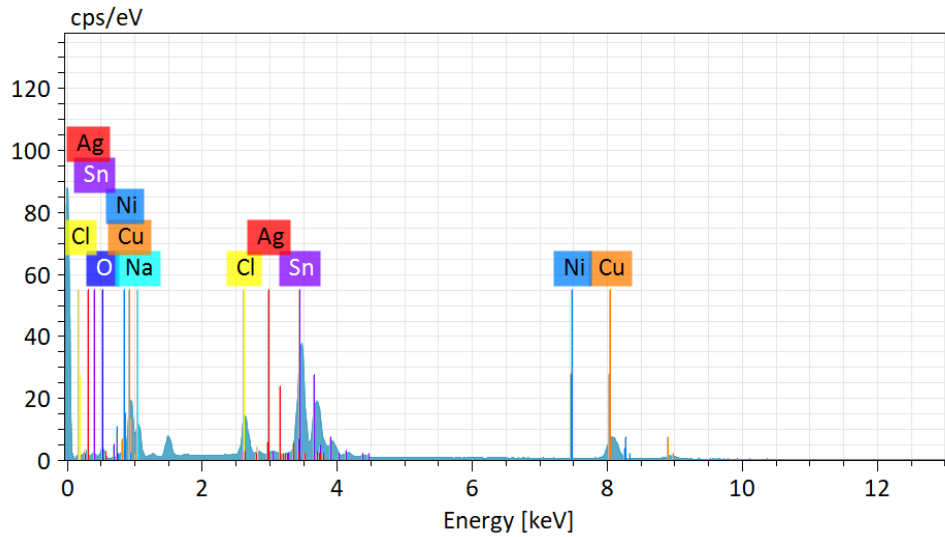
Fig. 8.1a EDS results of Sn-Cu-Ni samples immersed in 3.5% NaCl solution for 7 days
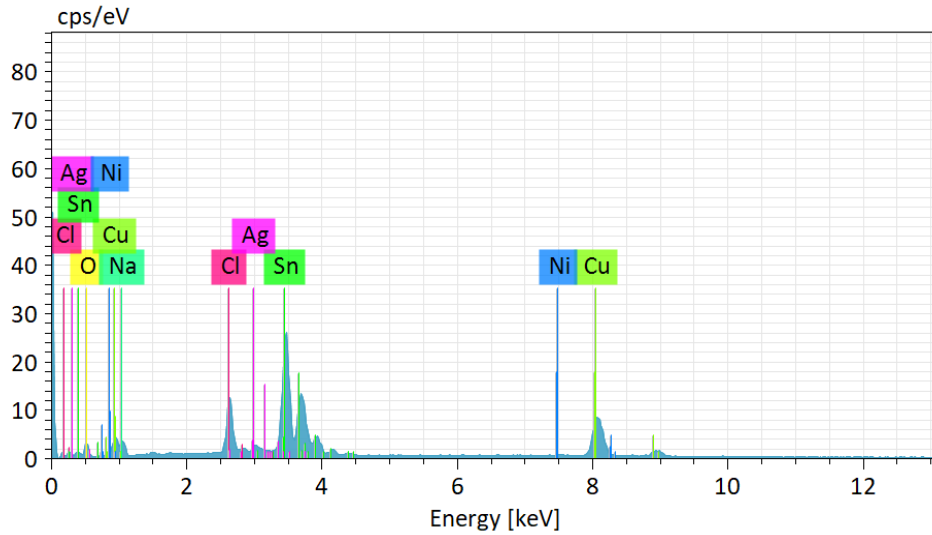
Fig. 8.1b EDS results of Sn-Cu-Ni samples immersed in 3.5% NaCl solution for 14 days
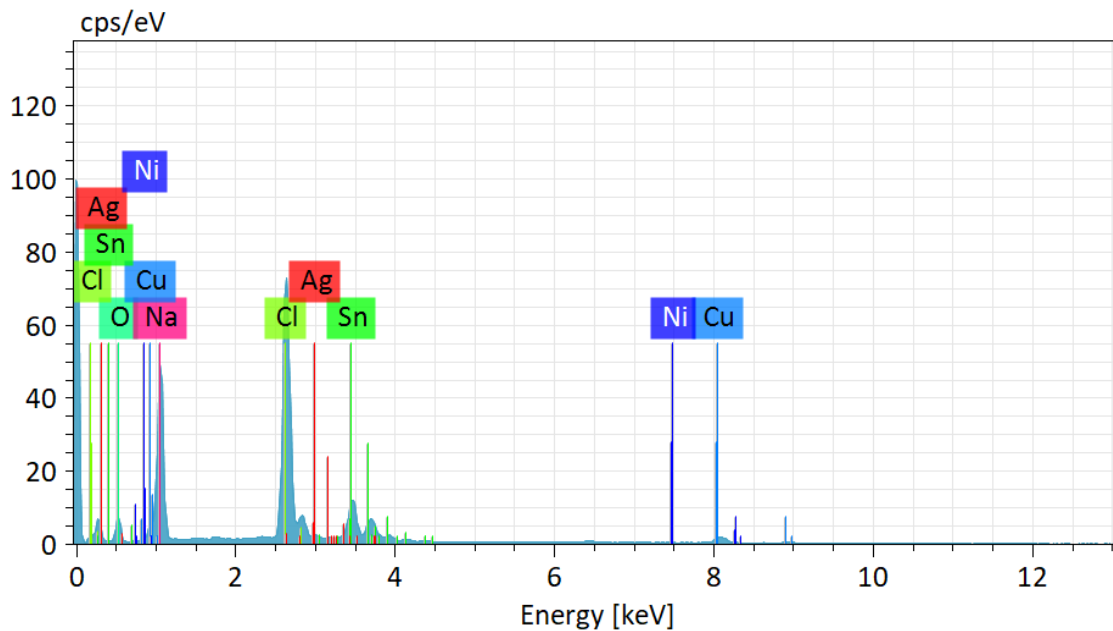
Fig. 8.2a EDS analysis of the surface of Sn-1Cu-1Ni-1Ag immersed in 3.5% NaCl after 7 days
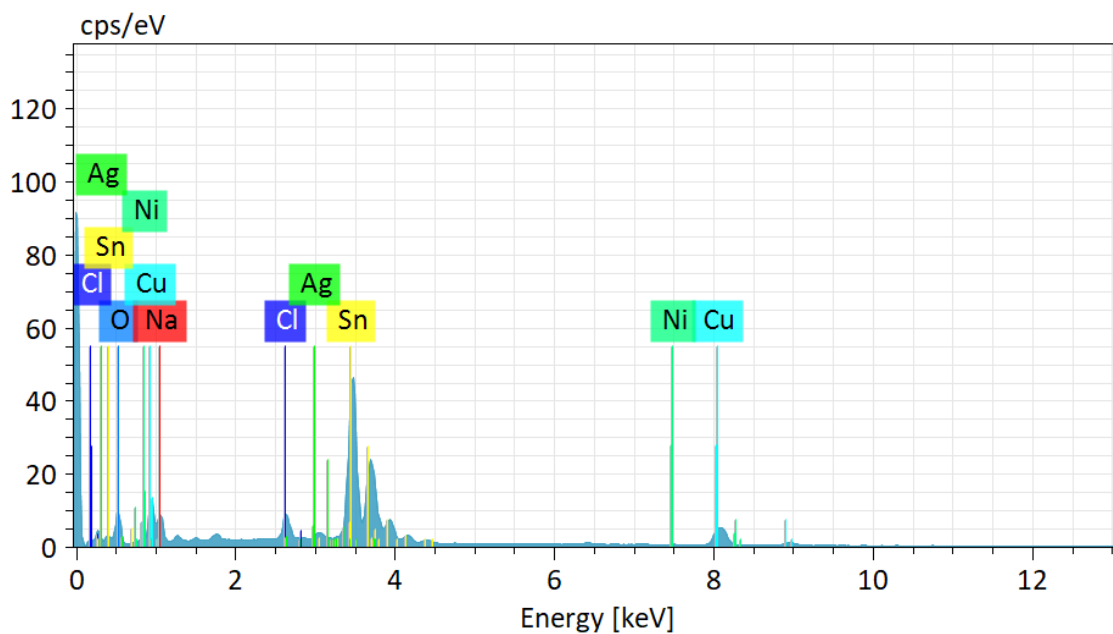
Fig. 8.2b EDS analysis of the surface of Sn-1Cu-1Ni-1Ag immersed in 3.5% NaCl after 14 days
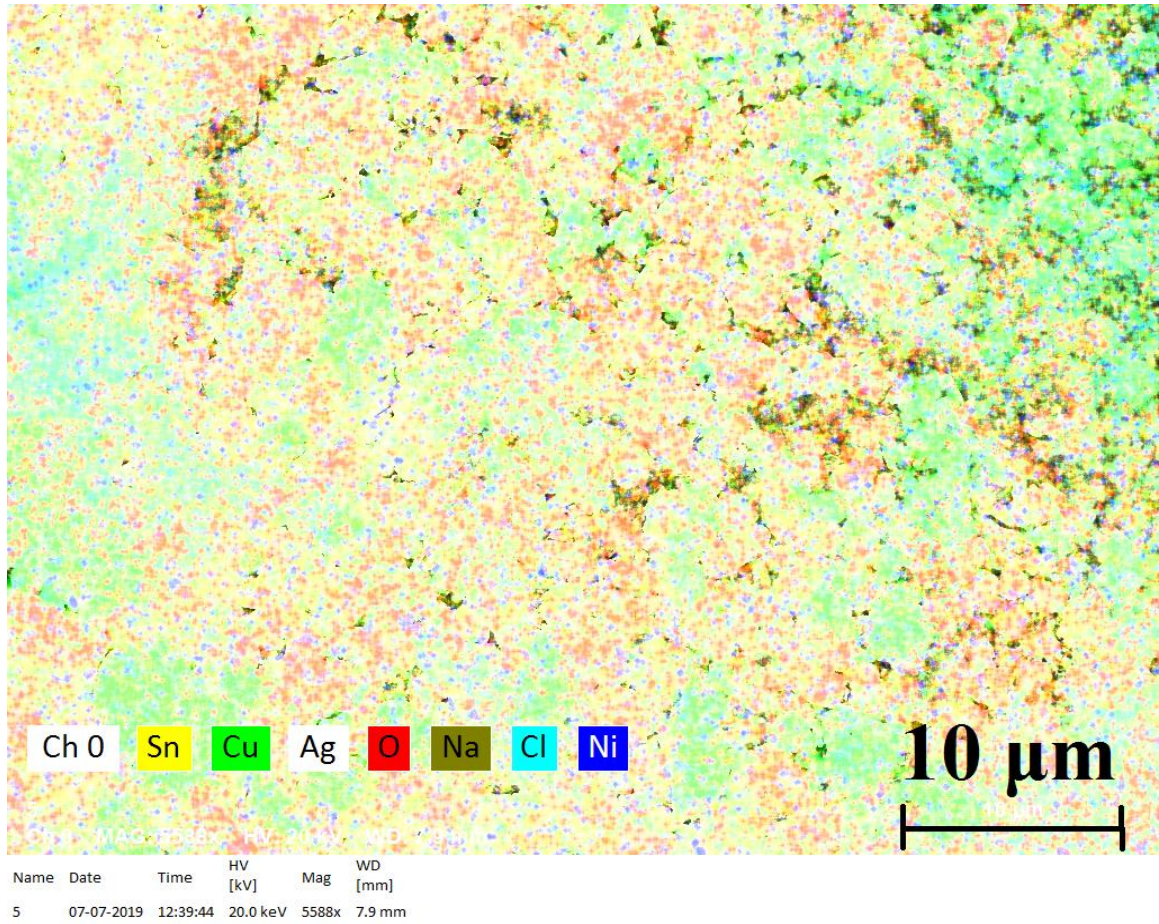
Fig. 8.3 Colour mapping of the surface of Sn-1Cu-1Ni-1Ag immersed in 3.5% NaCl solution after 7 days
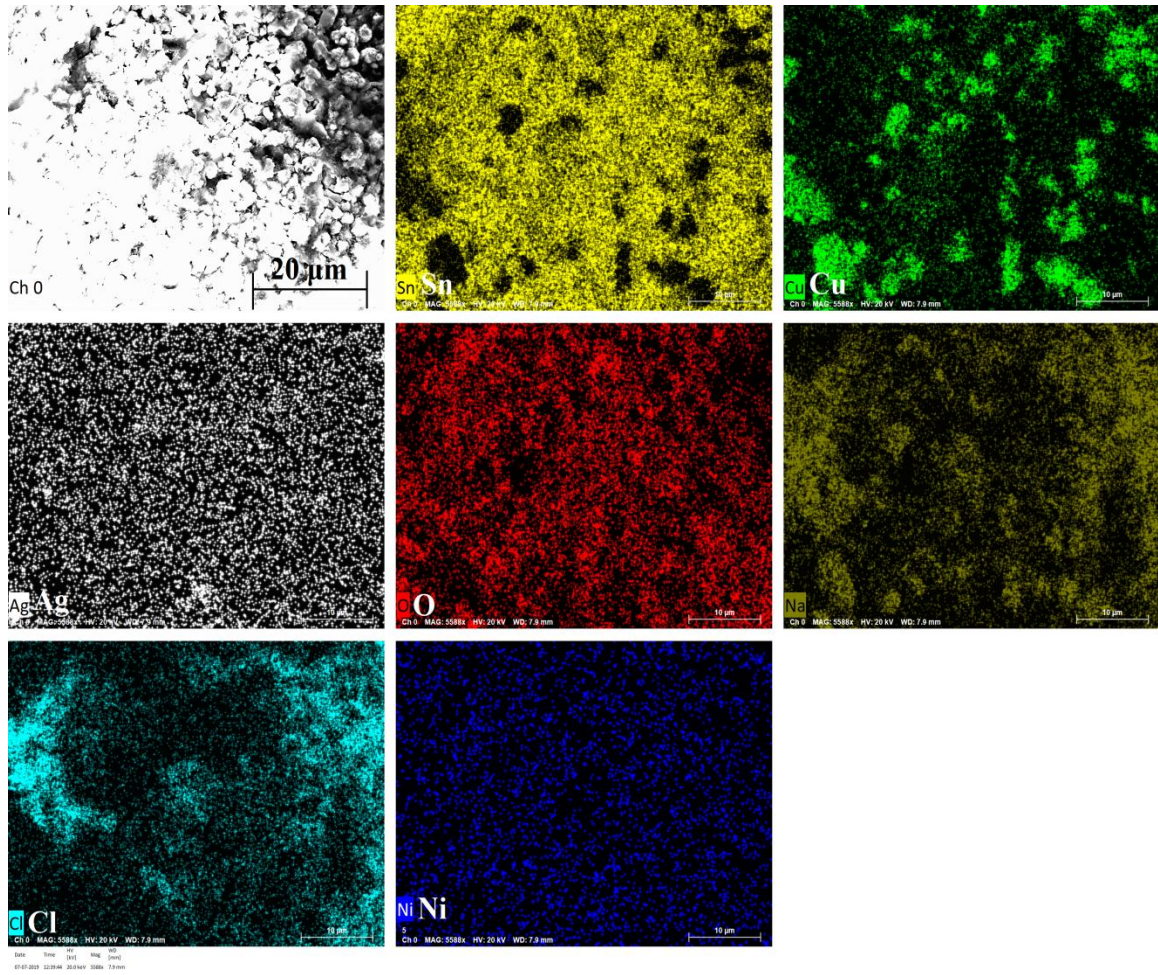
Fig. 8.4 Element wise Colour mapping of the surface of Sn-1Cu-1Ni-1Ag immersed in
3.5% NaCl solution after 7 days
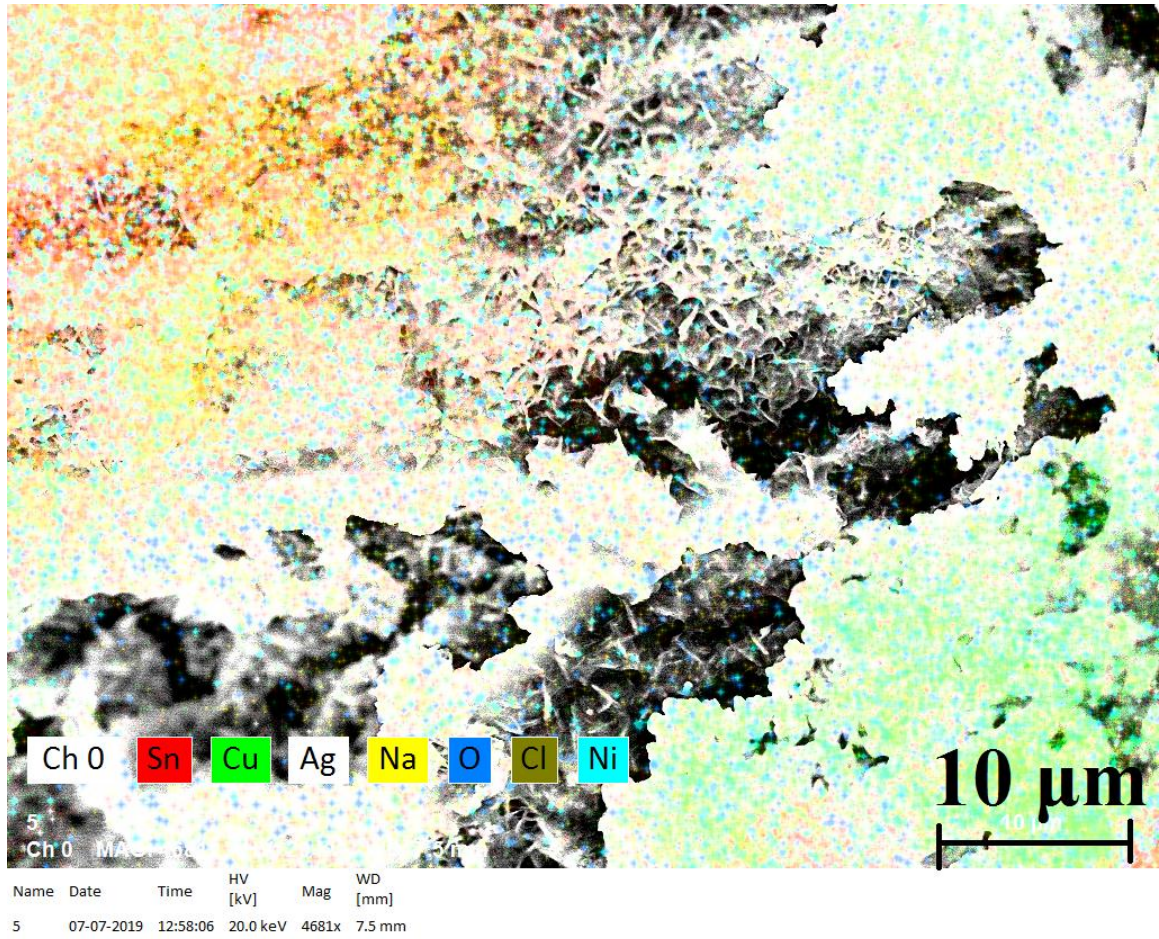
Fig. 8.5 Colour mapping of the surface of Sn-1Cu-1Ni-1Ag immersed in 3.5% NaCl solution after 14 days
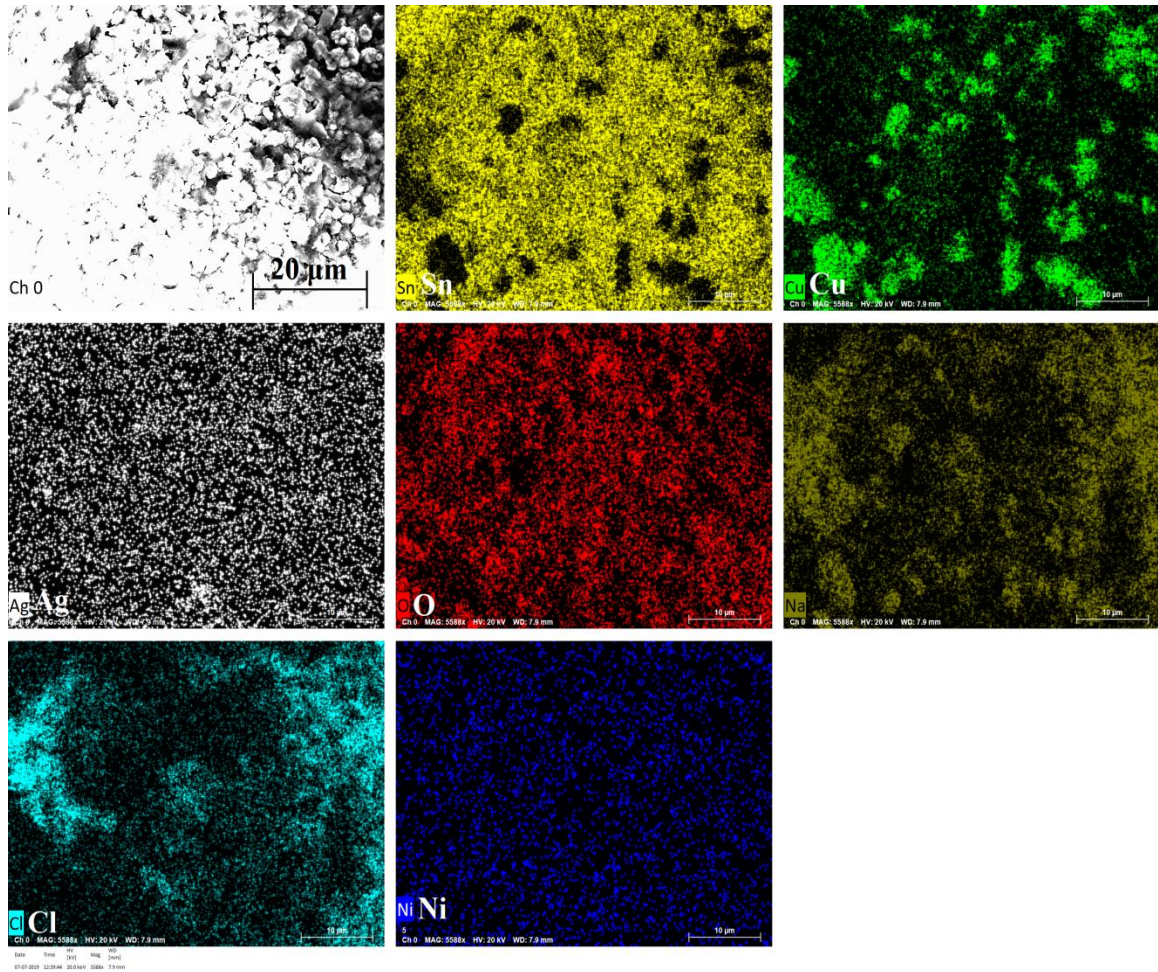
Fig. 8.6 Element wise Colour mapping of the surface of Sn-1Cu-1Ni-1Ag immersed in
3.5% NaCl solution after 14 days
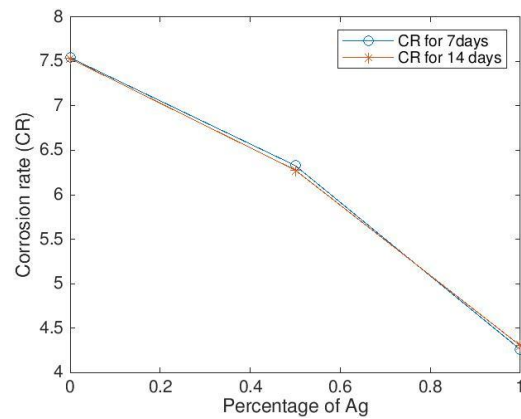
Fig. 8.7 Corrosion rate for 7 days and 14 days with the addition of Ag.
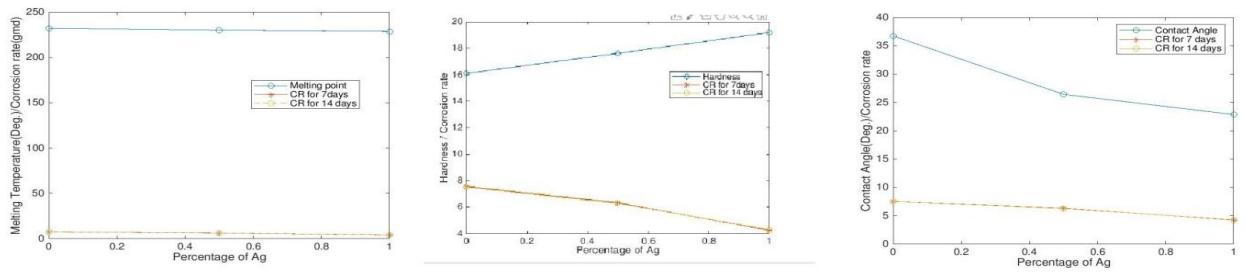
Fig. 8.8 Comparison of properties of Sn-1Cu-1Ni-xAg with corrosion rates
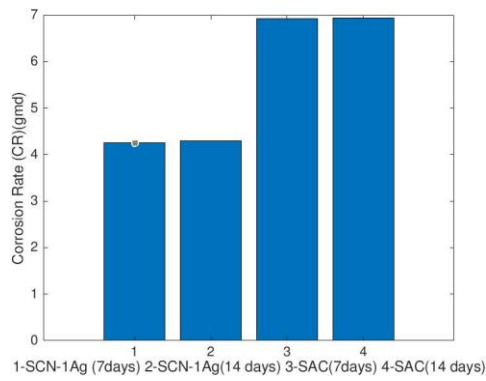
Fig. 8.9 Comparisons of Sn-1Cu-1Ni-1Ag and SAC
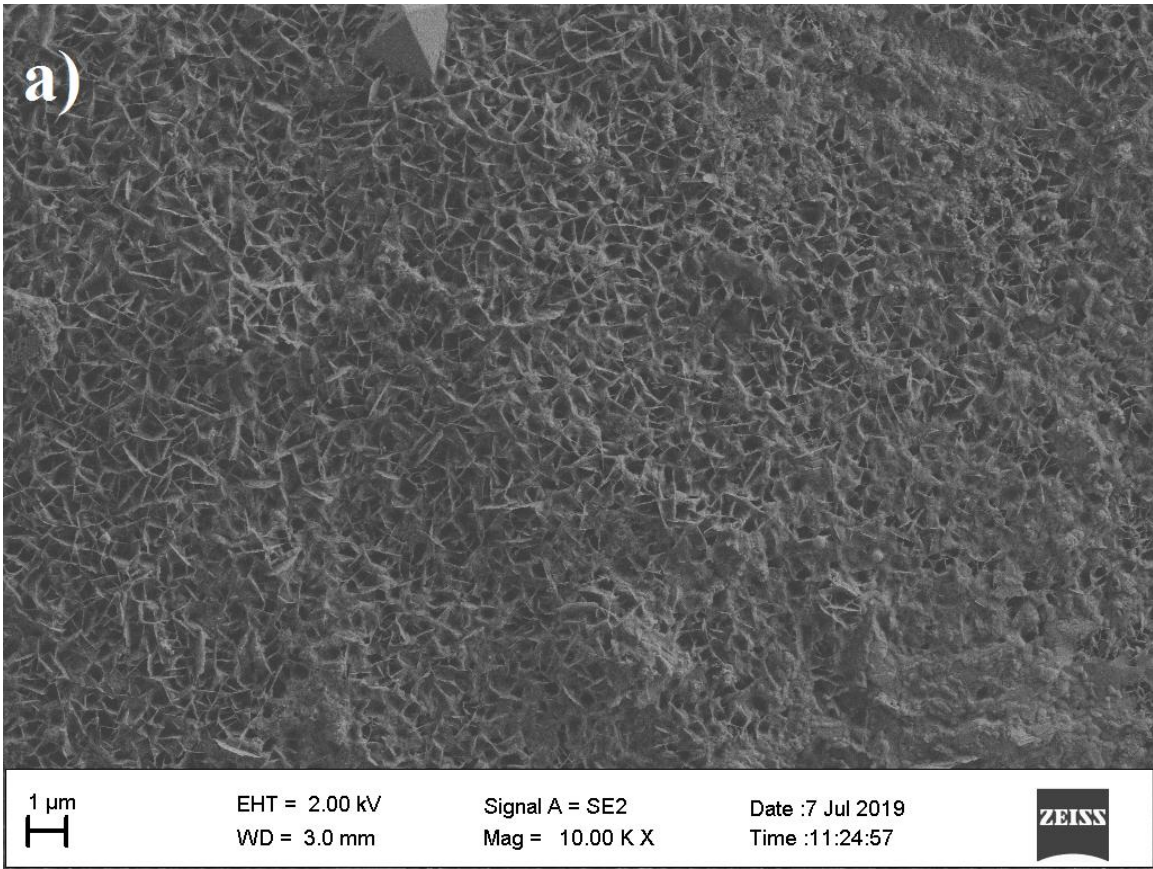
Fig. 8.10a The FE-SEM image of Sn-Cu-Ni immersed in 3.5% NaCl solution for 14 days
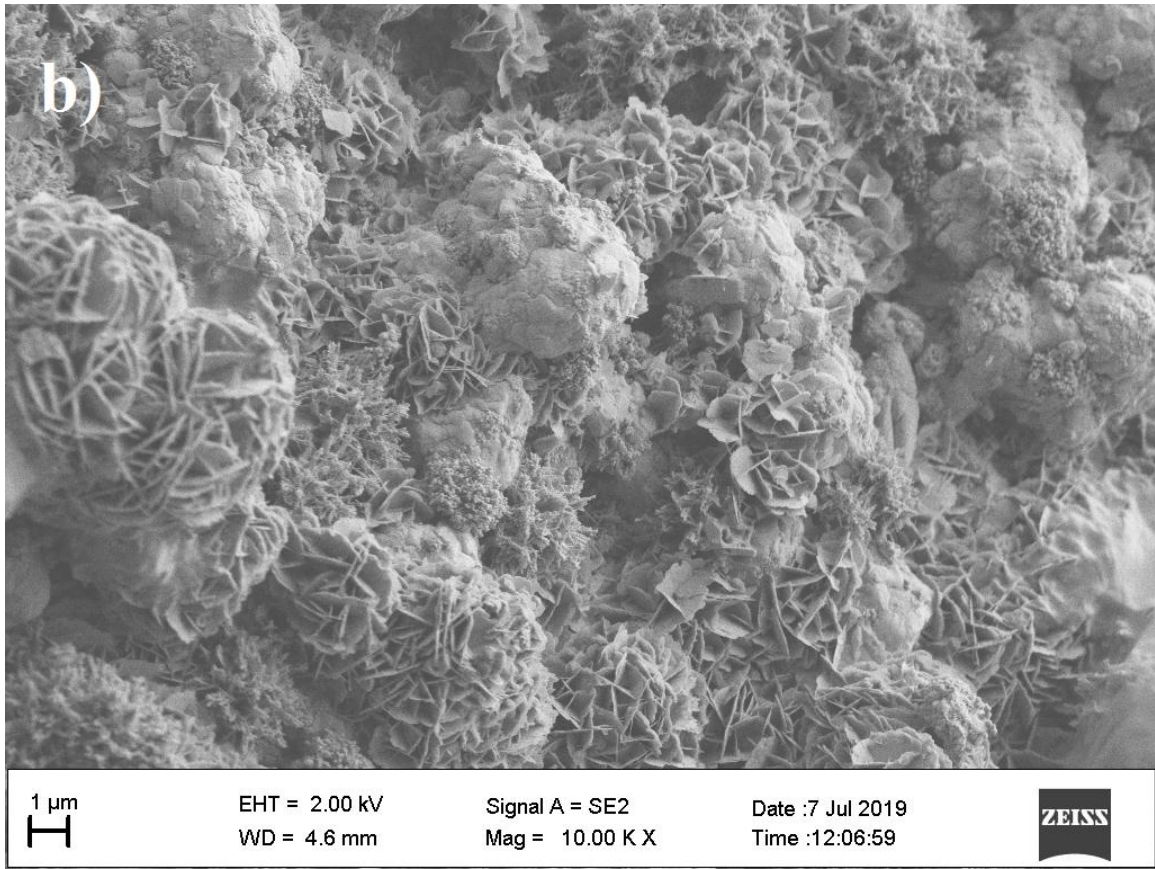
Fig. 8.10b The FE-SEM image of Sn-Cu-Ni-0.5Ag immersed in 3.5% NaCl solution for 14 days
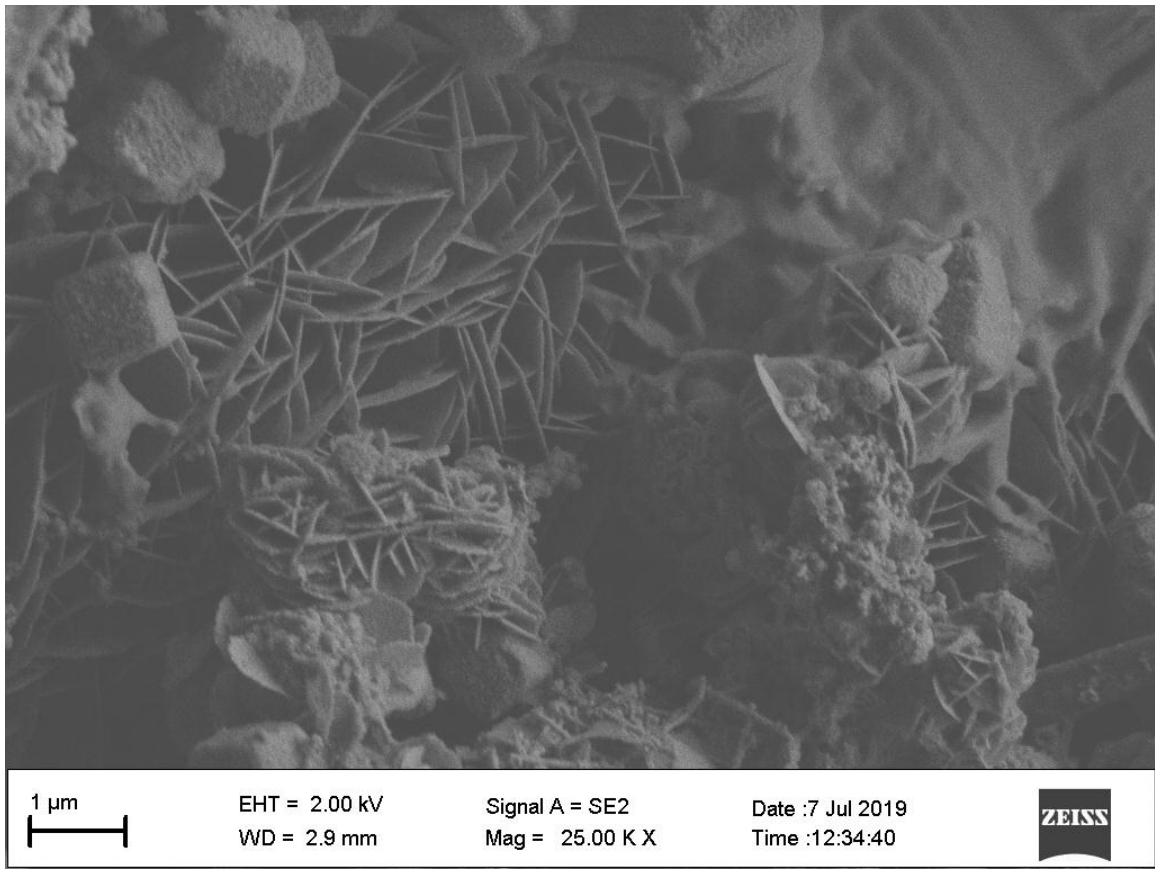
Fig. 8.11 The FE-SEM image of Sn-Cu-Ni-1Ag immersed in 3.5% NaCl solution for 14 days

In Sn-Pb alloy, corrosion products have two layers-Sn-rich outer layer and Pb-rich inner layer. The Pb-rich inner layer will cause harm in the corrosion phenomenon. Sn-Ag-Cu (SAC) alloys were famous lead free solder alloy which were popular in the market. The SAC has also lethal effect on medical equipment due to electrochemical migration. The new solder alloy should be corrosion resistant. It was reported that the addition of Ag into Sn-1Cu-1Ni alloy improve the properties like melting temperature, contact angle and hardness. In this chapter, the corrosion behaviours' of these alloys were studied. It was found that with addition of Ag by 1%, the corrosion rate is having a decreasing trend.

The corrosion rates of 7 days exposure and 14 days exposure were same. SnO and SnO_2 were found on the surface as the corrosion products. The presence of Ag_3Sn, Cu_6Sn_5, SnO, and SnO_2 are also identified. Ag_3Sn is nobler than the β-Sn phase in the solder alloy due to the retaining of Ag_3Sn. The comparison of Corrosion rates and the properties were shown in the figure 8.8. The decreasing value of CR with the addition of Ag can be correlated to the formation of Ag_3Sn and Cu_6Sn_5 which accelerates the resistance to the surface. The multi-color mapping and element wise color mapping is also reported in this study. The comparison of corrosion rates of Sn-1Cu-1Ni-1Ag with SAC shown in the figure 8.9 which shows that it has better corrosion resistance. Therefore combining the results from earlier chapter and the present study, it is clear that Sn-1Cu-1Ni-1Ag is a promising candidate among the lead free solder alloys.

CHAPTER 9

CONCLUSION

Sn-Pb cannot be used in solder alloy making because of the presence of toxic lead in it. SAC305 AND SAC405 are two famous alloys which came as a replacement for Sn-Pb. But they were not able to replace in all aspects. Also high cost of the alloy due to patent cost and silver content is another concern. In this investigation, two novel lead free solder alloys are successfully developed. Properties of these alloys were compared with the existing alloys. The addition of Ag into the alloys (1% by wt.) enhanced the properties (decrease in melting temperature, hardness, shear strength, wetting property and impact toughness). Corrosion analysis is also done and found that the new alloys were showing better properties than SAC305 and SAC405.

9.1 DEVELOPMENT OF TWO NEW NOVEL LEAD FREE SOLDER ALLOYS

Two novel lead-free solder alloys, one Sn-0.5Cu-3Bi (SCB305) and Sn-1Cu-1Ni (SCN110) are successfully developed. DoE was conducted at the initial stage. Melting temperature, hardness and contact angle of SCB305 are 231.15°C, 19.8Hv and 28.74° respectively. Melting temperature, hardness and contact angle of SCN 110 are 232.5°C, 16.1Hv and 36.75° respectively. All these properties were comparable with the existing SAC305 and SAC405 alloys. The cost of SCB305 and SCN110 are $23.05/Kg and $20.65/Kg respectively. Details of the cost of the alloys are shown in annexure I. The cost of SAC305 and SAC405 are $36.63/Kg and $41.89/Kg respectively. Cost wise comparison also suggests that new alloys are better. The patent cost of the SAC alloys will again make it a costlier alloy.

9.2   EFFECT OF ADDITION OF Ag INTO Sn-0.5cu-3bi (SCB305)

Effect of addition of Ag into SCB305 is investigated. Ag is added in 0.25, 0.5, 0.75, 1, 1.25, 1.5, and 1.75 % by wt. into the alloy. Melting temperature, hardness, contact angle, shear strength and impact toughness of these properties were analysed. From the investigation, it is found that optimum amount of Ag that should be added is 1% by wt. Melting point decreased from 231.20°C to 226.93°C, hardness increased from 19.8 Hv to 24.2 Hv, and contact angle reduced from 28.74° to 24.87°. These are the basic mechanical properties that should be satisfied. Shear strength and impact toughness are found to be increased from 23.4MPa to 28.0Mpa and 10.4 J to 11.3 J respectively. Microstructures of the alloys are also studied. Therefore with addition of 1% by wt. of Ag, the properties of SCB305 are found to be enhanced. Sn-0.5Cu-3Bi-1Ag can be considered as a potential candidate for lead free solder alloy.

9.3   ADDITION OF Ag INTO Sn-1Cu-1Ni (SCN110)

Effect of addition of Ag into SCN110 is investigated. Ag is added in 0.25, 0.5, 0.75, 1, 1.25, 1.5, and 1.75 % by wt. into the alloy. Melting temperature, hardness, contact angle, shear strength and impact toughness of these properties were analysed. From the investigation, it is found that optimum amount of Ag that should be added is 1% by wt. Melting point decreased from 232.2°C to 228.4°C, hardness increased from 16.1 Hv to 19.2 Hv, and contact angle reduced from 36.75° to 22.87°. These are the basic mechanical properties that should be satisfied. Shear strength and impact toughness are found to be increased from 27.4MPa to 29.7MPa and 9.4 J to 10.1 J respectively. Microstructures of the alloys are also studied. Therefore with addition of 1% by wt. of

Ag, the properties of SCN110 are found to be enhanced. Sn-1Cu-1Ni-1Ag can be considered as a potential candidate for lead free solder alloy.

9.4   CORROSION PROPERTIES OF Sn-0.5Cu-3Bi-xAg

Corrosion properties of SCB305-xAg (x = 0, 0.5, 1% by wt.) is investigated using weight loss method. This is an accelerated test using 3.5% by wt. NaCl for 7 days and 14 days. It is observed that the mean CR (Corrosion Rate) for Sn-Cu-Bi is 3.6386 gmd and 3.5643 gmd for 7 days and 14 days respectively. In case of Sn-Cu-Bi-0.5Ag, it is found that3.2643 gmd and 3.2464 are the mean CR values for 7 and 14 days respectively. The solder alloy in which more focus is given i.e. Sn-Cu-Bi-1Ag has 3.0929 gmd and 3.0726 gmd as the average CR values with the exposure of 7 and 14 days in order. The corrosion rate of a specific alloy remains almost same with 1 week and 2 weeks exposures. With the addition of Ag, the corrosion rate is found to be decreasing. Corrosion rates of the new alloy are better when compared to SAC305 and SAC405.

9.5   CORROSION PROPERTIES OF Sn-1Cu-1Ni-xAg

Corrosion properties of SCB305-xAg (x = 0, 0.5, 1% by wt.) is investigated using weight loss method. This is an accelerated test using 3.5% by wt. NaCl for 7 days and 14 days. It is observed that the mean CR (Corrosion Rate) for Sn-Cu-Ni is 7.5429 gmd and 7.5327 gmd for 7 days and 14 days respectively. In case of Sn-Cu-Ni-0.5Ag, it is found that 6.3286 gmd and 6.2782 are the mean CR values for 7 and 14 days respectively. The solder alloy in which more focus is given i.e. Sn-Cu-Ni-1Ag has 4.2571gmd and 4.3015 gmd as the average CR values with the exposure of 7 and 14 days in order. The corrosion rate remains almost same with 1 week and 2 weeks exposures. With the addition of Ag,

the corrosion rate is found to be decreasing. Corrosion rates of the new alloy are better when compared to SAC305 and SAC405.

9.6 COST OF THE SOLDER ALLOY

Details of cost of selected solder alloys are given in annexure I. Patent cost are not considered for the comparison. Sn-0.5Cu-3Bi-1Ag and Sn-1Cu-1Ni-1Ag are having costs $26.09/Kg and $25.13/Kg respectively. SAC305, SAC405 and Sn-Pb are having costs $36.63/Kg, $41.89/Kg and $13.86/Kg respectively. Comparison shows that the two new solder alloys were better than SAC305 and SAC405 existing lead free solder alloys in terms of cost.

Therefore it can be concluded that:

> ➢ Two novel lead free solder compositions are made with Sn, Cu, Bi, Ni

> ➢ Sn-0.5Cu-3Bi and Sn-1Cu-1Ni are the two novel compositions

> ➢ With 1% Ag addition into both the compositions enhanced the desirable properties of solder alloy(melting temperature decreased, hardness and shear strength increased, contact angle decreased).

> ➢ Sn-0.5Cu-3Bi-1Ag and Sn-0.5Cu-1Ni are found to be corrosion resistant than SAC305 and SAC405.

9.7 FUTURE SCOPE

- Application of machine learning and AI to develop new lead free solders materials.
- Thermal fatigue test and vibration analysis for the novel alloys.

- Investigate whether addition of foreign elements (other than Ag) enhances the properties of the alloy.

REFERENCES

1. B. Arfaei, F. Mutuku, K. Sweatman, N. Lee, E. Cotts, R. Coyle (2014) Dependence of solder joint reliability on solder volume, composition and printed circuit board surface finish, Electronic Components and Technology Conference (ECTC), IEEE 64th, pp. 655–665.

2. A. Choubey, D. Menschow, S. Ganesan, M. Pecht (2006) Effect of aging on pull strength of SnPb, SnAgCu and mixed solder joints in peripheral surface mount components, J. SMTA 19 (2), 33–37.

3. A. Schröter, Addressing the Challenge of Head-in-pillow Defects in Electronics Assembly, http://www.evertiq.com/news/14414 (Last accessed on February 2020)

4. A. Sharif, Y.C. Chan (2004) Dissolution kinetics of BGA Sn–Pb and Sn–Ag solders with Cu substrates during reflow, Material science and engineering, pp.126-131

5. A. Siewiorek, A. Kudyba, N. Sobczak, M. Homa, Z. Huber, Z. Adamek, J.Wojewoda- Budka (2013) Effects of PCB substrate surface finish and flux on solderability of lead-free SAC305 alloy, J. Mater. Eng. Perform. 22 (8), 2247–2252.

6. A.A. El-Daly, A.M. El-Taher, S.Gouda (2015) Materials and Designs, vol.65, pp. 796-805

7. A.A. El-Daly, G.S. Al-Ganainy, A. Fawzy,M.J. Younis (2015) Structural characterization and creep resistance of nano-silicon carbide reinforced Sn–1.0 Ag–0.5 Cu lead-free solder alloy, Mater. Des. 55, 837–845.

8. A.A. El-Daly, H. El-Hosainy, T.A. Elmosalami, W.M. Desoky (2015) Microstructural modifications and properties of low-Ag-content Sn–Ag–Cu solder joints induced by Zn alloying, J. Alloys Compd. 653, 402–410.

9. A.A.El-Daly, A.M. El-Taher, S. Gouda (2015) Journal of Alloys and Compounds, vol. 627, pp. 268-275

10. A.B. Frazier, R.O. Warrington, C. Friedrich (1995) IEEE Trans. Ind. Electron., 42 (5) , pp.423–430.

11. A.K. Gain, L. Zhang (2016), Growth mechanism of intermetallic compound and mechanical properties of nickel (Ni) nanoparticle doped low melting temperature tin–bismuth (Sn–Bi) solder, J. Mater. Sci. Mater. Electron., vol.27,pp. 781–794.

12. A.K. Gain, L. Zhang, Y.C. Chan (2015), J. Mater. Sci. Mater. Electron. 26

13. A.K. Gain, Y.C. Chan, K.C. Yung, A. Sharif, L. Ali (2009), Effect of nano Ni additions on the structure and properties of Sn–9Zn and Sn–Zn–3Bi solders in Au/Ni/Cu ball grid array packages, Mater. Sci. Eng. B,vol.162,pp. 92–98

14. Act for Resource Recycling of Electrical and Electronic Equipment and Vehicles, http://www.rsjtechnical.com/images/Documents/Korea_RoHS_ELV_April_2007 _ EcoFrontier.pdf

15. Anton Zoran Miric Angela Grusd, (1998),"Lead-free alloys", Soldering & Surface Mount Technology, Vol. 10 Iss 1 pp. 19 – 25

16. Australian Government, Investigation Into Lead-Free Solder in Australian Defence Force Applications, https://acc.dau.mil/adl/en-US/445103/file/57179/DSTO-TN-0970.pdf

17. B. Illés, B. Horváth, (2014), Tinwhisker growth fromlowAg contentmicro-alloyed SAC solders, Proceedings of the 2014 37th International Spring Seminar on Electronics Technology, IEEE pp. 152–157.

18. B. Sood, M. Osterman, M. Pecht, (2011) Tin whisker analysis of Toyota's electronic throttle controls, Circuit World 37 (3) , 4–9.

19. B.D. Cullity (1967), 'Elements of X-ray diffraction', Addison-Wesley, UK

20. B.-J. Lee, C.-S. Oh and J.-H. Shim, (1996), Thermodynamic assessments of the Sn-In and Sn-Bi binary systems J. Electron. Mater. 25, 983-991

21. B.P. Richards, K. Nimmo et al, 'Lead-free Soldering', Department of Trade and Industry, UK, (1999 and update 2000) (www.lead-free.org/) (last accessed on February 2020)

22. C. B. L. & S. B. J. J.W. Yoon, (2003), Mater. Sci. Technol., vol.19, pp. 1101-1106

23. C. Chen, H.M. Tong, K.N. Tu,(2010) Electromigration and thermomigration in Pb-free flipchip solder joints, Annu. Rev. Mater. Res. 40, 531–555.

24. C. Chung, Z.X. Zhu, C.R. Kao,(2015) Thermal stress of surface oxide layer on micro solder bumps during reflow, J. Electron. Mater. 44 (2), 744–750.

25. C. Hamilton, P. Eng, P. Snugovsky, (2007), Have High Cu Dissolution Rates of SAC305/405 Alloys Forced a Change in the Lead-free Alloy Used During PTH Processes? Celestica Inc., IBM Corporation, Toronto, ON, Canada.

26. C. Hamilton, P. Snugovsky, M. Kelly, Effects of SAC Alloy Copper Dissolution Rates on PTH Processes: Cost and Performance Justify Use of Certain Alternatives   to   SAC305/   405,

http://thor.inemi.org/webdownload/newsroom/Presentations/Celestica_iNEMI_Tech_Forum_07/Effects_of_SAC_alloy.pdf (accessed on February 2020).

27. C. Hillman, "Overview of Copper Pillar Technology", DfR Solutions, http://www. dfrsolutions.com/wp-content/uploads/2015/12/Overview-of-Copper-Pillar-Technology.pdf, (accessed on February 2020).

28. C. Hillman, N. Blattau, J. Arnold, S. Binfield,(2007), Derivation of test-to-field correlation for Sn-Ni-Cu+Ge (SN100C), DfR06-024 Report

29. C. Liu, C. Lai, M.Wang, M. Hon, (2006), Thermal behavior and microstructure of the intermetallic compounds formed at the Sn-3Ag-0.5Cu/Cu interface after soldering and isothermal aging, J. Cryst. Growth 290 (1), 103–110.

30. C. Yang, F. Song, S. Lee, (2014), Comparison of ball pull strength among various Sn-Cu-Ni solder joints with different pad surface finishes, J. Electron. Packag. 136 (1) 1001-1003.

31. C. Yang, F. Song, S.W.R. Lee, (2011), Effect of interfacial strength between Cu6Sn5 and Cu3Sn intermetallic on the brittle fracture failure of lead-free solder joints with OSP pad finish, IEEE Electronic Components and Technology Conference, pp. 971–978.

32. C.H.H.L.C. Tsao, C.H. Chunga, R.S. Chen, Mater. Sci. Eng. A (2012)

33. C.-S. Oh, J.-H. Shim, B.-J. Lee and D.N. Lee, (1996), A thermodynamic study on the Ag/Sb/Sn system, J. Alloys and Compounds 238, 155-166

34. Chang, S.Y., Jain, C.C., Chuang, T.H., Feng, L.P., and Tsao, L.C., (2011), Effect of addition of TiO2 nanoparticles on the microstructure, microhardness and interfacial reactions of Sn3.5AgxCu solder, Mater. Des., vol. 32, pp. 4720–4727

35. Choubey, H. Yu, M. Osterman, M. Pecht, F. Yun, L. Youghong, X. Ming, (2008), Intermetallics characterization of lead-free solder joints under isothermal aging, J. Electron. Mater. 37 (8), 1130–1138.

36. Cost of lead-free solder materials, A Research Report by the IPC Solder Products Value Council, May 2006.

37. D. Amir, R. Aspandiar, S. Buttars, W.W. Chin, P. Gill, (2009), Head-on-pillow SMT failure modes, Proceedings of SMTA International Conference.

38. D. Amir, S. Walwadkar, S. Aravamudhan, L. May, (2012), The challenges of non wet open BGA solder defect, Proceedings of SMTA International Conference.

39. D. Kim, D. Suh, T. Millard, H. Kim, C. Kumar, M. Zhu, Y. Xu, (2007) Evaluation of high compliant low Ag solder alloys on OSP as a drop solution for the 2nd level Pb-free interconnection, Proceedings of 57th ECTC, pp. 1614–1619.

40. D. Tian, H. Chen, C.Wang, (2005), Effect of thermal aging onmicrostructure, shear and mechanical shock failures for solder ball bonding joint, International Conference on Electronic Packaging Technology, pp. 1–7.

41. D.S. Jiang, Y.P.Wang, C.S. Hsiao, (2006), Effect ofminor doping elements on lead free solder joint quality, Electronic Packaging Technology Conference, 8th, Singapore, pp. 385–389.

42. D.Y.R. Chong, F.X. Che, J.H.L. Pang, K. Ng, J.Y.N. Tan, P.T.H. Low, (2006) Drop impact reliability testing for lead-free and lead-based soldered IC packages, Microelectron. Reliab. 46 (7), 1160–1171.

43. Da Yu, Abdullah Al-Yafawi, (2011), Microelectronics Reliability, vol.51, pp. 649-656

44. Directive 2002/95/EC of the European Parliament and of the Council, http://eurlex.europa.eu/LexUriServ/LexUriServ.do?uri=OJ:L:2003:037:0019:002 3:EN:PDF

45. Directive 2011/65/EU of the European Parliament and of the Council of 8 June 2011 on the Restriction of the Use of Certain Hazardous Substances in Electrical and Electronic Equipment (Text With EEA Relevance), http://data.europa.eu/eli/dir/ 2011/65/oj

46. Draft Proposal for a European Parliament and Council Directive on Waste Electrical and Electronic Equipment (WEEE), Brussels Belgium (2000)

47. E. George, M. Pecht, (2016) RoHS compliance in safety and reliability critical electronics, Microelectron. Reliab. 65, 1–7.

48. E. George, M. Pecht, (2014), Tin whisker analysis in an automotive engine control unit, Microelectron. Reliab. 54 (1), 214–219.

49. E.R. Monsalve, (1984), 'Lead Ingestion Hazard in Hand Soldering Environments', in Proceedings of the 8th Annual Soldering Technology and Product Assurance Seminar, Naval Weapons Center, China Lake, CA USA.

50. Ervina Efzan MhdNooraNurulakmal MohdSharifaCheong KuanYewaTadashiArigabAhmad BadriIsmailaZuhailawatiHussaina, (2010), Wettability and strength of In–Bi–Sn lead-free solder alloy on copper substrate, Journal of Alloys and Compounds Volume 507, Issue 1, Pages 290-296

51. European Parliament. Proposal for a Directive of the European Parliament and of the Council on Waste Electrical and Electronic Equipment and on the restriction

of the use of certain hazardous substances in electrical and electronic equipment. COM 2000;:347.

52. F. Cheng, H. Nishikawa, T. Takemoto, (2008), Microstructural and mechanical properties of Sn–Ag–Cu lead-free solders with minor addition of Ni and/or Co, J. Mater. Sci. 43 (10), 3643–3648.

53. F. Gao, T. Takemoto, H. Nishikawa, (2006), Effects of Co and Ni addition on reactive diffusion between Sn–3.5Ag solder and Cu during soldering and annealing, Mater. Sci. Eng. A 420, 39–46.

54. F. Gnecco, E. Ricci, S. Amore, D. Giuranno, G. Borzone, G. Zanicchi, R. Novakovic, (2007), Int. J. Adhes. Adhes. 27 (2007)

55. F.A. Stam, E. Davitt, (2001), Effects of thermomechanical cycling on lead and lead-free (SnPb and SnAgCu) surface mount solder joints, Microelectron. Reliab. 41 (11), 1815–1822.

56. F.H. Hayes, H.L. Lukas, G. Effenberg and G.Petzow, (1986), The ag-cu (silver-copper) system. Z. Metallkde. 77, 749-754

57. F.J. Wang, F. Gao, X. Ma, Y.Y. Qian, (2006), Depressing effect of 0.2wt.%Zn addition into Sn- 3.0Ag-0.5Cu solder alloy on the intermetallic growth with Cu substrate during isothermal aging, J. Electron. Mater. 35 (10), 1818–1824.

58. G. Davy, Relay failure caused by tin whiskers, Northrop Grumman Electronic Systems Technical Article, http://nepp.nasa.gov/whisker/ reference/tech_papers/davy2002-relay-failure-caused-by-tin-whiskers.pdf   (Last accessed on February 2020)

59. G. Demortier,(1989), Archeological Chemistry, 249

60. G. Elviz, M. Osterman, M. Pecht, R. Coyle, R. Parker, E. Benedetto, (2014), Thermal cycling reliability of alternative low-silver tin-based solders, J. Microelectron. Electron. Packag. 11 (4), 137–145.

61. G. Henshall, R. Healey, R. Pandher, K. Sweatman, K. Howell, R. Coyle, T. Stack, P. Snugovsky, S. Tisdale, F. Hua, (2008), iNEMI Pb-free alloy alternatives project report: State of the industry, Proceedings SMTAI, pp. 109–122.

62. G. Humpston, (2010), Cobalt: a universal barrier metal for solderable under bump metallization, J. Mater. Sci. Mater. Electron. 21 (6), 584–588.

63. G. Subbarayan, (2007), A Systematic Approach for Selection of Best PB-free Printed Circuit Board (PCB) Surface Finish (Ph.D dissertation) Binghamton University.

64. G. Zeng, S. McDonald, K. Nogita, (2012), Development of high-temperature solders: review, Microelectron. Reliab. 52 (7), 1306–1322.

65. Gayle, F.W., Becka, G., Syed, (2001), High temperature lead-free solder for microelectronics. JOM 53, 17–21.

66. Guo, F., Lucas, J.P. & Subramanian, (2001), Creep behavior in Cu and Ag particle-reinforced composite and eutectic Sn-3.5Ag and Sn-4.0Ag-0.5Cu non-composite solder joints. Journal of Materials Science: Materials in Electronics 12, 27–35.

67. H Wang, Song-bai Xue, (2016), Effect of Ag on the properties of solders and brazing filler metals, J. Mater. Sci. Mater. Electron., pp. 1–13.

68. H. Ma, T. Lee, D. Kim, H.G. Park, S. Kim, K. Liu, (2011), Isothermal aging effects on the mechanical shock performance of lead-free solder joints, IEEE Trans. Compon. Packag. Manuf. Technol. 1 (5), 714–721.

69. H. Tong, Y. Lai, C.P.Wong, (2012), Advanced Flip Chip Packaging, Springer, US.

70. H. Watanabe, N. Hidaka, I. Shoji, M. Ito, (2006), Effect of Ni and Ag on interfacial reaction and microstructure of Sn-Ag-Cu-Ni-Ge lead-free solder, Materials Science & Technology 2006 Conference and Exhibition (MS&T Partner Societies), 12, pp. 1399–1410.

71. H.J. Fecht, M.-X. Zhang, Y.A. Chang and J.H. Perepezko, (1989), Metastable phase equilibria in the lead-tin alloy system: Part II. Thermodynamic modelling, Metall. Trans. A, 20A, 795-803

72. H.R. Kotadia, P.D. Howes, S.H. Mannan, (2014), A review: on the development of low melting temperature Pb-free solders, Microelectron. Reliab. 54 (6), 1253–1273.

73. Handwerker C., Kattner U., Moon KW. (2007) Fundamental Properties of Pb-Free Solder Alloys., Lead-Free Soldering. Springer, Boston, MA.

74. He Wang, Song-bai Xue, (2016), Effect of Ag on the properties of solders and brazing filler metals, J. Mater. Sci. Mater. Electron., pp. 1–13.

75. www.merckmillipore.com/IN/en/product/Tin,MDA_CHEM107806#anchor_order ingcomp (accessed on February 2020)

76. www.rankem.in (accessed on February 2020)

77. www.hitachi-hightech.com/global/products/science/tech/ana/icp/descriptions/icp-oes.html (last accessed on February 2020)

78. www.lobachemie.com/lab-chemicals/bulk-packs.aspx (accessed on February 2020)

79. I. E. Anderson and R. L. Terpstra, (2001), "Lead-free solder," US Patent No. US6231691B1.

80. I.E. Anderson, B.A. Cook, J. Harringa, R.L. Terpstra, (2002), Microstructural modifications and properties of Sn-Ag-Cu solder joints induced by alloying, J. Electron. Mater. 31 (11), 1166–1174.

81. I.E. Anderson, J.L. Harringa, (2004), Elevated temperature aging of solder joints based on Sn-Ag-Cu: effects on joint microstructure and shear strength, J. Electron. Mater. 33 (12), 1485–1496.

82. I.E. Anderson, J.L. Harringa, (2006), Suppression of void coalescence in thermal aging of Tin-Silver-Copper-X solder joints, J. Electron. Mater. 35 (1), 94–106.

83. InfoMine, http://www.infomine.com/investment/metal-prices/ (Last accessed on February 2020).

84. IPC Solder Products Value Council, Electrical/Electronic Enduser: Cost of Lead-free Solder Materials, http://www.adhesivesmag.com/articles/86921-electrical-electronicenduser-cost-of-lead-free-solder-materials (Last accessed on February 2020).

85. IPC-A-610F, (2014), Acceptability of Electronic Assemblies.

86. J. Glazer, (1994), Microstructure and mechanical properties of Pb-free solder alloys for low-cost electronic assembly: A review, J. Electron. Mater., vol.23 (8) , pp. 693–700.

87. J. H. L. Pang and B. S. Xiong, (2005), "Mechanical Properties for 95.5Sn–3.8Ag–0.7Cu Lead-Free Solder Alloy," in IEEE Transactions on Components and Packaging Technologies, vol. 28, no. 4, pp. 830-840.

88. J. Keller, D. Baither, U. Wilke, G. Schmitz, (2011), Mechanical properties of Pb-free SnAg solder joints, Acta Mater. 59, 2731–2741.

89. J. Kim, Y. Lee, S. Lee, S. Jung, (2014), Effect of surface finishes on electromigration reliability in eutectic Sn–58Bi solder joints, Microelectron. Eng. 120, 77–84.

90. J. Varghese, A. Dasgupta, Test methodology for durability estimation of surface mount interconnects under drop testing conditions, Microelectron. Reliab. 47 (1) (2007) 93–107.

91. J. Zhao, L. Qi, X. M. Wang, and L. Wang, (2004), J. Alloys Compd., vol.375, pp. 196-201

92. J. Zhao, Y. Miyashita, Y. Mutoh, (2001), Fatigue crack growth behavior of 96.5Sn–3.5Ag lead-free solder, International Journal of Fatigue, Volume 23, Issue 8, Pages 723-731.

93. J. Zürcher, K. Yu, G. Schlottig, M. Baum, M. Taklo, B. Wunderle, P. Warszyński, T. Brunschwiler, (2015), Nanoparticle assembly and sintering towards all-copper flip chip interconnects, IEEE 65th Electronic Components and Technology Conference (ECTC), pp. 1115–1121.

94. J.C.J. Koo, Y.W. Lee, S.J. Hong, K.-S. Kim, H.M. Lee, (2014), New Sn–0.7Cu-based solder alloys with minor alloying additions of Pd, Cr and Ca, J. Alloys Compd., vol.608, pp.126–132.

95. J.D. Raby, R.W. Johnson, (1999), Electronic Packaging &Production 8(18).

96. J.H. Shim, C.-S. Oh, B.-J. Lee and D.N. Lee, (2006), Thermodynamic description of the CuAlZn and CuSnZn systems in the copper-rich corner Z. Metallkde. 87 ,205-212

97. J.Y. Kim, J. Yu, S.H. Kim, (2009), Effects of sulfide-forming element additions on the Kirkendall void formation and drop impact reliability of Cu/Sn–3.5Ag solder joints, Acta Mater. 57, 5001–5012.

98. Japanese Industry Standard JIS Z 3198-6, (2003), Test Method for Lead-free solders − Part 6: Methods for 45° Pull Test of Solder Joints on QFP Lead(Tokyo, Japan).

99. JC.-S. Oh, J.-H. Shim, B.-J. Lee and D.N. Lee, (1996), Metallurgy, Processing and Reliability of Lead-Free Solder Joint Interconnections, J. Alloys & Compds. 238, 155-166

100. J-Moss (Japanese RoHS), http://home.jeita.or.jp/eps/jmoss_en.htm

101. Joint Industry Guide (JIG) - IPC, http://www.ipc.org/4.0_Knowledge/4.1_Standards/Free/JIG-101-Ed-4.0.pdf

102. K. Gilleo, (1994), Circuits Assembly, **10** (30).

103. K. Sweatman, (2016), The latest trends in R&D of high reliability of no-Ag and low Ag leadfree solders, China International Solder Technology Forum (CISTF).

104. K. Zeng, R. Stierman, T. Chiu, D. Edwards, K. Ano, K.N. Tu, (2005), Kirkendall void formation in eutectic SnPb solder joints on bare Cu and its effect on joint reliability, J. Appl. Phys. 97 (2), 024508–024508-8.

105. K.L. Xiaowu Hu, Z. Min, (2013), J. Alloys Compd., vol.566, pp. 239–245.

106. K.Tu, H.Hsiao, C.Chen, (2013), Microelectronics Reliability, 53.

107. Kim, Y.M., Harr, K. & Kim, (2010), Mechanism of the Delayed Growth of Intermetallic Compound at the Interface between Sn−4.0Ag−0.5Cu and Cu−Zn Substrate. Electron. Mater. Lett. 6, 151–154.

108. L. Dorso, E. Bigot-Corbel, J. Abadie, M. Diab, S. Gouard, F. Bruchertseifer, A. Morgenstern, C. Maurel, M. Chérel, F. Davodeau, (2016) , Long-term toxicity of 213Bi-labelled BSA in mice, PLoS ONE 1–23.

109. L. Kondrachova, S. Aravamudhan, R. Sidhu, D. Amir, R. Aspandiar, (2012), Fundamentals of the non-wet open BGA solder joint defect formation, Proceedings of the International Conference on Soldering and Reliability (ICSR).

110. L. Zhang, K.N. Tu, (2014), Mater. Sci. Eng. R , vol.82, pp. 1–32

111. L. Zhang, K.N. Tu, (2014), Structure and properties of lead-free solders bearing micro and nano   particles, Mater. Sci. Eng. R 82, 1–32

112. L.C.T.J.C. Leong, C.J. Fang, C.P. Chu, (2011), J. Mater. Sci. Mater. Electron., 2011, vol.22, pp. 1443–1449

113. Lead-free Solder Project: Final Report'; NCMS, (1997), Ann Arbor Michigan USA.

114. Lee, T., Choi, W., Tu, K., Jang, J., Kuo, S., Lin, J.,Kivilahti, J. (2002). Morphology, kinetics, and thermodynamics of solid-state aging of eutectic SnPb

and Pb-free solders (Sn–3.5Ag, Sn–3.8Ag–0.7Cu and Sn–0.7Cu) on Cu. Journal of Materials Research, 17(2), 291-301.

115. LIU Yang, SUN Fenglian, LIU Xiaojing,(2010), Improving Sn-0.3Ag-0.7Cu Low-Ag Lead-free Solder performance by Adding Bi Element, International Forum on Strategic Technology 2010, pp 343-346

116. London Metal Exchange, http://www.lme.com C. Hamilton, P. Snugovsky, M. Kelly, Effects of SAC Alloy Copper Dissolution Rates on PTH Processes: Cost and Performance Justify Use of Certain Alternatives to SAC305/405, http://thor.inemi.org/webdownload/newsroom/Presentations/Celestica_iNEMI_Tech_Forum_07/Effects_of_SAC_alloy.pdf

117. Longjun Chena, Bálint Medgyesc, Zhi Zhanga, Shujun Gaod and László Jakabc, (2017), Electrochemical migration of Sn and Sn solder alloys: a review, DOI: 10.1039/C7RA04368F (Review Article) RSC Adv., 7, 28186-28206

118. M. A. A. MohdSalleh, R. M. Said, N. Saud, H. Yasuda, S. D. McDonald, and K. Nogita, (2016), KeyEng. Mater., vol.700, pp. 161-172

119. M. Amagai, (2008), A study of nanoparticles in Sn–Ag based lead free solders, Microelectron. Reliab. 48 (1), 1–16.

120. M. Guarnieri, V. Di Noto, F. Moro, (2010), A dynamic circuit model of a small direct methanol fuel cell for portable electronic devices, IEEE Trans. Ind. Electron. 57 (6), 1865–1873.

121. M. H. Mahdavifard, M. F. M. Sabri, D. A. Shnawah, S. M. Said, I. A. Badruddin, and S. Rozali, (2015), Microelectron. Reliab., vol.55, pp. 1886-1890

122. M. Harada and R. Satoh, (1990), "Mechanical characteristics of 96.5 Sn/3.5 Ag solder in microbonding," in IEEE Transactions on Components, Hybrids, and Manufacturing Technology, vol. 13, no. 4, pp. 736-742

123. M. Holtzer, 92013), Low temperature SMT process conditions, Proceedings of the 2013 IPC APEX Conference, (San Diego, CA).

124. M. J. Rizvi, Y. C. Chan, C. Bailey, H. Lu, and M. N. Islam, (2006), J. Alloys Compd., vol.407,no. 1–2, pp. 208-214

125. M. Lee, M. Yoo, J. Cho, S. Lee, J. Kim, C. Lee, D. Kang, C. Zwenger, R. Lanzone, (2009), Study of interconnection process for fine pitch flip chip, 59th Electronic Components and Technology Conference, pp. 720–723.

126. M. Lu, D. Shih, C. Goldsmith, T.Wassick, (2009), Comparison of electromigration behaviorsof SnAg and SnCu solders, IEEE International Reliability Physics Symposium, pp. 149–154.

127. M. Lu, D. Shih, P. Lauro, C. Goldsmith, D.W. Henderson, (2008), Effect of Sn grain orientation on electromigration degradationmechanism in high Sn-based Pb-free solders, Appl. Phys. Lett. 92 (21), 211909.

128. M. Uchida, H. Ito, K. Yabui, H. Nishiuchi, T. Togasaki, K. Higuchi, H. Ezawa, (2007), Lowstress interconnection for flip chip BGA employing lead-free solder bump, Proceedings of 57th ECTC, pp. 885–891.

129. M. Yunus, K. Srihari, J.M. Pitarresi, A. Primavera, (2003), Effect of voids on the reliability of BGA/CSP solder joints, Microelectron. Reliab. 43 (12), 2077–2086.

130. M.I.I. Ramli, N.Saud, M.A.A. mohdSalleh, M.N.Derman, R. Mohd Said, (2016), Microelectronics reliability , vol.65, pp. 255-264

131. M.J.H. van Dal, A.M. Gusak, C. Cserháti, A.A. Kodentsov and F.J.J. van Loo, (2001), Microstructural Stability of the Kirkendall Plane in Solid-State Diffusion, Phys. Rev. Lett. 86, 3352

132. M.M. Salleh, A.M. Al Bakri, M. Zan, F. Somidin, N.F.M. Alui, Z.A. Ahmad, (2012), Mechanical properties of Sn–0.7Cu/Si3N4 lead-free composite solder, Mater. Sci. Eng. A, vol.556, pp.633–637.

133. M.N. Bashir, A.S.M.A. Haseeb, A.Z.M.S. Rahman, M.A. Fazal, C.R. Kao, (2015), Reduction of electromigration damage in SAC305 solder joints by adding Ni nanoparticlesthrough flux doping, J. Mater. Sci. 50 (20), 6748–6756.

134. Management Methods for Restriction of the Use of Hazardous Substances in Electrical and Electronic Products, http://www.chinarohs.com (Last accessed on February 2020).

135. Marcus Vitruvius Pollio, 'De Architectura, liber VIII' (www.ukans.edu/history /index/europe/ancient_rome/) (Last accessed on February 2020).

136. Michael Krachler, Rafael Alvarez-Sarandes, and Gert Rasmussen, (2016), High-Resolution Inductively Coupled Plasma Optical Emission Spectrometry for 234U/238Pu Age Dating of Plutonium Materials and Comparison to Sector Field Inductively Coupled Plasma Mass Spectrometry, Anal. Chem. 2016, 88, 17, 8862-8869

137. MineralPrices, http://mineralprices.com (accessed on February 2020)

138. MineralPrices.com http://mineralprices.com (accessed on February 2020).

139. O. Beattie, J. Geiger and J.J. Geiger, (2000), 'Frozen in Time', Greystone Publishing Vancouver Canada.

140. O. Chen, J. Gao, T. Pan, K.K. Tang, R. Aspandiar, K. Byrd, B. Zhou, S.Mokler, A.Molina, (2016), Solder joint Reliability onmixed SAC-BiSn ball grid array solder joints formed with resin reinforced Bi-Sn metallurgy solder pastes, 2016 SMTA International Conference, Chicago, USA.

141. O. Krammer, T. Garami, B. Horváth, T. Hurtony, B. Medgyes, and L. Jakab, (2015), J. Alloys Compd., vol.634, pp. 156-162

142. O. Teppo, J. Niemelä, P. Taskinen, Thermochim, (1990), An assessment of the thermodynamic properties and phase diagram of the system Bi-Cu, Acta 173, 137-150

143. P. Biocca, C. Rivas, (2007), Case study on the validation of SAC305 and SnCu-based solders in SMT wave and hand-soldering at the contract assembler level, Proceedings of the 12th International Symposium IEEE Advanced Packaging Material Processing Properties Interfaces, pp. 152–157.

144. P. Biocca, Lead-free Hand Soldering – Ending the Nightmares, http://www. emsnow.com/cnt/files/White%20Papers/biocca_hand_soldering.pdf

145. P. Chauhan, M. Osterman, M. Pecht, (2009), Impact of thermal aging on the growth of Cu- Sn intermetallic compounds in Pb-free solder joints in 2512 resistors, Proceedings of the ASME International Mechanical Engineering Congress and Exposition, IMECE2009, 10169.

146. P. Davuluri, S. Shetty, A. Dasgupta, S. Young, (2011), Thermomechanical durability of high I/O BGA packages, Transactions of the ASME, vol. 124, pp. 226–270.

147. P. Hagler, P. Henson, R.W. Johnson, (2011), Packaging technology for electronic applications in harsh high temperature environments, IEEE Trans. Ind. Electron. 58 (7), 2673–2682.

148. P. L. Sudan Ahmed, MunshiBasit, Jeffrey C. Suhling, (2016), Effects of aging on SAC-Bi solder materials, 15th IEEE Intersociety Conf. on Thermaland Thermomechanical Phenomena in Electronic Systems, pp. 746-754

149. P. Lall, C. Bhat, M. Hande, V. More, R. Vaidya, K. Goebel, (2011), Prognostication of residual life and latent damage assessment in lead-free electronics under thermomechanical loads, IEEE Trans. Ind. Electron. 58 (7), 2605–2616.

150. P.L. Liu, J.K. Shang, (2001), Interfacial segregation of bismuth in Cu/Sn-Bi solder interconnect, Scr. Mater. 44, 1019–1023.

151. P.T. Vianco and D.R. Frear, (1993), Issues in the replacement of lead bearing solders, J. of Met. 7, 14-23.

152. R. Aspandiar, K. Byrd, K.K. Tang, L. Campbell, S. Mokler, (2015), Investigation of low temperature solders to reduce reflow temperature, improve SMT yields and realize energy savings, Proceedings of the 2015 APEX Conference.

153. R. Berni, M. Catelani, C. Fiesoli, V.L. Scarano, (2016), A comparison of alloy-surface finish combinations considering different component package types and their impact on soldering reliability, IEEE Trans. Reliab. 65 (1), 272–281.

154. R. Boyle, A. Plant, K. Vijay, Low Ag SAC Alloys, http://www.smartgroup.org/wpcontent/ uploads/2013/04/Low-Silver-SAC-Alloys-February-2015.pdf (last accessed on February 2020).

155. R. Brandt, J. Knarren, G. Manders, (1999), "Lead-free Solders for Electronic Applications", Internal Report, MDP Project Group "Lead-free Soldering", Eindhoven University of Technology, Eindhoven the Netherlands.

156. R. Coyle, K. Sweatman, B. Arfaei, (2015), Thermal fatigue evaluation of Pb-free solder joints: Results, lessons learned, and future trends, J. Miner. Met. Mater. Soc. 67 (10), 2394–2415.

157. R. Lim, (2010), Investigation into lead-free solder in Australian defense force applications, Air Vehicles Division Defence Science and Technology Organization, DSTO-TN- 0970.

158. R. Pandher, B. Lewis, R. Vangaveti, B. Singh, (2007), Drop shock reliability of lead-free alloys effect of micro-additives, Proceedings of the 57th Electronic Components and Packaging Conference, pp. 669–676.

159. R. Pandher, R. Healey, (2008), Reliability of Pb-Free solder alloys in demanding BGA and CSP applications, Proceedings of the 58th Electronic Components and Technology Conference, pp. 2018–2023.

160. R. Schueller, N. Blattau, J. Arnold, C. Hillman, (2010), Second generation Pb-free alloys, SMTA J. 23 (1), 18–27.

161. R.R. Tummala, E.J. Rymaszewski, A.G. Klopfenstein, (1989), 'Microelectronics Packaging Handbook, subsystem Packaging part III', second edition Chapman & Hall, New York USA, 221

162. R.W. Wu, L.C. Tsao, R.S. Chen, (2009), Effect of 0.5 wt% nano-TiO2 addition into low-Ag Sn0.3Ag0.7Cu solder on the intermetallic growth with Cu

substrateduring isothermal aging, J. Mater. Sci. Mater. Electron. 26 (3), 1858–1865.

163. Restrictions on the Use of Certain Hazardous Substances (RoHS) in Electronic Devices, https://www.dtsc.ca.gov/HazardousWaste/RoHS.cfm (accessed on February 2020)

164. S. Ahmed, M. Basit, J.C. Suhling, P. Lall, Effects of aging on SAC-Bi solder materials, 2016 15th IEEE Intersociety Conference on Thermal and Thermomechanical Phenomena in Electronic Systems (ITherm), IEEE 2016, pp. 746–754 (Lead Free Alloys) http:// www.kester.com/knowledge-base/lead-free-solutions/ (Last accessed on February 2020).

165. S. Han, S. Meschter, M. Osterman, M. Pecht, (2012), Evaluation of effectiveness of conformal coatings as tin whisker mitigation, J. Electron. Mater. 41 (9), 2508–2518.

166. S. Kim, J. Yu, (2010), Effects of Ag on the Kirkendall void formation of Sn–xAg/Cu solder joints, J. Appl. Phys. 108, 083532.

167. S. Menon, E. George, M. Osterman, M. Pecht, (2015), High lead solder (over 85%) solder in the electronics industry: RoHS exemptions and alternatives, J. Mater. Sci. Mater. Electron. 26 (6), 4021–4030.

168. S. Meschter, P. Snugovsky, Z. Bagheri, E. Kosiba, M. Romansky, J. Kennedy, L. Snugovsky, D. Perovic, (2014), Whisker formation on SAC305 soldered assemblies, J. Miner. Met. Mater. Soc. 66 (11), 2320–2333.

169. S. Mokler, R. Aspandiar, K. Byrd, O. Chen, S.Walwadkar, K.K. Tang, M. Renavikar, S. Sane, (2016), "The application of Bi-based solders for low

temperature reflow to reduce cost while improving SMT yields in client computer systems", Proceedings of the 2016 SMTA International Conference, Sept. 25-29, Chicago, IL.

170. S. Seo, S. Kang, D. Shih, H. Lee, (2009), The evolution of microstructure and microhardness of Sn–Ag and Sn–Cu solders during high temperature aging, Microelectron. Reliab. 49 (3), 288–295.

171. S. Wang, C. Liu, (2007), Coupling effect in Pt/Sn/Cu sandwich solder joint structures, Acta Mater. 55 (10), 3327–3335.

172. S. Wiese, M. Roellig, K. Wolter, (2007), Creep of thermally aged SAC solder joints, Microelectron. Reliab. 47 (2–3), 223–232.

173. S.C.O. Mathuna, P. Byrne, G. Duffy,W. Chen, M. Ludwig, T. O'Donnell, P. McCloskey, M. Duffy, (2004), Packaging and integration technologies for future high-frequency power supplies, IEEE Trans. Ind. Electron. 51 (6), 1305–1312.

174. S.K. Kang, D. Leonard, D.Y. Shih, L. Gignac, D.W. Henderson, S. Cho, J. Yu, (2005), Interfacial reactions of Sn-Ag-Cu solders modified by minor Zn alloying addition, J. Electron. Mater. 35 (3), 479–485.

175. S.K.K.W.M. Chen, C.R. Kaoa, (2012), J. Alloys Compd.,vol.520, pp. 244–249.

176. Shunfeng Cheng, Chien-Ming Huang, Michael pecht, (2017), A review of lead-free solders for electronics applications, Microelectronics Reliability, 75, 77-95

177. SMART Group, "Solder Dross," EMT Worldwide, http://www.emtworldwide.com/ article.aspx?ArticleID=21838 16 January 2009 (accessed on February 2020)

178. Solder Value Final Report.indd - IPC, http://www.ipc.org/3.0_Industry/3.5_Councils_Associations/3.5.1_Industry_Assoc/spvc_bro/SVPC_Final_ExecSumm.pdf (accessed on February 2020)

179. Solder-ball Manufacturing and Attachment for BGAs, http://www.indium.com/technicaldocuments/whitepaper/solderball-manufacturing-and-attachment-forbgas (accessed on February 2020)

180. Solder-ball Manufacturing and Attachment for BGAs, http://www.indium.com/technical-documents/whitepaper/solderball-manufacturing-and-attachment-forbgas (Last accessed on February 2020).

181. T. Laurila, J. Hurtig, V. Vuorinen, J.K. Kivilahti, (2009), Effect of Ag, Fe, Au and Ni on the growth kinetics of Sn–Cu intermetallic compound layers, Microelectron. Reliab. 49, 242–247.

182. T. Laurila, V. Vuorinen, M.P. Kröckel, (2010), Impurity and alloying effects on interfacial reaction layers in Pb-free soldering, Mater. Sci. Eng. R 68.

183. T. Nishimura, M. Dekui1, S. Sawada, K. Sweatman, K. Howell, G. Zeng, K. Nogita, (2015), The Performance of solid solution strengthened no silver lead free solder, Proceedings of the International Conference on Soldering and Reliability (ICSR).

184. T. Woodrow, (2003), The effects of trace amounts of lead on the reliability of six lead-free solders, IPC Proceedings of the 3rd International Conference on Lead-free Components and Assemblies, San Jose, CA.

185. T.C. Chiu, K. Zeng, R. Stierman, D. Edwards, K. Ano, (2004), Effect of thermal aging on board level drop reliability for Pb-free BGA packages, Proceedings of the 54th Electronic Components and Technology Conference, vol. 2, pp. 1256–1262.

186. T.P. Vianco, Development of alternatives to lead-bearing solders, in: Proceedings of the Technical Program on Surface Mount International, 19 August±2 September 1993, San Jose, CA.

187. TCNCP, http://www.amkor.com/go/technology/tcncp/tcncp (accessed on February 2020).

188. Turkey Announces RoHS Legislation, http://www.intertek.com/news/2008/10-28-turkey-announces-rohs-legislation (accessed on February 2020)

189. U.R. Kattner and W.J. Boettinger, (1994), Phase diagrams for lead-free solder alloys, J. Electron. Mater. 23, 603-610

190. W. Peng, K. Zeng and J.K. Kivilahti, (2000)'A Literature Review on Potential Leadfree Solder Systems', Internal Report, Helsinki University of Technology, Espoo Finland.

191. W.J. Plumbridge, (1996), Solders in electronics, J. Mat. Sc., 2501

192. W.K. Loh, R. Kulterman, H. Fu, M. Tsuriya, (2016), Recent trends of package warpage and measurement metrologies, 2016 International Conference on Electronics Packaging (ICEP), IEEE, pp. 89–93.

193. W.Wondrak, R. Held, E. Niemann, U. Schmid, (2011), SiC devices for advanced power and high-temperature applications, IEEE Trans. Ind. Electron. 48 (2), 307–308.

194. www.metallurgy.nist.gov (Last accessed on February 2020)

195. www.service.chimie.pagesproorange.fr/2Ele/LEAD_FREE_SOLDERS_IN_ELE CTRONICS.htm (Last accessed on February 2020)

196. X. Liu, L.Wang, J.Wang, Y. Lv, (2010), Effects of Ce addition on properties of Sn-0.3 Ag-0.7 Cu low-Ag lead-free solder, Electronic Packaging Technology & High Density Packaging (ICEPT-HD), pp. 176–180.

197. X. Xu, A.S. Gurav, P.M. Lessner, C.A. Randall, (2011), IEEE Trans. Ind. Electron. 58.

198. X.L.Z.a.M. Gupta, (2008), J. Phys. D. Appl. Phys. 41 (2008).

199. Y. Liu, F. Sun, X. Liu, (2010), Improving Sn-0.3 Ag-0.7 Cu low-Ag lead-free solder performance by adding Bi element, Strategic Technology (IFOST), 2010 International Forum on, IEEE.

200. Y. Zhong, W. Liu, C. Wang, X. Zhao, and J. F. J. M. Caers, (2016), Mater. Sci. Eng. A, 652, pp. 264-270

201. Y. Zhou, A. Dasgupta, (2007), Vibration durability assessment of Sn3.0Ag0.5Cu & Sn37Pb solders under harmonic excitation, ASME International Mechanical Engineering Congress and Exposition, Seattle, Washington.

202. Y.-H. Lee, (2008), Microstructure and mechanical properties of Sn-Ag-xNi composite solder, IEEE International Nanoelectronics Conference, pp. 175–178.

203. Y.K. Jee, Y.H. Ko, J. Yu, (2007), Effect of Zn on the intermetallics formation and reliability of Sn-3.5Ag solder on a Cu pad, J. Mater. Res. 22 (7), 1879–1887.

204. Y.M. Kim, K.M. Harr, Y.H. Kim, (2010), Mechanism of the delayed growth of intermetallic compound at the interface between Sn−4.0Ag−0.5Cu and Cu−Zn substrate, Electron. Mater. Lett. 6 (4), 151−154.

205. Y.W. Wang, C.R. Kao, (2009), Minimum effective Ni addition to SnAgCu solders for retarding Cu3Sn thickness, ASE Technol. J. 2 (2), 137−142.

206. Y.W. Wang, Y.W. Lin, C.T. Tu, C.R. Kao, (2009), Effects of minor Fe, Co, and Ni additions on the reaction between SnAgCu solder and Cu, J. Alloys Compd. 478, 121−127.

207. Z.L. Ma, S.A. Belyakov, C.M. Gourlay, (2016), Effects of cobalt on the nucleation and grain refinement of Sn-3Ag-0.5 Cu solders, J. Alloys Compd. 682, 326−337.

208. Fan Yang, Liang Zhang, (2016), Properties and Microstructures of Sn-Bi-X Lead-Free Solders, Adv. Mat.sci. Engg, 2016, 15

209. M.kamal, B M manoharan, H I Farag (2011), Newton's metal as a new home-made shielding material, Radiation Effects and Defects in Solids, Volume 162, Issue 1

COST CALCULATION AND COMPARISON

10.1 INTRODUCTION

Cost is an important factor that needs to be considered while selecting a lead free solder alloy along with their properties. Sn-Pb is a very low cost alloy. Ever since the implementation of RoHS, Sn-0.5Cu-3Ag (SAC305) has been the good lead free solder alloy used in the electronic industry. But the 3% Ag will add the cost; therefore the industry is looking for a less expensive lead free solder alloy along with good properties. Corrosion is yet another factor. Solder material (alloy, flux) cost, cost for production/manufacturing the solder material in their specific form, cost for patent are the major costs coming into picture

Major elements in the lead free solder alloys were identified and cost of these elements were tabulated. Costs of the solder alloys were calculated. Composition of the elements (in wt. %) in the alloy and Cost of the elements were takes as the variables. Only material costs were considered in this paper. Patent cost and manufacturing costs were not considered in this analysis. All other cost will remain almost constant regardless of the change in the composition. Equation for finding the cost of an alloy is proposed in terms of material composition and cost of each element. 22 lead free solder alloys and Sn-Pb alloy were included in this study. These 22 solder alloys and Sn-Pb alloy are represented in table 10.1

Table 10.1 List of the solder alloys selected

Sl no.	Solder alloy
1	96.5Sn-3.5Ag
2	96.5Sn-3Ag-0.5Cu
3	95.5Sn-4Ag-0.5Cu
4	95.5Sn-3.8Ag-0.7Cu
5	95Sn-4Ag-1Cu
6	93.6Sn-4.7Ag-1.7Cu
7	99.3Sn-0.7Cu
8	96.7Sn-2Ag-0.8Cu-0.5Sb
9	91.8Sn-3.4Ag-4.8Bi
10	93.5Sn-3.5Ag-3Bi
11	95.5Sn-0.5Cu-3Bi -1Ag
12	97Sn-1Cu-1Ni-1Ag
13	90Sn-2Ag-7.5Bi-0.5Cu
14	42Sn-58Bi
15	95Sn-5Sb
16	65Sn-25Ag-10Sb
17	52In-48Sn
18	86.4Sn-11In-2Ag-0.6Sb
19	95Sn-3.5Ag-1.5In
20	77.2Sn-20In-2.8Ag
21	91Sn-9Zn
22	99.25Sn-0.7Cu-0.05Ni
23	63sn-37Pb

10.2`METHOD AND CALCULATION

10.2.1 Costs

In this paper 10 elements are short listed which are used to manufacture the solder alloys. Cost of the element and the composition of elements are taken as the variables. Cost of the alloy may be distributed into cost of the solder material. Patent cost, cost of solder in different forms (sphere, bar and wire) and paste forms and the manufacturing cost are not considered in the study. This will help to compare the lead free solder alloys with Sn-Pb alloy.

10.2.2 Cost of the solder material

The elements in the lead free solder joints are identified. Costs of these elements (in $ US/Kg) is also identified as of December 2019. This is shown in the table 9.2.

Table 10.2, Element prices as of December 2019

Material	Price $ US /Kg
Tin (Sn)	20.94
Gold (Au)	45467.37
Copper (Cu)	5.94
Bismuth (Bi)	19.82
Nickel (Ni)	11.6
Antimony (Sb)	8.42
Indium (In)	408.2
Zinc (Zn)	2.5
Silver (Ag)	546.73
Lead (Pb)	1.8

10.2.3 Patent costs

While selecting an appropriate lead-free solder alloy, patent royalties should be considered. A major group of lead free alloys that are having good properties are protected by North American and Japanese patents. The manufacturers of the solder should pay the corresponding royalties on behalf of the Original Equipment manufacturer or the electronics manufacturing services (EMS) firms (IPC Solder Products Value Council).

10.2.4 Cost of solder in sphere, bar, wire, and paste forms

Solder alloys are present in the market in various forms like sphere, bar, wire and paste and it depends on the application of use. Sequential flow or reflow process is used to manufacture solder spheres which is followed by degreasing and classification. Solder bars and ingots are produced by melting the individual portions of the alloy recipe and transferring into molds of designed shapes. The solder wire manufacturing process is mainly containing formulating flux for the core, billet casting the alloy, extruding the cored wire-product, drawing the wire to the desired diameter, and making the wire onto reels or bobbin. Smaller-diameter wires are more expensive because of the longer wire length, increased drawing steps and longer manufacturing times. Solder paste production involves much higher costs compared to solders produced in other forms. In this study the composition of the elements and cost of the element are considered. All other costs were taken as constants.

10.2.5 Cost of solder alloy equations

$$Cost\ of\ the\ alloy = a * C_a + b * C_b + c * C_c + d * C_d + e * C_e + f * C_f + g * C_g +$$

$$h * C_h + i * C_i + j * C_j + C_P + C_F + C_M \tag{10.1}$$

$$= \Sigma(\text{Composition of the element} * \text{Cost of the Element})$$

Where $a, b, c, d, e, f, g, h, i$ $and j$ are Composition (in wt. %) of Tin (Sn), Gold (Au), Copper(Cu), Bismuth(Bi),Nickel(Ni), Antimony(Sb), Indium(In), Zinc(Zn), Silver(Ag) and Lead(Pb) respectively

$C_a, C_b, C_c, C_d, C_e, C_f, C_g, C_h, C_i, C_j$ are the costs ($US/Kg) of Tin (Sn), Gold (Au), Copper(Cu), Bismuth(Bi),Nickel(Ni), Antimony(Sb), Indium(In), Zinc(Zn), Silver(Ag) and Lead(Pb) respectively

$C_P, C_F,$ $and\ C_M$ are Patent cost, Cost to make in different forms and manufacturing cost respectively.

10.3 Results

10.3.1 Cost of the solder alloys

Cost of the solder alloys were determined using equation (1). The price of the different solder alloys are tabulated in the table 3. All the price are in US$. From the table 3 we can see that lead-tin alloy is having the lowest price of $13.85/Kg. This alloy has to be replaced by a lead free solder alloy. Table 4 shows a comparison of these alloys with Sn-Pb alloy which is represented as a cost ratio with Sn-Pb alloy. While analyzing the remaining 21 lead free alloys, 91Sn-9Zn, 42Sn-58Bi, 95Sn-5Sb, 99.25Sn-0.7Cu-0.05Ni,

99.3Sn-0.7Cu, 97Sn-1Cu-1Ni-1Ag and 95.5Sn-0.5Cu-3Bi -1Ag are having cost less than $30/kg.

Table 10.3 Price of the solder alloy calculated

Composition	Price $ US /Kg
96.5Sn-3.5Ag	39.34265
96.5Sn-3Ag-0.5Cu	36.6387
95.5Sn-4Ag-0.5Cu	41.8966
95.5Sn-3.8Ag-0.7Cu	40.81502
95Sn-4Ag-1Cu	41.8216
93.6Sn-4.7Ag-1.7Cu	45.39713
99.3Sn-0.7Cu	20.835
96.7Sn-2Ag-0.8Cu-0.5Sb	31.2732
91.8Sn-3.4Ag-4.8Bi	38.7631
93.5Sn-3.5Ag-3Bi	39.30905
95.5Sn-0.5Cu-3Bi -1Ag	26.0893
97Sn-1Cu-1Ni-1Ag	25.13
90Sn-2Ag-7.5Bi-0.5Cu	31.2968
42Sn-58Bi	20.2904
95Sn-5Sb	20.314
65Sn-25Ag-10Sb	151.1355
52In-48Sn	222.3152
86.4Sn-11In-2Ag-0.6Sb	73.97928
95Sn-3.5Ag-1.5In	45.15155
77.2Sn-20In-2.8Ag	113.11412
91Sn-9Zn	19.2804
99.25Sn-0.7Cu-0.05Ni	20.83033
63sn-37Pb	13.8582

Table 10.4 Comparison with Sn-Pb

Composition	Price $ US /Kg	Ratio to 63Sn-37Pb
63sn-37Pb	13.86	1
91Sn-9Zn	19.28	1.391053391
42Sn-58Bi	20.29	1.463924964
95Sn-5Sb	20.31	1.465367965
99.25Sn-0.7Cu-0.05Ni	20.83	1.502886003
99.3Sn-0.7Cu	20.84	1.503607504
95.5Sn-0.5Cu-3Bi -1Ag	26.09	1.882395382
96.7Sn-2Ag-0.8Cu-0.5Sb	31.27	2.256132756
90Sn-2Ag-7.5Bi-0.5Cu	31.3	2.258297258
96.5Sn-3Ag-0.5Cu	36.64	2.643578644
91.8Sn-3.4Ag-4.8Bi	38.76	2.796536797
93.5Sn-3.5Ag-3Bi	39.31	2.836219336
96.5Sn-3.5Ag	39.34	2.838383838
95.5Sn-3.8Ag-0.7Cu	40.82	2.945165945
95Sn-4Ag-1Cu	41.82	3.017316017
95.5Sn-4Ag-0.5Cu	41.9	3.023088023
95Sn-3.5Ag-1.5In	45.15	3.257575758
93.6Sn-4.7Ag-1.7Cu	45.4	3.275613276
86.4Sn-11In-2Ag-0.6Sb	73.98	5.337662338
77.2Sn-20In-2.8Ag	113.11	8.160894661
65Sn-25Ag-10Sb	151.14	10.9047619
52In-48Sn	222.32	16.04040404

Cost calculation of the 23 selected solder alloys was done. The cost of the constituent element and the percentage of composition (% by wt.) are taken as the variables in the analysis. Costs of the solder alloys were calculated. From the analysis of the results we can see that Sn-0.5Cu-3Bi-1Ag and Sn-1Cu-1Ni-1Ag are having better cost ratio when compared to the other alloys. These two alloys can be regarded as an alternative solder joints to replace Sn-Pb solder alloy.

LIST OF PUBLICATIONS

SUBMITTED ON THE BASIS ON THESIS

REFEREED JOURNALS

1. Jayesh, S., Elias, J. Experimental Investigation on the Effect of Ag Addition on Ternary Lead Free Solder Alloy –Sn–0.5Cu–3Bi. Met. Mater. Int. 26, 107–114 (2020). https://doi.org/10.1007/s12540-019-00305-3 (Springer) (Scopus-Indexed)

2. Jayesh, S., Elias, J. Experimental Investigations on Impact Toughness and Shear Strength of Lead Free Solder Alloy Sn–0.5Cu–3Bi–xAg. Trans. Electr. Electron. Mater. (2020). https://doi.org/10.1007/s42341-019-00167-x (Springer) (Scopus-Indexed)

3. Jayesh, S., Jacob, E. An Experimental Investigation on the Properties of Two Novel Ternary Solder Alloys Sn–0.5Cu–3Bi and Sn–1Cu–1Ni Replacing Lead. Phys. Metals Metallogr. 120, 1398–1403 (2019). https://doi.org/10.1134/S0031918X1913009X (Springer) (Scopus-Indexed)

4. Jayesh, J. Elias, Experimental investigations on the effect of addition of Ag into ternary lead free solder alloy Sn-1Cu- 1Ni, Lett. Mater. 9, 239–242 (2019) https://doi.org/10.22226/2410-3535-2019-2-239-242 (Scopus-Indexed)

5. Jayesh, S., & Elias, J. (2019). Experimental Investigations on Impact Toughness and Shear Strength of Novel Lead Free Solder Alloy Sn-1Cu-1Ni-XAg, Powder Metallurgy Progress, 19(2), 90-96. doi: https://doi.org/10.1515/pmp-2019-0009 (Scopus-Indexed)

6. Jayesh S., Elias, J. Investigations on the Corrosion Properties of Sn–0.5Cu–Bi–xAg Lead Free Solder Alloys in 3.5% NaCl Solution. Trans. Electr. Electron. Mater. (2020). https://doi.org/10.1007/s42341-020-00219-7 (Springer) (Scopus-Indexed)

7. Jayesh S, Jacob Elias, Manoj Guru, Factorial design and design of experiments for developing novel lead free solder alloy with Sn, Cu and Ni, Int. J. Simul. Multidisci. Des. Optim. 11, 18 (2020) (Scopus-Indexed)

INTERNATIONAL CONFERENCES

1. Jayesh S, J Elias, Asif S, Cost-benefit Analysis of Sn-0.5Cu-3Bi-1Ag and Sn-1Cu-1Ni-1Ag lead free solder alloys considering Elemental Cost, Hardness, Contact angle and Melting Temperatures, Taylor and Francis , AICERA, 2019.

PATENTS

1. Jayesh S, Jacob Elias, Lead free solder alloy for moderately high temperature applications, Application no. 201941028296, dt. 15-07-2019 (Published)

2. Jayesh S, Jacob Elias, Lead Free Solder Alloy Tin-Copper-Bismuth-Silver, Application no. 201941005271, dt. 11/02/2019 (Published)

CURRICULUM VITAE

1. Name : **JAYESH S**

2. Date of Birth : 10.06.1988

3. Educational Qualifications

2010 Bachelor of Technology (B. Tech)

Institution : Government Engineering College, Thrissur, Kerala

Specialization : Mechanical Engineering

2014 Master of Engineering (M.E.)

Institution : PSG College of Technology, Coimbatore

Specialization : Product Design

Doctor of Philosophy (PhD)

Institution : Cochin University of Science and Technology,
Kochi, Kerala Registration

Date of Reg. : 26.11.2015